

UNIVERSITY COLLEGE LONDON

**SOLID POLYMER ELECTROLYTES
FOR ION SELECTIVE MEMBRANES**

by

Yut-Mei Tang

PhD, 1996

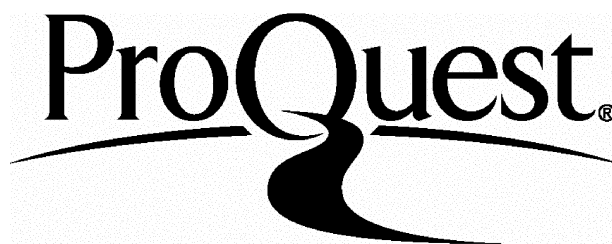
ProQuest Number: 10055393

All rights reserved

INFORMATION TO ALL USERS

The quality of this reproduction is dependent upon the quality of the copy submitted.

In the unlikely event that the author did not send a complete manuscript and there are missing pages, these will be noted. Also, if material had to be removed, a note will indicate the deletion.



ProQuest 10055393

Published by ProQuest LLC(2016). Copyright of the Dissertation is held by the Author.

All rights reserved.

This work is protected against unauthorized copying under Title 17, United States Code.
Microform Edition © ProQuest LLC.

ProQuest LLC
789 East Eisenhower Parkway
P.O. Box 1346
Ann Arbor, MI 48106-1346

This thesis is dedicated to my parents

ABSTRACT

The work described in this thesis was carried out as part of a project to explore the use of solid polymer electrolytes as pH electrodes, the properties of which would be superior to those of the fragile glass membranes traditionally used. To this end, potentiometry was used to study ion transport in membranes which were composites of poly(vinyl chloride) and poly(ethylene oxide). The idea was that the hydrophilic polymer (PEO) would interact with water molecules and ionic species, and the hydrophobic polymer (PVC) would serve as an inert matrix, intimately tangled with the hydrophilic polymer to prevent its diffusion into the aqueous solution phase.

It was shown that membranes prepared by co-casting polymers from solution were indeed stable in water and that the properties could be changed by change in fabrication procedure which changed the microstructure. This thesis describes the development of the membrane preparation procedure from initially pure PEO gels to processed pure PEO membranes then co-cast composite PEO and PVC membranes and finally rotary evaporated PEO-PVC membranes. The effect of the preparation procedure on the potential difference response of these membranes was investigated to correlate any structural changes to the membrane electrochemical behaviour. Membranes prepared by the various procedures were tested with thermal analysis, FTIR and polarised light optical spectroscopy to observe any trends in physical characteristics associated with structural changes. The electrical properties of these membranes were correlated with the microscopic and macroscopic membrane structure and chemical composition.

It is postulated that the membranes are a nano-scale composite structure comprising interpenetrating networks of hydrophobic and hydrophilic regions of size determined by the preparation procedure. The size of these regions determine the transport properties of ions moving through the membrane. It is proposed that the dominant effect on permselectivity in the membranes studied here is a modification of the interaction between ions and water within the membrane channels formed by a hydrated hydrophilic polymer.

TABLE OF CONTENTS

	PAGE
Title page	1
Abstract	3
Table of contents	4
Table of figures	9
Table of tables	13
Table of abbreviations	15
Table of symbols	16
Acknowledgement	18

CHAPTER 1. INTRODUCTION

1.1. Glass electrode	21
1.2. Poly(ethylene oxide)	22
1.2.1. General Introduction	22
1.2.2. Anhydrous poly(ethylene oxide)	24
1.2.3. Solution properties of poly(ethylene oxide)	25
1.2.4. Association complexes of poly(ethylene oxide)	25
1.2.5. Ionic complexes	26
1.3. Poly(vinyl chloride) membranes	27
1.4. Ion Selective Electrodes	30
1.4.1. Ion Selective Membranes	30
1.4.2. Development of Specific membranes Electrodes	32
References	33

CHAPTER 2. THEORY

2.1. Ion-water interactions	36
2.1.1. Interactions of ions with water-effects on local water structure	36
2.1.2. Effects of ionic concentration on solution	38

	Page
viscosity and conductivity	
2.1.3. Interaction of non-ionic species with water	40
2.1.4. Complex mixtures	41
2.1.5. Interaction of PEO and water	41
2.1.6. Interaction of PEO with ionic species in aqueous solution	42
2.1.7. Structure of water in polymer membranes	43
2.2. Development of membrane potential	44
2.2.1. The permeable membrane	45
2.2.2. The semipermeable membrane	53
2.2.3. The permselective membrane	55
2.2.4. Glass membranes	56
2.2.5. Other types of practical permselective membranes	58
2.2.6. Permselective site free membrane	59
2.2.7. Permselective fixed site membrane	60
2.2.8. Permselective mobile site membrane	60
2.2.9. Selectivity coefficients and interferences	62
2.2.10. Time dependant effects	64
2.3. The electrified interface	65
2.3.1. The streaming potential	68
References	71

CHAPTER 3. EXPERIMENTAL TECHNIQUES AND EQUIPMENT

3.1. Materials	75
3.2. Membrane preparation	75
3.2.1. Aqueous PEO membranes	75
3.2.2. Processed PEO gels	76
3.2.3. Composite PEO-PVC membranes	76

	Page
3.3. Aqueous PEO membranes	77
3.3.1. Density and viscosity measurements	77
3.3.2. Conductivity measurements	78
3.3.3. Stoichiometry and stability constant of Ag/PEO complex	78
3.4. Processed PEO gels	79
3.4.1. A. C. Impedance	79
3.5. Potentiometry	79
3.6. Composite PEO-PVC membranes, non-electrochemical methods	81
3.6.1. Thermal analysis	81
3.6.2. Differential scanning calorimetry (DSC)	82
3.6.3. Thermo-mechanical analysis (TMA)	83
3.6.4. Thermogravimetry (TG)	84
3.6.5. Fourier transform infrared spectroscopy	84
3.6.6. Optical microscopy	85
3.6.7. ^2H nuclear magnetic resonance spectroscopy	86
References	87

CHAPTER 4. ELECTROCHEMICAL RESULTS

4.1. Development of the film preparation method	89
4.2. Background studies on aqueous PEO solutions	92
4.2.1. Conductivity of salt solutions containing PEO	92
4.2.2. Viscosity results	92
4.2.3. Complexation of Ag^+ by PEO: potentiometry titration	95
4.2.4. Potentiometry measurements of salt complexation by PEO	96

	Page
4.3. Potentiometric behaviour of pure PEO membranes	97
4.3.1. Supported aqueous PEO membranes	97
4.3.2. Processed PEO membranes	98
4.4. Potentiometric behaviour of co-cast PEO-polymer membranes	100
4.4.1. Potentiometric behaviour of slowly dried PEO-PVC membranes	101
4.4.2. Potentiometric behaviour of quickly dried PEO-PVC membranes	107
4.4.3. Potentiometric behaviour of PVC-polymer membranes	116
4.4.3.1. Potentiometric behaviour of PVC-PMA and PVC-PVMK membranes	116
4.4.3.2. Potentiometric behaviour of co-cast PEO-PVC (fluka chemicals) membranes	120
4.4.3.3. Potentiometric behaviour of co-cast PEO-carboxylated PVC membranes	125
4.4.3.4. Rotary evaporated PEO-carboxylated PVC membranes	126
References	129

CHAPTER 5. NON-ELECTROCHEMICAL RESULTS

5.1. Differential scanning calorimetry (DSC)	131
5.2. Thermo-mechanical analysis (TMA)	133
5.3. Thermogravimetry (TG)	135
5.4. FTIR spectroscopy	138
5.5. Optical spectroscopy	144
5.6. Solid state NMR spectroscopy	149
References	151

	Page
CHAPTER 6. DISCUSSION	
6.1. Conductivity of ions in aqueous solutions containing PEO	153
6.2. Discussions of PEO membranes	155
6.2.1. Supported PEO membranes	155
6.2.2. Behaviour of processed PEO membranes	157
6.3. Behaviour of the co-cast PEO-PVC membranes	159
6.3.1. Evidence for different forms of water in the membrane	159
6.3.2. Correlation of forms of water and potential response of co-cast membranes	161
6.3.3. Evidence for variations in microstructure in the co-cast membrane	162
6.3.4. Correlation of microstructure and membrane potential	165
6.3.5. Effect of variation of PVC in the membrane	168
6.3.6. Effect of changing the hydrophilic polymer in the membrane	169
6.4. Model for the co-cast PEO-PVC membrane potential response based on membrane structure	169
References	176
CHAPTER 7. CONCLUSION	178

TABLE OF FIGURES

	Page
1.1 The structure of PEO	22
1.2 A model of the water structure of water proposed by Sheraga and Nemathy	27
1.3 The structure of PVC	28
2.1 The potentiometric response of an ideal semipermeable and permselective membrane	55
2.2 The regions of a glass membrane	56
3.1 The doctor-blading co-casting machine	77
3.2 The concentration cell used in the potentiometry experiments	80
3.3 The DSC recording instrument with control mechanism	82
3.4 The thermo-mechanical analysis instrument	83
3.5 The thermogravimetry analysis instrument	84
4.1 Potentiometry and A. C. Impedance response of a processed PEO membrane in NaCl solution	91
4.2 Molar conductivity vs. the square root of salt concentration in water and PEO solution	93
4.3 Variation of $\ln[(\eta/CV)-1]$ vs. $\ln V$	96
4.4 The effect of PEO on salt activity measured using potentiometry	97
4.5 Potential difference response vs. log activity ratio of HCl solution on aqueous supported PEO membranes	98
4.6 Potential difference measurement on aqueous supported PEO membranes in various salts	99
4.7 Potential difference response vs. log activity ratio of NaCl for processed PEO membranes	99
4.8 Potential difference vs. time response for slowly dried co-cast PEO-PVC membrane in NaCl solution	102

	Page
4.9 Potential difference response vs. log activity ratio of NaCl for slowly dried co-cast PEO-PVC membrane in NaCl	103
4.10 Potential difference vs. time response for slowly dried PEO-PVC membranes in HCl solution after immersion in NaCl	104
4.11 Potential difference response vs. log activity ratio of HCl solution for slowly dried PEO-PVC membranes	105
4.12 Potential difference vs. time response for quickly dried co-cast PEO-PVC membranes in HCl solution	109
4.13 Potential difference vs. time response for quickly dried co-cast PEO-PVC membranes in HCl, then immersed in NaCl solution	110
4.14 Potential difference response vs. log activity of various acids for quickly dried co-cast PEO-PVC membranes	111
4.15 Potential difference response vs. log activity ratio of various salts for 5% quickly dried co-cast 5% and 20% PEO-PVC membranes	112
4.16 Potential difference response of quickly dried co-cast PEO-PVC membranes in mixed salt solutions	113
4.17 Potential difference response for quickly dried co-cast PVC-PMA and PVC-PVMK membranes in HCl	117
4.18 Potential difference response for quickly dried co-cast PVC-PMA and PVC-PVMK membranes in HCl and NaCl solution	118
4.19 Potential difference response for quickly dried co-cast PVC-PMA and PVC-PVMK membranes in mixed HCl and NaCl salt solutions	118
4.20 Potential difference response of slowly dried co-cast PEO-PVC (fluka) membrane in HCl, NaCl and pH solution	121
4.21 Potential difference response of quickly dried co-cast PEO-PVC (fluka) membranes in HCl, NaCl and pH solution	122

	Page
4.22 Potential difference response of slowly dried co-cast PEO-PVC (fluka) membranes in mixed HCl, NaCl salt solution	123
4.23 Potential difference response of quickly dried co-cast PEO-PVC (fluka) membranes in mixed HCl, NaCl solution	123
4.24 Potential response of quickly dried co-cast PEO-carboxylated PVC membrane in HCl solution	125
4.25 Potential difference response of quickly dried co-cast PEO-carboxylated PVC in various salt solution	126
4.26 Potential difference response of rotary evaporated PEO-carboxylated PVC membrane in HCl solution	127
4.27 Potential difference response of rotary evaporated PEO-carboxylated PVC membrane in various salt solution	127
5.1 DSC traces of slowly dried co-cast PEO-PVC membranes	132
5.2 DSC traces of quickly dried co-cast PEO-PVC membranes	132
5.3 Thermogravimetry transition for slowly dried co-cast PEO-PVC membrane	137
5.4 FTIR spectrum of slowly dried co-cast PEO-PVC membranes	140
5.5 FTIR spectrum of quickly dried co-cast PEO-PVC membranes	141
5.6 FTIR spectrum of quickly dried PMA-PVC membranes	142
5.7 FTIR spectrum of cast PVC, PEO and cyclohexanone	143
5.8 Polarised light optical photomicrograph of slowly dried co-cast PEO-PVC membranes	145
5.9 Polarised light optical photomicrograph of quickly dried co-cast PEO-PVC membranes	146

	Page	
5.10	Polarised light optical photomicrograph of quickly dried PMA-PVC membrane	147
5.11	Polarised light optical photomicrograph of quickly dried PVMK-PVC membrane	148
5.12	Solid state nmr spectrum of conditioned quickly dried co-cast 20% PEO-PVC membrane at 213 K	149
5.13	Solid state nmr spectrum of conditioned quickly dried co-cast 20% PEO-PVC membrane at 298 K and pure D ₂ O at 250 K	150
6.1	Potential response of supported aqueous PEO membrane in HCl solution compared to the response of an ideal semipermeable and permselective membrane	156
6.2	Potential difference response of the processed PEO gel membrane compared to the ideal semipermeable and permselective membrane	158
6.3	Expected potential difference response of a membrane composed of non-intersecting channels of permselective channels of conductance	175

TABLE OF TABLES

	Page
1.1 The structure of polymers similar to PEO	23
4.1 The limiting molar conductivity ratios for salts in PEO and water compared to literature values	94
4.2 Concentrations and viscosities of aqueous PEO solutions of various concentrations	94
4.3 The apparent transport number of various salts in supported PEO membranes compared to literature value	100
4.4 Apparent transport numbers of NaCl in slowly dried co-cast PEO-PVC membranes	106
4.5 Apparent transport numbers of HCl in slowly dried co-cast PEO-PVC membranes	106
4.6 Apparent transport numbers of HCl in quickly dried co-cast PEO-PVC membranes	114
4.7 Apparent transport numbers of NaCl in quickly dried co-cast PEO-PVC membranes	114
4.8 Apparent transport numbers of various salts in quickly dried co-cast PEO-PVC membranes	115
4.9 Apparent transport numbers of HCl and NaCl in quickly dried co-cast PVC-PMA membranes	119
4.10 Apparent transport numbers of HCl and NaCl in quickly dried co-cast PVC-PVMK membranes	119
4.11 Apparent transport numbers of HCl and NaCl in slowly dried co-cast PEO-PVC (fluka) membranes	124
4.12 Apparent transport numbers of HCl and NaCl in quickly dried co-cast PEO-PVC (fluka) membranes	124
4.13 Apparent transport numbers of various salts in co-cast and rotary evaporator dried PEO- carboxylated PVC membranes	128
5.1 Thermo-mechanical transitions for slowly dried co-cast and rotary evaporated dried PEO-PVC membranes	136

	Page
5.2 Thermogravimetry transitions for slowly dried co-cast PEO-PVC membranes	137
6.1 Effect of the supported aqueous PEO membrane on the relative ionic mobility of various salts	156
6.2 The membrane to aqueous ionic mobility ratio and viscosity B coefficient of the cation and anion for the supported aqueous PEO and processed PEO membrane	158

TABLE OF ABBREVIATIONS

PEO	Poly(ethylene oxide)
PVC	Poly(vinyl chloride)
PMA	Poly(methacrylate)
PVMK	Poly(vinyl methylketone)
PET	Poly(ethylene terephthalate)
DOP	Diethyl phthalate
IPM	Isopropyl myristate
DOS	Bis-(2-ethylhexyl) sebecate
o-NPOE	o-nitrophenyl octyl ether
DVB	Divinyl benzene
PSSA	Polystyrene sulphonic acid
KTpCIPB	Potassium tetrakis(p-chlorophenyl) borate
NaTPB	Sodium tetraphenyl borate
NapTS	Sodium p-toluene sulphonate
NaDDS	Sodium dodecylsulphate
DSC	Differential scanning calorimetry
TMA	Thermo-mechanical analysis
TG	Thermogravimetry
FTIR	Fourier transform infra-red
SCE	Saturated calomel electrode

TABLE OF SYMBOLS

ROMAN

a_i	Activity of species i
C_i	Concentration of species i
D_i	Diffusional coefficient
E	Experimentally determined potential difference
F	Faraday constant
f_i	Frictional coefficient of species i
G	Gibbs free energy
I	Ionic strength
J	Flux
K	Equilibrium constant
K_{ij}	Potentiometry selectivity constant for species i, j
$K_{\text{ext},i}$	Interfacial extraction coefficient
L	Avogadro number
N_j	Number of permselective channels in the membrane
n_i	Number of moles of species i
Q_i	Charge carried by ion i
r	Position of shear plane of the double layer
S_j	The total relative conductance of channels j
t_i	Transport number of species i
U_i	Mobility of species i
V_i	The partial molar volume of species i
X	The number of binding sites in a permselective membrane
x_A	Debye length/ion atmosphere thickness
z_i	The charge of species i

TABLE OF SYMBOLS

GREEK

α	The degree of dissociation of a weak electrolyte
γ_{\pm}	Mean activity coefficient
ϵ_0	Permittivity of free space
ϵ	Dielectric constant
ζ	streaming potential
η_0	Viscosity of a pure solvent
η	Experimentally determined viscosity
κ	conductivity
Λ_0	Molar conductance at infinite dilution
Λ	Molar conductance
μ_i	Electrochemical potential of species i
ρ	Space charge density
σ	Net surface charge density
σ_j	Conductance of permselective channel j
τ	Exchange times of water molecules
v_i	Particle velocity
Φ_i	Electric potential of species i

ACKNOWLEDGEMENT

This project was sponsored by the DTI, Unilever and ABB Kent Taylor Ltd.

I would like to thank Professor D. E. Williams for his encouragement and guidance. Thanks also to Dr. Roger Hutton for his support, which was very much appreciated.

My thanks are due to a number of people whose expertise was appreciated: Ms. Marianne Odlyha, Dr. A. Aliev, Mr. Dave Knapp and the staff in the mechanical workshop.

I especially would like to thank my family, Terence and my dearest friends Paula, Ruth, Navjot and Yemi, for their patience and encouragement.

CHAPTER 1
INTRODUCTION

CHAPTER 1. INTRODUCTION

The work described in this thesis was carried out as part of a project to explore the use of solid polymer electrolytes as pH electrodes, in order to obtain mechanical properties superior to those of the fragile glass membranes traditionally used.

It was hypothesised that by co-casting composite polymer membranes from hydrophilic and hydrophobic polymers, ion transport properties could be controlled. The hydrophilic polymer would interact with water molecules and ionic species, and the hydrophobic polymer would serve as an inert matrix, intimately tangled with the hydrophilic polymer to prevent its diffusion into the aqueous solution phase. The physical and chemical properties of the membrane could be further controlled by varying the membrane fabrication process, which would effect the micro-structure of the membrane and size of the micro-cavities. These structural changes would in turn alter the ionic transport properties.

This thesis describes the development of the membrane preparation procedure. Firstly, pure poly(ethylene oxide) membranes then processed pure poly(ethylene oxide) membranes. These films were followed by co-cast composite poly(ethylene oxide)-poly(vinyl chloride) membranes and finally, rotary evaporated poly(ethylene oxide)-poly(vinyl chloride) membranes. The effect of the preparation procedure on the potential difference response of these membranes was investigated to correlate any structural changes with the membrane electrochemical behaviour.

Membranes prepared by the various procedures were studied using thermal analysis, FTIR and polarised light optical microscopy to observe any trends in physical characteristics associated with structural changes. The electrical properties of these membranes were correlated with the microscopic and macroscopic membrane structure and chemical composition.

It was shown that subtle changes in the membrane structure indeed influence ionic transport. The transport of ions across the membrane is modelled as a

liquid junction potential where the ions diffuse across the membrane under the influence of the electrochemical potential gradient.

1.1. THE GLASS ELECTRODE

The structure and the mechanism of ions transport in the glass membrane can be used to explain the transport properties in the composite polymer film. The magnitude of the phase boundary potential between the glass membrane and the electrolyte solution, in which the electrode is immersed, is determined by the hydrogen ion and other cation concentrations in solution [1]. The H⁺ selective glass membrane is composed typically of 72.2 mole % SiO₂, 6.4 mole % CaO and 21.4 mole % Na₂O. Hughes [2] showed that the composition of the glass membrane is an important factor in the behaviour of the electrode. Glasses have a three-dimensional network of oxygen and silicon atoms in which there is a residual negative charge. The charge of the macro-ion is balanced by cations which occupy holes in the network and are held in different energy levels by electrostatic forces centred on the neighbouring oxygen atoms [3]. The glass membrane undergoes structural changes when brought into equilibrium with aqueous solution. In solutions of pH between 1 and 9, the glass exhibits a noticeable swelling. This structural change is accompanied by deviation in the potential response due to interferences from cations other than H⁺. At low pH's and in non-aqueous solutions the membrane suffers from dehydration of the swollen surface layer [3].

Horovitz [4] regarded the glass membrane as a solid electrolyte, the potential difference between the glass and the solution phases depending on the concentration of ions in both the phases. The electrode junction is limited to those ions which are able to migrate into the glass phase. The ions are exclusively cations with the hydrogen ion being the most labile. The behaviour at the glass-solution interface of the pH electrode has been described by Dole et al [5] in terms of a semipermeable membrane (Gibbs-Donnan equilibrium)

and the liquid junction potential.

The increase in the error in solutions of low pH was attributed to progressive absorption of acid by the outer swollen layer. The time dependence of the alkaline error can be attributed to a loss of hydrogen ions from the swollen layer when the electrode is immersed into a highly alkaline solution. Thus the optimum condition of operation is obtained when the swollen layer contains a constant hydrogen ion concentration: this is in the pH region of 2 to 9, when the electrode is substantially error free [3].

1.2. POLY(ETHYLENE OXIDE)

1.2.1. GENERAL INTRODUCTION

Poly(ethylene oxide) is a crystalline, water-soluble polymer with the general formula $X-(OCH_2CH_2-)_n Y$. The end groups are known to be hydroxyl groups only in the case of the lower molecular weight polymers which are known as poly(ethylene glycol), with the value of n up to about 150. Higher molecular weight members are known as poly(ethylene oxide) and include all the molecular weights higher than $n \sim 150$, and are commercially available up to $n \approx 2 \times 10^6$. The physical properties of the glycols vary from viscous fluids to wax like solids as n increases. Higher molecular weight polymers are typically crystalline or amorphous solids [6]. The structure of poly(ethylene oxide) is shown in figure 1.1. No side branching is observed: this structure is confirmed by x-ray crystallography [7].

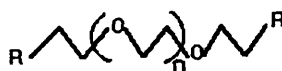


Figure 1.1: The structure of poly(ethylene oxide).

Poly(ethylene oxide)s regardless of weight are soluble in water unlike similar polymers such as poly(methylene oxide), poly(acetaldehyde) and higher molecular weight (greater than 1000) poly(propylene oxide) and poly(trimethylene oxide), which are water insoluble [7]. The structures of these are shown in table 1.1. The water solubility of poly(ethylene oxide) may be due to the regularity of the alternate ethylene units (hydrophobic character) and the oxygens (hydrophilic character) supporting hydrogen bonds between the water molecules and the ether oxygens, resulting in a negative entropy and enthalpy of dilution.

Polymer	Structural unit
Poly(ethylene oxide)	$-(\text{CH}_2-\text{CH}_2-\text{O})_n$
Poly(methylene oxide)	$-(\text{CH}_2-\text{O})_n$
Poly(acetaldehyde)	$-(\text{CH}(\text{CH}_3)-\text{O})_n$
Poly(propylene oxide)	$-(\text{CH}_2-\text{CH}(\text{CH}_3)-\text{O})_n$
Poly(trimethylene oxide)	$-(\text{CH}_2-\text{CH}_2-\text{CH}_2-\text{O})_n$

Table 1.1: The structures of polymers similar to poly(ethylene oxide).

Poly(ethylene oxide) precipitates from solution with increasing temperature due to increasing thermodynamic activity. As the temperature of the aqueous solution is increased to the boiling point of water, poly(ethylene oxide) is precipitated. The precipitation temperature depends on the polymer concentration and molecular weight. In dilute solutions (0.2 weight %), the precipitation is observed as a cloud point, and for more concentrated solutions (0.5 weight % or more) the polymer precipitates as a gel which shrinks and retains the shape of the container.

When poly(ethylene oxide) of molecular weight greater than 10^6 is dissolved in water at concentrations greater than ~0.5 weight %, a characteristic structure in the solutions is observed. Studies on these solution show a pseudoplastic behaviour [6]. Bailey et al have shown that a concentration of 1 weight % poly(ethylene oxide) has a 10% increase in viscosity from water and a 3 weight % solution has a 40% change in viscosity from that of water [7]. Aqueous solutions containing more than 5 weight % polymer are elastic gels. The activity of neutral molecules can also be increased by the addition of salts [8]. It appears that the limiting solubility decreases with concentration and the effectiveness of the salts is determined by the nature of the anion. The salting out effects are reflected in a collapsing of the polymer coil in solution. This collapse is a result of the gradual decrease of the hydrodynamic volume as the salt content increases [9].

These unique properties enable poly(ethylene oxide) to be used in a wide range of commercial applications: low molecular weight polymers are formulated as tablet coatings and viscous solutions suitable for lubricants in the pharmaceutical industry. High molecular weight poly(ethylene oxide) (M_w = several million or more) are used as a flocculant for finely dispersed solids in water, as an adhesive when combined with products such as lignin sulphonic acids and as a binder in the tobacco industry [7].

1.2.2. ANHYDROUS POLY(ETHYLENE OXIDE)

The interactions between anhydrous PEO and alkali metal salt in, for example, solid state batteries, can be used to understand the mechanism of ion transport in composite PEO membranes. Armand et al [10] studied the behaviour of poly(ethylene oxide) with LiClO_4 . The ion-conducting polymer was considered as a solid solution of alkali metal salt in the polymer. The salts were able to dissociate into free ions under the coordinating effect of the ether group in the

neighbouring polymer segments. The location of ions may change due to the rearrangement of polymer segments. It was proposed that, for high conductivity, the coordinating polymer should have the following physical properties: high dielectric constant to ensure efficient salt dissociation (dipole moment of poly(ethylene oxide) is 1.13); low glass transition temperature for polymer chain flexibility (so that the polymer segmental motion occurs easily); and low crystallinity to lower the barrier for ion movement (glass transition temperature of polyethylene oxide is $-53\text{ }^{\circ}\text{C}$) [11].

Amorphous poly(ethylene oxide)- LiClO_4 gels have been made with the EO/Li ratio at 20. The conductivity of the poly(ethylene glycols) ($M_w = 2000$) was found to be $5 \times 10^{-6}\text{ S cm}^{-1}$ at $25\text{ }^{\circ}\text{C}$ and the conductivity of poly(ethylene glycol) ($M_w = 5700$) was $1 \times 10^{-3}\text{ S cm}^{-1}$ at $90\text{ }^{\circ}\text{C}$ when the polymer electrolyte was completely amorphous [12].

1.2.3. SOLUTION PROPERTIES OF POLY(ETHYLENE OXIDE)

As well as water, poly(ethylene oxide) is soluble in a number of organic solvents such as acetonitrile, chloroform and ethylene dichloride. It is insoluble in aliphatic hydrocarbons such as diethylene glycol, ethylene glycol and glycerine, an effect of molecular weight. The polymer shows an inverse solubility-temperature relationship.

1.2.4. ASSOCIATION COMPLEXES OF POLY(ETHYLENE OXIDE)

A solution of 3% poly(ethylene oxide) in benzene forms complexes with urea or thiourea. If the complexation takes place in a thin walled capillary, the progress of the complexation can be observed microscopically. The particles change when the fibrils of the complex grow from the crystal plane edges. The

stoichiometry of the complex is two to three moles of urea to every oxyethylene unit [13].

The structure of water in association complexes of poly(ethylene oxide) have been studied [14] using a model based on a "broken down" ice structure with the existence of extensive hydrogen bonded regions. Nemethy et al [15] developed this model further to include energies from water interactions as shown in figure 1.2. This model shows the entropy gain from disruption of the water structure.

Formation of association complexes of poly(ethylene oxide) in water solutions occurs at the expense of the water molecules associated with the polymer and the disruption of the water structure provides an added entropic driving force favouring complex formation.

An aqueous solution of poly(ethylene oxide) forms an inter-molecular complex when mixed with an aqueous solution of poly(acrylic acid) in equal proportions. The precipitate can be recovered by filtration, dried and pressed into a water insoluble film [7]. Association complexes are also formed with poly(methacrylic acid) resulting in a stoichiometry of three ethylene oxide units per methacrylic acid unit.

1.2.5. IONIC COMPLEXES

Complex formation between poly(ethylene glycol) and metal cations occur when the electron deficient metal cation coordinates with the oxygen atoms, after which the metal is rendered hydrophobic. Selectivity is exhibited by poly(ethylene glycol) since the polymer can adopt a helical conformation with cavities of preferred sizes [6]. This property is utilised in phase transfer catalysis. The transfer of the metal cation in KMnO_4 from a solid phase to benzene, for example, is accompanied by the anion across the phases to

maintain electrical neutrality.

Salts have limited interactions with aqueous poly(ethylene oxide) solutions other than a small salting out effect observed with potassium iodide. When the potassium iodide is milled into poly(ethylene oxide) at room temperature, an amorphous and elastic substance is achieved at high salt concentrations [9]. Aqueous solutions of poly(ethylene oxide) of molecular weight $\sim 1 \times 10^6$ have been found to form complexes with aqueous solutions of mercuric chloride and cadmium chloride with a stoichiometry of: $[(-\text{CH}_2-\text{CH}_2-\text{O})_4 \text{HgCl}_2]_x$.

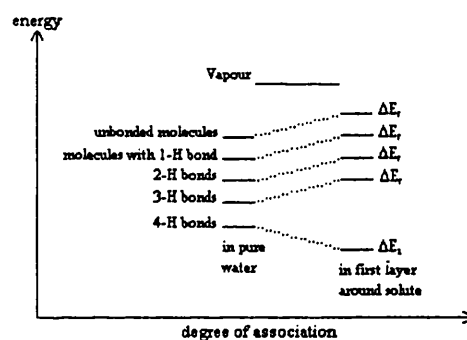


Figure 1.2: A model proposed by Nemethy and Scheraga for the structure of water encasing a non-polar solute [15].

1.3. POLY(VINYL CHLORIDE) MEMBRANES

Poly(vinyl chloride) has been widely used in the construction of membranes in the development of ion-selective sensors. The structure of poly(vinyl chloride) is shown in figure 1.3 [16].

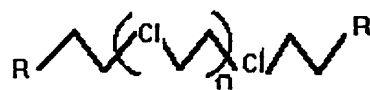


Figure 1.3: The structure of poly(vinyl chloride).

Pure poly(vinyl chloride) membranes have a very high resistance and form glassy, impermeable and inflexible membranes (the glass transition temperature of PVC, molecular weight 1×10^6 , is $82 \text{ }^\circ\text{C}$) [17]. Incorporation of plasticisers and ionophores endow the membrane with flexibility and conductivity respectively, for use as an ion selective membrane [18]. The role of the poly(vinyl chloride) serves to be a membrane matrix which holds the components of the membrane together, hence PVC is used in this work as an inert matrix.

Poly(vinyl chloride) membranes have been prepared by casting from solutions with plasticiser dioctyl phthalate (DOP) in tetrahydrofuran. Membranes formed by the petri dish casting method were transparent, colourless, possessed slight elasticity and retained their structural integrity provided they were carefully handled. The cast membrane was then cut out to cover the area of the probe to form a sensor. Alternatively the poly(vinyl chloride) membrane could be cast directly onto dialysis membranes or onto "dipstick" devices by pipetting a small amount of the dissolved polymer and plasticiser on the sensor area. Other methods include the use of spin casting [19].

Changes in the preparation procedure have been found to affect the potentiometric properties of the resulting membrane. Christie et al [19] found that slow solvent evaporation in cast membranes resulted in the full incorporation of the plasticiser isopropyl myrisate (IPM) whilst quick

evaporation of THF resulted in some of the IPM remaining in liquid form on the membrane surface. The incorporation of dioctyl phthalate into the poly(vinyl chloride) membrane was not affected by the casting method. The quickly cast membranes were found to be less responsive to the electroactive species by 25% [19].

Plasticisers incorporated into poly(vinyl chloride) membranes include dioctyl adipate [20], bis(1-butylpentyl) adipate (DNA), bis(2-ethylhexyl) sebacate (DOS) and *o*-nitrophenyl octyl ether (*o*-NPOE) [21] to give the membrane strength and flexibility in handling. Common ionophores reported to have been used are: valinomycin, potassium tetrakis(*p*-chlorophenyl) borate (KTPCIPB), sodium tetraphenylborate (NaTPB) and functional groups attached to the poly(vinyl chloride) backbone such as carboxylated PVC [22]. These ionophores are anionic in nature and confer cationic selectivity when incorporated into the membrane. Valinomycin selectively transports the K^+ ion across the membrane by forming the complex $Kval^+$.

Poly(vinyl chloride) membranes made with plasticisers and ionophores show a high permselectivity for cations Mg^{2+} and Ca^{2+} , both having a selectivity coefficient of ~ -5 [23]. Membranes which have been made by incorporation of ionophores may suffer from: interferences from ions which compete to bind with the active site, a decrease in selectivity due to loss of the ionophore through diffusion into the test solution and failure of the ionophore to dissociate resulting in lower active site concentrations [24].

To conclude, there needs to be developed a membrane system that does not suffer from the leaching out problems normally associated with conventional poly(vinyl chloride) membranes, as well as retaining the ionic selectivity and minimising interferences from ions not intended to be measured.

1.4. ION SELECTIVE ELECTRODES

1.4.1. ION SELECTIVE MEMBRANES

In the past thirty years, many types of ion-selective membranes have been developed. Incorporating these membranes into electrode devices enables the recognition of the desired ion in a sample solution of mixed ions. Ion-selective membranes are typically composed of: a zeolite, clay, collodion or synthetic resin. Membranes can be composed of a single phase or a multilayer [25].

Wyllie et al [26] developed clay type membranes incorporated into a plastic matrix. Examples of these membranes are synthetic faujasite and synthetic sodium analcite embedded in polystyrene, polythene or polymerised methyl methacrylate [27]. These membranes are prepared by mixing finely ground zeolite with a powdered thermoplastic and pressure moulding them into discs. These zeolite membranes are cation-selective to Na^+ ions [26].

There are many studies of membranes based on collodion [28,29]. These membranes have been prepared by casting two successive films of collodion cotton from a 4% solution of 1:1 ether-alcohol solution in a test tube. After solvent evaporation, the film was coagulated in water, oxidised to produce carboxylic groups and immersed in *N* sodium hydroxide solution to produce the salt complex and dried (irreversibly) to the desired thickness and porosity. These membranes became anion-selective after soaking in 2% protamine sulphate solution at pH 10.5 for several days. The collodion membranes are easily hydrolysed in acid solutions and are not responsive to alkaline earth ions, which combine chemically with the carboxylate groups. Neihof [30] developed collodion membranes with the carboxylic groups replaced by sulphonic acid groups. This was achieved by dissolving polystyrene sulphonic acid in the initial casting solution or by soaking the cast membrane in aqueous sodium polysulphonate solution. The ion-selectivity response of collodion

membranes is usually stable for several days but they are susceptible to deterioration.

Ion-selective membranes based on synthetic resins are widely studied [31,32]. Examples of such synthetic resin range from: cross-linked polymethacrylic acid, sulphonated phenol-formaldehyde, sulphonated polystyrene and poly(vinyl chloride) incorporated with ionophores. The membranes may be prepared by mixing a solution such as methacrylic acid with a cross linking agent and containing it between two glass plates. Other membranes may be prepared by casting from a monomer. Anion selective membranes can be prepared, for example, by polymerisation of ethyleneimine cross linked with epichlorohydrin.

Ion-selectivity is conferred to these membranes by incorporating ion exchange materials. This can be done by the graft polymer technique which involves chemically bonding two polymers by irradiation. Alternatively the ion exchange material, such as sulphonated or aminated polystyrene, can be mixed thoroughly with a plastic binder and moulded by application of pressure into a flexible sheet. These membranes were less porous and permeable than the parent polystyrene resin material, showing a closer approach to the ideal membrane electrode. The pressure moulded membranes were easily handled, clamped and mounted as a membrane electrode.

Multilayered membranes involve building parallel layers of insoluble salt such as calcium stearate between two electrolyte solutions. The transport of the potential determining calcium ions is in the direction at right angles to the axis of orientation of the molecules in the monolayers [33]. These membranes had a high resistance ($\approx 50 \text{ M}\Omega$) and a high impedance voltameter was required to measure the membrane potentials.

1.4.2. DEVELOPMENT OF SPECIFIC MEMBRANE ELECTRODES

One limitation of membrane electrodes is their lack of specificity towards ionic species of same charge [34]. In solutions containing more than one electrolyte, the membrane potential responds to the total cationic or anionic concentration. The exception to this behaviour is when one of the diffusible ions has unusual properties such as high mobility (in the case of the glass electrode which is sensitive to H^+ and Na^+ ions), or large size (such as a macro-ion). In this situation, some distinction can be made between the contribution of the target ion to the total membrane potential and the contribution from the other ions. There are two types of specificity which are possible: physical and chemical.

The sizes of ions may be distinguished by the membrane if the membrane pores are small and inelastic rather like a molecular sieve, as in the case of zeolite materials. Montmorillonite membranes are insensitive to divalent ions and could be used to distinguish alkali ions in the presence of calcium and barium ions. This ion-sieve effect has been shown by Barrer et al [35]. They showed that synthetic analcite will selectively transport sodium and potassium ions but exclude cesium ions. Chemical specificity can be attained by incorporating a species which reacts specifically by complex formation with the ion which is to be detected. Examples of this type of membrane are: dipicrylamine (which show a selectivity of potassium over sodium ions) and calcium oxalate suspended in paraffin wax (sensitive to calcium ions over potassium ions) [36].

REFERENCES FOR CHAPTER 1

- [1] G. A., Perly, *Anal. Chem.*, **21**, 559, (1949).
- [2] W. S., Hughes, *J. Am. Chem. Soc.*, **44**, 2860, (1922).
- [3] D. J. G., Ives, G. J., Janz, "Reference Electrodes, Theory and Practice", ch. 5, Plenum Press, New York, 1961.
- [4] K. Z., Horovitz, *Physik*, **15**, 369, (1923).
- [5] M., Dole, *J. Am. Chem. Soc.*, **53**, 4260, (1931).
- [6] J. M., Harris (ed), "Poly(ethylene glycol) Chemistry", ch. 1, Plenum Press, New York, 1992.
- [7] F. E., Bailey, J. V., Koleske, "Poly(ethylene oxide)", ch. 1, Academic Press, London, 1976.
- [8] F. E., Bailey, R. W., Callard, *J. Appl. Polym. Sci.*, **1**, 272, (1959).
- [9] F. E., Bailey, J. V., Koleske, "Poly(ethylene oxide)", ch. 5, Academic Press, London, 1976.
- [10] M. B., Armand, J. M., Chabagno, M., Duclot, *Second International Meeting on Solid Electrolytes*, St. Andrews, Scotland, 20-22, Sept. 1978.
- [11] J., McBreen, Y. O., Kamoto, H. S., Lee, T. A., Skotheim, Q., Yang, Z. S., Yu, *J. Electrochem. Soc.*, **141**, 4, (1994).
- [12] J. C., Salamore, J. S., Riffle, "Contemporary Topics in Polymer Science", vol. 7, p. 237, Plenum Press, New York.
- [13] F. E., Bailey, J. V., Koleske, "Poly(ethylene oxide)", ch. 6, Academic Press, London, 1976.
- [14] J. D., Bernal, R. H., Fowler, *J. Chem. Phys.*, **1**, 515, (1933).
- [15] G., Nemethy, H. A., Scheraga, *J. Chem. Phys.*, **36**, 3382, (1962).
- [16] C. E. H., Bawn, "Chemistry of High Polymers", ch. 1, Butterworths Scientific Press, London, 1948.
- [17] L. A., Wood, *J. Polym. Sci.*, **28**, 319, (1958).
- [18] H. L., Wu, R. Q., Yu, *Talanta*, **34**, 6, 577, (1987).
- [19] I. M., Christie, P. H., Treolar, P. Vadgama, *Anal. Chim. Acta*, **269**, 65, (1992).

- [20] X., Li, D. J., Harrison, *Anal. Chem.*, **63**, 2168, (1991).
- [21] M. L., Inglehart, R. P., Buck, E., Pungor, *Anal. Chem.*, **60**, 290, (1988).
- [22] B., Fu, E., Bakker, V., Yang, J. H., Yun, M. E., Mayerhoff, *Anal. Chem.*, **66**, 2250, (1994).
- [23] E., Lindler, E., Graf. Z., Neigreisz, K., Toth, E., Pungor, R. P., Buck, *Anal. Chem.*, **60**, 295, (1988).
- [24] R. P., Buck, J. H., Boles, R. D., Porter, J. A., Margolis, *Anal. Chem.*, **46**, 2, 255, (1974).
- [25] N., Lakshminarayanaiah, "Transport Phenomena in Membranes", ch. 2, Academic Press, New York, 1969.
- [26] M. R. J., Wyllie, H. W., Patnode, *J. Phys. Chem.*, **54**, 204, (1950).
- [27] R. M., Barrer, S. D., James, *J. Phys. Chem.*, **64**, 417, 421, (1960).
- [28] K., Sollner, I., Abrams, C. W. Carr, *J. Gen. Physiol.*, **24**, (1941).
- [29] K., Sollner, J., Anderson, *J. Gen. Physiol.*, **27**, (1943).
- [30] R., Neihoff, *J. Phys. Chem.*, **58**, 916, (1954).
- [31] G. J., Hills, J. A., Kitchener, P. J., Ovenden, *T. Faraday Soc.*, **51**, 719, (1955).
- [32] T. R. E., Kressman, *J. Appl. Chem.*, **4**, 123, (1954).
- [33] H. P., Gregor, H., Schonhorn, *J. Am. Chem. Soc.*, **79**, 1507, (1957).
- [34] K., Sollner, *J. Phys. Chem.*, **49**, 47, (1945).
- [35] R. M., Barrer, D. C., Sammon, *J. Chem. Soc.*, 675, (1956).
- [36] D. J. G., Ives, G. J., Janz, "Reference Electrodes, Theory and Practice", ch. 9, Plenum Press, New York, 1961.

CHAPTER 2
THEORY

CHAPTER 2. THEORY

This chapter outlines the structure of water and polymers in salt solutions. The properties of the membrane-electrolyte interface and models of ion transport across membranes are also described.

2.1. ION-WATER INTERACTIONS

This thesis advances the view that a central element of the permselectivity shown by non-ionic composite membranes is the effect of the hydrophilic polymer on the solvation of aqueous ions. Therefore this chapter considers the interactions of salt solutions, polymers and water. This analysis gives an insight into the expected behaviour of aqueous PEO solution containing salts, and the hydration of membrane. The hypothesis is that the interaction of water, solute and polymer provides a mechanistic framework for the understanding of the potentiometric results.

2.1.1. INTERACTIONS OF IONS WITH WATER-EFFECTS ON LOCAL WATER STRUCTURE

Studies on the spatial arrangement of water molecules in pure water revealed ordered groups of tetrahedrally arranged hydrogen bonded water molecules [1]. Results from x-ray scattering show that at room temperature, the average number of closest neighbours for each water molecules is 4.5. The size and position of these ordered groups is constantly fluctuating in the timescale of 10^{-10} seconds, between ordered and disordered domains of water molecules.

The structure of liquid water is modified when ions are dissolved. This is evident from measurements such as viscosity and ion mobility.

The organisation of water molecules about a dissolved ionic species is usually considered as composed of five structurally different regions. First, the water molecules adjacent to the ions are strongly orientated and usually have lost all rotational energy. Further away, molecules are appreciably affected by the ionic electric field and partially orientated. At even greater distances from the central ion, the water molecules are least affected by the field of the ion, but the water structure can still be distinguished into 2 further regions. At remote distances from the ion, the water structure is unchanged from the unassociated state of tetrahedrally structured molecules. In the region closer to the ion, the water structure is partly orientated.

The way in which ions change the structure of water can be shown if a neutral molecule of similar size replaces a water molecule. For an uncharged species there is negligible effect on the local water structure. The absence of nearby dipole forces from the neighbouring water molecules prevent the perturbation of the tetrahedral structure of water. However, as the charge on the ion is increased, the orienting tendency of the charged particle, at some point, will neutralise the forces from the water dipoles. Thus, for a charged species, the water structure is altered and the favourable tetrahedral structure is lost.

Samoilov [2] observed this effect through self diffusion experiments. The average time that a water molecule spends in the close vicinity of an ion, compared to the exchange times for molecules in pure water, was calculated. This ratio (τ/τ_0) can either be greater than or less than 1. Values greater than 1 imply a binding of the ion and water and values less than 1 imply a loosening of the water structure by the ion. Typical values are $\text{Li}^+ = 3.48$, $\text{Na}^+ = 1.46$, $\text{K}^+ = 0.65$, $\text{Cs}^+ = 0.57$, $\text{Cl}^- = 0.63$, $\text{I}^- = 0.58$. The critical radius is when τ/τ_0 value passes through 1. The time ratio values for the alkali metal ions pass through unity and can be related to the crystal radii and the ionic surface charge density [3]. Thus the order-disorder behaviour of ions seems to be a

simple function of ionic radius and charge and is the case in simple solutions that are not concentrated.

2.1.2. EFFECT OF IONIC CONCENTRATION ON SOLUTION VISCOSITY AND CONDUCTANCE

Ionic interactions can be examined by considering viscosity and conductance changes. Generally, the viscosity of dilute electrolyte solutions up to the concentration of 0.1 mol dm^{-3} obeys the equation [3]:

$$\eta/\eta_0 = 1 + AC^{1/2} + BC \quad (2.1)$$

where η_0 is the viscosity of the pure solvent, η the viscosity of the solution, C is the concentration and A and B are constants. The $AC^{1/2}$ term is due to interionic forces and is always positive as interionic attraction increases viscosity. The B coefficient may be either positive or negative in aqueous solution and has been interpreted as the effect of an ion on the solvent. The B coefficient has a positive temperature coefficient, so an increase in temperature would increase the viscosity of the solution. The value of the B coefficient is approximately additive [1], examples of ions with a negative B coefficient are NO_3^- , ClO_3^- and Cs^+ : these ions have a low temperature coefficient of mobility indicating a decrease in water structure about the ion.

The conductivity κ of dilute electrolyte solutions is dependent on the ion concentration, C_i , and mobility, U_i , in the following way:

$$\kappa = \sum_i F |z_i| U_i C_i \quad (2.2)$$

Interionic forces may also influence ion mobility through the electrophoretic effect which arises from the interaction of opposing ion movement in an electric field.

Onsager developed equations to incorporate the electrophoretic effect at high dilution [1]. Thus the Onsager limiting law is given as:

$$\Lambda = \Lambda^0 - (B_1 \Lambda^0 + B_2) \sqrt{C} \quad (2.3)$$

where B_1 and B_2 are constants which take into account the effect of interionic forces at higher concentrations up to 0.1 mol dm^{-3} . The Onsager equation is modified for weak univalent electrolytes, to the form:

$$\Lambda = \alpha [\Lambda^0 - (B_1 \Lambda^0 + B_2) \sqrt{\alpha C}] \quad (2.4)$$

where α is the degree of dissociation of the weak electrolyte. Thus the conductivity depends linearly on the square root of the electrolyte concentration, but for weak electrolytes the conductivity behaviour differs to include the degree of dissociation α .

The characterisation of the salt solution viscosity and conductivity given here are used to help explain the results observed with the behaviour of aqueous PEO solutions containing salts.

2.1.3. INTERACTION OF NON-IONIC SPECIES WITH WATER

Polar organic molecules interact strongly with water, the extent of which depends on: the number of hydrogen bonds in relation to the size of the non polar residue, the number of internal degrees of freedom of the solute and the hydrocarbon chain and the relative positions of the polar groups [3]. A common feature of such solutions is the pronounced concentration dependence of physical properties, particularly in dilute solutions. For example, this effect is partially responsible for the formation of clathrate hydrates.

The behaviour of mono-functional polar solutes in water is governed by the association of the alkyl-group, polar group and water molecules. For example, ethanol-water mixtures form ordered structures [3].

¹H NMR studies of acetone-water and tetrahydrofuran-water mixtures, show increasing the solute concentration results in a general slowing down of the diffusional motions of the water molecules. The main features of monofunctional solute-water mixtures summarised: dilute solutions resemble hydrocarbons rather than polyfunctional polar compounds. The solute has a pronounced effect on the surrounding water molecules, reducing rotational and diffusion motion. These effects reach a well defined maximum at a given solute concentration. More concentrated solutions behave like mixtures of non-aqueous polar molecules.

The polyfunctional solutes show specific interactions between polar groups and water and thermodynamic properties are sensitive to minor stereochemical differences. The variation of observed physical characteristics with concentration are minimal [3]. No evidence of solute clustering is observed, but strong short range interactions usually exist [4].

For example, ^1H NMR and dielectric investigations of glucose in water reveal that water molecules interact specifically with hydroxyl sites [3]. Water molecules are exchanged between the bound and unbound water at the hydroxyl sites. Similar structure promoting behaviour is exhibited by other sugars such as galactose and manose.

2.1.4. COMPLEX MIXTURES

It is evident that the chemical potential of any species in solution is changed as a consequence of the introduction of any other species. In aqueous solution, the interaction between ionic and non-ionic species is demonstrated by the phenomena of "salting in" and "salting out".

Salting-out is the result of the addition of an electrolyte to an aqueous solution of a non-electrolyte, resulting in the transfer of a part of the free water to the hydration sheath of the ion, thus decreasing the amount of "free solvent". This effect in turn results in the lowering of the solubility of the electrolyte [5, 6, 7]. For example, proteins can be salted out of solution. The first is the association of electrostatic forces between the two species without direct combination. The second type involves actual ion-protein combination.

Solubility studies on β -lactoglobulin showed a one hundred fold decrease with NaCl concentration increasing from 0 to 0.01 mol dm^{-3} , and a ten fold decrease for glycine solubility when the NaCl concentration change was from 0 to $\sim 0.4 \text{ mol dm}^{-3}$ [6].

2.1.5. INTERACTION OF PEO AND WATER

Poly(ethylene oxide) molecules in water are strongly hydrated. Evidence for this is that, in aqueous solution, the polymer occupies a larger volume than

macromolecules of similar molecular weight such as proteins [8, 9, 10, 11]. Differential scanning calorimetry studies indicate 2 water molecules bond per polymer repeat unit [12, 13] (with molecular weights less than 100). For higher molecular weights, 2-3 water molecules are associated with each repeat unit [14]. This rises to 3 water molecules for molecular weights greater than 600 due to the formation of a trihydrate structure around each ether unit. The proposed trihydrate structure is helical, a configuration which is possible when the number of ether groups in the chain is sufficient to form at least 2 coils of helix [15].

Kjellander [16, 17] suggests that a minimum of 2 and often 3 hydrogen bonded water molecules are needed to hydrate each ether unit of PEO. This PEO-water interaction effectively excludes other molecules such as proteins but not ions [18].

Solid PEO swells in water, the magnitude of which is an indicator of the strength of interaction. Swelling decreases with increasing temperature. Calorimetric studies showed initial swelling of the partially crystalline dry PEO to be endothermic, followed by absorption of approximately 30% in weight of water into the polymer, the swelling process becoming exothermic [9, 10].

2.1.6. INTERACTION OF PEO WITH IONS IN AQUEOUS SOLUTION

The swelling of PEO in aqueous solution is often modified by the presence of dissolved salts which may compete with the polymer for water of hydration [19]. The effect of added salts is not straightforward, some salts diminish swelling due to osmotic competition [20] whereas with other salts (e.g. LiCl, urea) swelling increases.

2.1.7. STRUCTURE OF WATER IN POLYMER MEMBRANES

Water and ions in a membrane should not be considered merely as a structureless dielectric [21]. For example, sulphonate membranes are more selective to the alkali metal ions in the order of $\text{Li} < \text{Na} < \text{K}$, whereas the carboxylate resin membranes have the opposite affinity [22]. One explanation for this phenomenon is the "localised hydrolysis" theory [23] in which OH^- and CH_3COO^- can accept a proton from an oriented or polarised water molecule in the hydration shell of an ion, X^+ , thereby forming a temporary bond. Thus for the smaller the ion (eg. Li^+), the stronger electrical field results in a stronger bond. Such bonding effects are similar to the "structure making" or "structure breaking" ability of an ion.

The interaction of water and the polymer is important in the understanding of ion transport. Pepper and Greggor [24], Held and Bellin [25] studied the water sorption in sulphonated cross linked polystyrene resins. The water content of certain resins have been determined for hydrophilic, swelling gels and hydrophobic polymers [24]. The $-\text{SO}_3$ group of the cross-linked polystyrene sulphonic acid resin showed, through differential scanning calorimetry measurements, an initial sorption of 1 mole of water attached to the functional group of the polymer at relative humidities (p/p_0) less than 0.2. This water was found to be strongly bound. At relative humidities, between about 0.2 and 0.8, the second, third and fourth molecules of water were taken up. These water molecules are thought to cluster around the hydrophilic groups of the polymer causing the membrane to swell. At relative humidities greater than 0.8, water molecules enter as "normal" unbound water molecules, separating the membrane polymer chains. At high relative humidities, the uptake of water causes the polymer chains to extend which result in tension developing in the polymer network which opposed further expansion and established an equilibrium volume. Some studies [25] on resins made from polystyrene

sulphonic acids and stretched nylon, reveal that at low relative humidities, between 0 and 0.1, the dry material is hydrophobic due to strong association of the hydrocarbon chains.

Thermodynamic investigations [26] found the free energies of hydration, heats and entropy values of some polystyrene sulphonic acid resins to be negative. The sorption of water is a spontaneous, exothermic process in which most of the water molecules are presumed immobilised about the ionic groups.

Dissociated functional groups facilitate the sorption of water (undissociated H-resins absorb 0.08 mol whilst dissociated resin absorbs 0.22 mol of water per gram of dry resin) [25]. The amount of swelling is minimal at cross linkages of 0.2 to 8 % below relative humidities of 0.8 [26, 27]. Exceptionally low swelling can be attributed to ion-polymer interaction. This is demonstrated in the trimethylphenylamine (Me_3PhN^+) form of the polystyrene sulphonic acid (PSSA) resin, a strong interaction between the phenyl groups of the cation and the resin could account for lowered swelling between these species [27].

Thus, the swelling of the membrane and the binding of water molecules to the membranes depends on the following factors:

- (1) the functional group,
- (2) the amount of cross-linking,
- (3) the ion-ion-interaction and the ion-polymer interaction,
- (4) Rigidity of the polymer backbone.

Thus, consideration of water and the membrane interactions is important when attempting to interpret membrane behaviour.

2.2. DEVELOPMENT OF MEMBRANE POTENTIAL

Porous membranes can be classified into three main types [28]: permselective membranes, through which only one ion permeates; semipermeable

membranes, where all but one ion does not travel through and permeable membranes, where all ions pass through the membrane but travel with different mobilities. The potentiometric behaviour of each type of membrane is described below.

2.2.1. THE PERMEABLE MEMBRANE

In this model [28] the membrane is permeable to all ions but each have different mobilities. In the absence of an electric field ion movement can be modelled using Ficks law of diffusion [29]. Alternatively, assumptions can be made which result in the generalised Nernst-Plank and Henderson equations when ion movement occurs under an electrochemical potential. Descriptions of both these approaches are given below:

For systems not at equilibrium [28], the potential difference is usually diffusion controlled. The general driving force for ions in membranes is the gradient of the electrochemical potential. When the osmotic pressure is considered, it is given as:

$$\mu_i = \mu_i^0 + RT \ln a_i + pV_i + Z_i F \Phi \quad (2.5)$$

where μ_i is the electrochemical potential for the species i , p is the pressure exerted on the system, V_i is the partial molar volume of the species i and Φ is the electric potential.

The rate at which ions move, the flux, for each species of charge z_i is a product of concentration and velocity, therefore at constant temperature,

$$J_i = C_i v_i = C_i U_i \frac{d\mu_i}{dx} \quad (2.6)$$

where U_i is the mobility of ion i , C_i is the local concentration, v_i is the particle velocity which is controlled by the chemical and electrical gradient through the distance dx . When an electrochemical potential gradient is introduced, Ficks Law is no longer valid and the velocity is described by the Nernst-Plank equation:

$$v_i = -\frac{1}{f_i} \frac{kT d \ln(a_i)}{dx} + \frac{z_i e d\Phi}{dx} \quad (2.7)$$

Where f_i denotes a frictional coefficient arising due to the movement of ions through the solution. This equation gives the flux in terms of the diffusional concentration and electromigration factors. If the electric potential is uniform and the activity is non-uniform, the Nernst-Plank equation reduces to:

$$J_i = -\frac{C_i U_i}{L} \frac{RT d \ln(a_i)}{dx} \quad (2.8)$$

where L denotes Avogadro's number. Substituting for the activity $a_i = C_i \gamma_i$, equation 2.8 becomes,

$$J_i = -\frac{C_i U_i RT}{a_i L} \left[\frac{\gamma_i d \ln(C_i)}{dx} + \frac{C_i d \ln(\gamma_i)}{dx} \frac{dC_i}{dx} \right] \quad (2.9)$$

If the activity coefficient is independent of concentration (i.e. for an ideal solution, a homogeneous excess of another electrolyte or low concentration), the flux reduces to,

$$J_i = -\frac{U_i RT}{L} \frac{dC_i}{dx} \quad (2.10)$$

Which gives Ficks first law of diffusion, with the diffusional coefficient, D_i :

$$D_i = \frac{RTU_i}{L} \quad (2.11)$$

The solution may be generalised from consideration of forms of variation of γ with C . To calculate the potential, the Nernst-Planck equation must be combined with Poisson's equation relating the local potential and charge density (in one dimension),

$$\frac{d^2 \Phi}{dx^2} = \frac{-\rho}{\epsilon} \quad (2.12)$$

The relationship between local charge density and ionic concentration is,

$$\rho = \sum_i C_i z_i e \quad (2.13)$$

The requirement for overall electroneutrality of the system is that, integrated over some volume, ρ is zero.

The interface between a porous membrane and electrolyte solutions may alternatively be described by a liquid junction potential [29, 30]. This potential develops across the test membrane when it separates two electrolyte solutions (phase α , β) such as in a concentration cell. The membrane serves to slow down diffusion as the system is not at equilibrium and the electrolytes will eventually mix. The liquid junction potential arises due to diffusion between the two phases. If one electrolyte is present and the phases differ only in concentration (i.e. $C^\alpha > C^\beta$) and diffusion will take place from phase α to β . The diffusion coefficient of anions and cations may differ, for example, when the cations move faster than the anions. This will give rise to an electrical potential difference which will eventually retard the unequal diffusion of the ions. The potential difference between the two phases may be derived by solution of the Nernst-Planck and Poisson equation.

The change in electrochemical potential when the ions move through the electrical potential difference $d\Phi$ across distance dx is

$$d\mu_i = RT \ln(a_i) + Fz_i d\Phi \quad (2.14)$$

Since the Gibbs free energy change of a reversible process is zero, the total change in free energy for the transport across the membrane of charge

$\delta Q = \sum_i z_i \delta n_i$ is,

$$\delta G = \sum d\mu_i \delta n_i = 0$$

The fraction of charge carried by each ion is termed the transference number t_i ,

$$t_i = z_i F \frac{\delta n_i}{\delta Q} \quad (2.15)$$

where F is Faradays constant. Thus,

$$\delta G = \left[\frac{RT}{F} \sum \frac{t_i}{z_i} d \ln(a_i) + \sum t_i d\Phi \right] \delta Q = 0 \quad (2.16)$$

δG is equal to zero since it is assumed that the charge transport through the phase boundary is reversible. The bracketed term must be zero and independent of δQ .

The bracketed term can be rearranged so obtain the electric potential change,

$$d\Phi = -\frac{RT}{F} \sum \frac{t_i}{z_i} d\ln(a_i) \quad (2.17)$$

When integrated over the phase boundary (α and β), the following expression is obtained,

$$\Delta\Phi = -\frac{RT}{F} \int_{\alpha}^{\beta} \sum_i \frac{t_i}{z_i} d\ln(a_i) \quad (2.18)$$

The link between this treatment and that starting from the Nernst-Planck equation is that the latter method develops explicitly the variation of transport number and activity with position within the membrane, usually based on some model of the membrane. Some cases are treated later.

In a simplified situation where there is only one binary electrolyte species present, differing only in concentration across the membrane, the liquid junction potential difference can be derived if the transference numbers (defined in equation 2.15) are assumed to be invariant with position.

The mean activity coefficient of the binary electrolyte $A_M B_N$ is defined as,

$$\gamma_{\pm} = (\gamma_A^{z_1} \gamma_B^{z_2})^{\frac{1}{(z_1+z_2)}} \quad (2.19)$$

The activity of ions are given as $a_A = \gamma_{\pm} C_A$, $a_B = \gamma_{\pm} C_B$ and the activity of the salt is $a_{\text{salt}} = \gamma_{\pm} C$.

The concentration of ions are given as $C_A = (z_1/z_1 + z_2)C$ and $C_B = (z_2/z_1 + z_2)C$, hence the activity of the ions may be expressed as,

$$a_A = \gamma_{\pm} z_1 C / (z_1 + z_2) \text{ and } a_B = \gamma_{\pm} z_2 C / (z_1 + z_2).$$

For a (1:1) binary electrolyte ($z_1 = 1$ and $z_2 = -1$), the electrical potential difference is,

$$\Delta \Phi = -\frac{RT}{F} [t_1 \ln \frac{a_{1,\beta}}{a_{1,\alpha}} - t_2 \ln \frac{a_{2,\beta}}{a_{2,\alpha}}] \quad (2.20)$$

Furthermore, for a 1:1 electrolyte, $a_1^{\alpha} = a_2^{\alpha} = a^{\alpha}$ and $a_1^{\beta} = a_2^{\beta} = a^{\beta}$. Thus, when two solutions differing only in concentration of an 1:1 electrolyte are in contact, the liquid junction potential is,

$$\Delta \Phi = \frac{RT}{F} (t_1 - t_2) \ln \frac{a^{\alpha}}{a^{\beta}} \quad (2.21)$$

For example, a membrane separating a 0.1 mol dm^{-3} and 1 mol dm^{-3} NaCl solution gives a potential difference of -12 mV.

Equation 2.21 has been used in the present work. It assumes the ions diffuse through the membrane and that there are no fixed charges in the membrane. Such charges could arise from local changes in the membrane composition such as ions incorporated from previous measurements and dissociated functional groups.

For mixtures of several electrolytes, the potential can be derived if the assumption is made that there is a linear concentration gradient of each ion across the boundary i.e. steady state as described by Henderson [29]. Thus, if the activity coefficients of ions across the boundary are assumed to be invariant with position, and the mobilities are assumed to be independent of concentration and hence position, the following is true,

$$d\ln(a_i) = \frac{\delta \ln(a_i)}{\delta x} \delta x = \frac{1}{C_i} \frac{\delta C_i}{\delta x} \delta x = \frac{C_{i,\beta} - C_{i,\alpha}}{C_i(x)} dx \quad (2.22)$$

The transference number can be expressed in terms of concentrations and mobilities,

$$t_i = \frac{|z_i| C_i(x) U_i}{\sum_j |z_j| C_j(x) U_j} \quad (2.23)$$

where the mobilities are assumed to be independent of concentration and position. For the transport numbers t_i ,

$$\sum t_i = 1 \quad (2.24)$$

Substitution into equation 2.17 then leads to the Henderson equation:

$$\Delta \Phi = -\frac{RT}{F} \frac{\sum_i (|z_i|/z_i) U_i (C_i^\beta - C_i^\alpha)}{\sum_i |z_i| U_i (C_i^\beta - C_i^\alpha)} \ln \frac{\sum_i |z_i| U_i C_i^\beta}{\sum_i |z_i| U_i C_i^\alpha} \quad (2.25)$$

This is the general solution for liquid junction potential of mixed electrolytes. The equation simplifies when there is a common cation (this gives a prelogarithmic term of RT/F) or anion present (the prelogarithmic term reduces to $-RT/F$) of the same concentration in both phases α and β . The potential difference is then given by,

$$\Delta \Phi = \pm \frac{RT}{F} \ln \frac{\sum_i |z_i| U_i C_i^\alpha}{\sum_i |z_i| U_i C_i^\beta} \quad (2.26)$$

This equation was used in the present work to fit data from potentiometric experiments where the membrane was tested with more than one salt.

2.2.2. THE SEMIPERMEABLE MEMBRANE

A membrane may alternatively be modelled as a semipermeable membrane as initially proposed by Donnan [29, 30]. In a solution containing species with a small ionic radius and charged macromolecules, the membrane only allows the free passage of the small ions and solvent molecules. Since the system is at true equilibrium, the ionic electrochemical potentials on both sides of the membrane should be equal. The potential difference across the membrane is

the difference between the potential in the two solutions (namely phase α and β):

$$\Delta\Phi = \frac{RT}{F} \ln \frac{a_{1,\alpha}}{a_{1,\beta}} = \frac{-RT}{F} \ln \frac{a_{2,\alpha}}{a_{2,\beta}} \quad (2.27)$$

Consequently,

$$a_1^\alpha a_2^\alpha = a_1^\beta a_2^\beta \quad (2.28)$$

The activity coefficients in phases α and β are equal, electroneutrality requires that $C_1^\alpha - C_2^\alpha = 0$. Phase β contains the macromolecule, of charge z_M and concentration C_M , so that the electroneutrality condition is,

$$C_1^\beta - C_2^\beta + z_m C_m = 0 \quad (2.29)$$

An example of the potential response of a ideal semipermeable behaviour as a function of HCl activity is given in figure 2.1. Assumptions for the permselective membrane are: selectivity is towards H^+ ions only and there are no interferences from other ions.

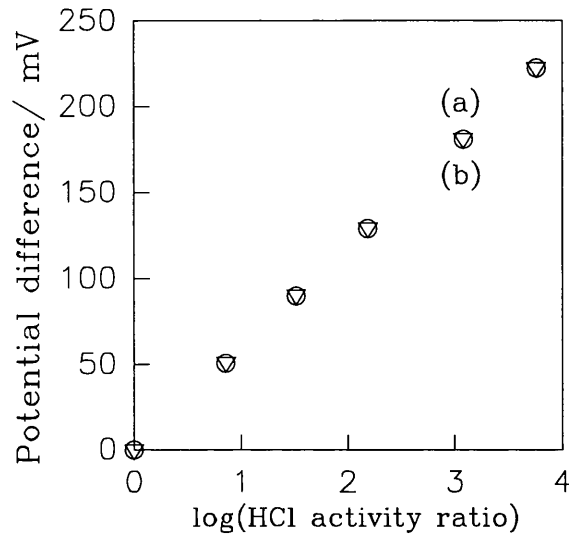


Figure 2.1: The potentiometric response of an a) an ideal semipermeable membrane and (b) a permselective membrane in HCl solution with a constant HCl solution of $0.001 \text{ mol dm}^{-3}$ on one side of the membrane.

2.2.3. THE PERMSELECTIVE MEMBRANE

In this model [28], the system is at true equilibrium. The electrochemical potential for the species, i , is equal on both sides of the membrane:

$$\begin{aligned} \mu_i &= \mu_{i,\alpha}^\theta + RT \ln a_{i,\alpha} + z_i F \phi_\alpha \\ &= \mu_{i,\beta}^\theta + RT \ln a_{i,\beta} + z_i F \phi_\beta \end{aligned} \quad (2.30)$$

where α and β denote the phases divided by the membrane.

The total electrochemical potential is described for two diffusing species i and j , where ion i is permeable to the membrane and j is not permeable. The behaviour of the various types of permselective membranes are described below.

2.2.4. GLASS MEMBRANES

A permselective membrane, such as a glass pH electrode, may be examined in terms of a summation of electrochemical potentials that arise from different regions of the membrane itself. The membrane can be divided up into five regions, as shown in figure 2.2:

α	external electrolyte solution
β	hydrated glass layer
γ	unhydrated glass core
β'	hydrated glass layer
α'	internal electrolyte solution

Figure 2.2: The regions of a glass membrane. The total membrane potential difference arises from a summation of the potential differences across its interfaces.

The total membrane potential therefore has contributions from each of the interfacial regions. The total membrane potential is expressed as,

$$\Delta \Phi_m = \Delta \Phi_{(\alpha\beta)} + \Delta \Phi_{(\beta\gamma)} + \Delta \Phi_{(\gamma\beta')} + \Delta \Phi_{(\beta'\alpha')}$$

The assumptions are that the solution and hydrated membrane interface of $\alpha\beta$ and $\beta'\alpha'$ are in equilibrium and Donnan equilibria (section 2.2.2.) can be used

to describe the potential. The potential at the hydrated membrane and the internal membrane core interface of $\beta\gamma$ and $\gamma\beta'$ is a result from differences in the mobilities of the diffusing species, which may be described using the Henderson equation.

Thus,

$$\Delta\Phi_{\alpha\beta} + \Delta\Phi_{\beta'\alpha'} = \frac{RT}{F} \ln \frac{a_{i,\alpha} a_{i,\beta'}}{a_{i,\beta} a_{i,\alpha'}} \quad (2.31)$$

If, in the interior of the membrane the anions are assumed to be immobile, such that the potential difference arises because of the differing mobilities of the cations, application of the Henderson equation 2.26 gives:

$$\Delta\Phi_{\beta\gamma} + \Delta\Phi_{\gamma\beta'} = \frac{RT}{F} \ln \frac{\sum (U_j/U_i) a_j^\beta + a_i^\beta}{\sum (U_j/U_i) a_j^{\beta'} + a_i^{\beta'}} \quad (2.32)$$

where U_j denotes the mobility of ion j .

The total membrane potential is then,

$$\Delta\Phi_m = \frac{RT}{F} \ln \frac{(U_j/U_i) K a_j^\alpha + a_i^\alpha}{(U_j/U_i) K a_j^{\alpha'} + a_i^{\alpha'}} \quad (2.33)$$

where K is the equilibrium constant for ion exchange across the α, β interface. The potentiometric selectivity coefficient, $K_{i,j}$, is expressed as,

$$K_{i,j} = K(U_j/U_i) \quad (2.34)$$

If simplifications are made such that the interior solution concentration is kept constant, then the denominator can be replaced by a constant and the general result can be given as,

$$\Delta\Phi_m = \text{constant} + \frac{RT}{F} \text{Ln} [a_i + \sum_j K_{i,j} a_j] \quad (2.35)$$

where the principal diffusing species is i and $K_{i,j}$ is the potentiometric selectivity coefficient for j relative to i . For the glass electrode, the diffusing species i is the H^+ ion and species j is usually the Na^+ ion. In the present work, potentiometric results will be compared to this theoretical behaviour (figure 2.1).

2.2.5. OTHER TYPES OF PRACTICAL PERMSELECTIVE MEMBRANE

The permselective membranes used in the construction of ion-selective electrodes usually consist of an ion-exchanger incorporated into a polymer matrix plasticised with a water immiscible solvent. Generally, such membranes have binding sites to which ions associate during transportation through the membrane. The nature of the binding sites may vary with composition and preparation. Films may have fixed sites, whose co-ordinates within the film are

constant as the ions move through, or mobile sites where the concentration associated sites and ions vary across the film. Alternatively, the film may be site-free with ions free to diffuse through. Each membrane type will be discussed below. The transport of ions across the film may be described using the Nernst-Planck equation [30]. The necessary conditions under which these electroneutral membranes develop potential differences are,

- 1) one or more concentration gradients of charged species exist;
- 2) fluxes of ions are non-zero;
- 3) mobilities of the charged species are different.

2.2.6. PERMSELECTIVE SITE-FREE MEMBRANES

Consider a charged membrane permeable to ions of one sign [28]. The assumptions of this model are: the Debye thickness (section 2.3) is greater than the membrane thickness, the activity coefficient, standard chemical potential and mobility are each independent of position, all ions are of the same charge and the net current flow is zero. The sum of the interfacial potentials give the total membrane potential. When the membrane is permeable to more than one ion of a given charge, the potential is given by:

$$\Delta \Phi_m \sim \frac{RT}{zF} \ln \left[\frac{\sum_i U_i K_{ext,i} a_i / \gamma_i}{\sum_i U_k K_{ext,k} a_k / \gamma_k} \right] \quad (2.36)$$

where a_i denotes activity of ions i on the left of the membrane and a_k is the activity of ions k on the right and $K_{ext,i}$ denotes the interfacial extraction coefficient of ion i .

2.2.7. PERMSELECTIVE FIXED SITE MEMBRANES

These membranes have a high site density to assure permselectivity [28, 31]. The idea is that the selected ion binds strongly to the membrane sites compared to all other ions. The assumptions in this model are the same as for the site-free membrane description (section 2.2.6).

The general expression for the total membrane potential for a multi-ionic case, at zero current is,

$$\Delta \Phi_m = \frac{nRT}{zF} \ln \left[\frac{a_i^{1/n} + \sum_j (K_{ij}^{pot} a_j)^{1/n}}{a_k^{1/n} + \sum_l (K_{kl}^{pot} a_l)^{1/n}} \right] \quad (2.37)$$

where i cations of charge z on the left of the membrane and k cations on the right of the membrane. K_{ij} is the potentiometric selectivity coefficient for ions i, j on the left of the membrane, K_{kl} is the potentiometric selectivity coefficient for ions k, l on the right of the membrane. a_i denotes the activity of cations i on the left of the membrane, a_k denotes ion activity of cations k on the right of the membrane. The membrane potential response time depends only on the time required to charge surfaces and establish ion exchange equilibrium.

2.2.8. PERMSELECTIVE MOBILE SITE MEMBRANE

These membranes are the liquid ion exchanger type [28, 32]. The assumptions are the same as the site-free membrane, however, the sites conferring selectivity are free to move within the membrane but confined to the

membrane interior. The confinement of sites in the membrane means that,

$$\int_0^d \bar{X}(x) dx = X_0 d \quad (2.38)$$

where $X \rightarrow X_0$ means that the binding sites in the membrane are located within the membrane boundaries. Typical site concentration values are 1.10^{-6} mol dm^{-3} [34].

Alternatively, the inner concentration of exchanged ions may redistribute in space and time. Equations for fixed sites only apply for the steady-state in these membranes. Site concentrations are higher than average at the side where permeable ions enter and lower at the exiting side. The total steady-state potential [34] is,

$$\Delta \Phi_m = \frac{RT}{F} \ln \left[\frac{a_i + \sum_j K_{i,j}^{pot} a_j}{a_k + \sum_l K_{k,l}^{pot} a_l} \right] + \int_0^d t \, d \ln \left| \frac{\sum_i U_{is} K_{is} C_i}{\sum_i U_i C_i} \right| \quad (2.39)$$

where $K_{i,j}$ is the potentiometric selectivity coefficient for ions i and j on the left of the membrane and $K_{k,l}$ is the potentiometric selectivity coefficient for ions k and l on the right of the membrane which is similar to the fixed site membrane.

a_i is the activity of cations i to the left of the membrane and a_k is the activity of cations k on the right side of the membrane.

U is the mobility of free sites, $U_{i,s}$ is the mobility of occupied sites and t , the

term which represents the potential difference contribution from the inner concentration of exchanging ions which vary with time as the sites continue to redistribute in time and space, is defined as,

$$t = \frac{\overline{U_s C_s}}{(\overline{U_s C_s} / \sum_i \overline{U_{i,s} C_{i,s}} + 1) (\sum_i \overline{U_i C_i} + \overline{U_s C_s})}$$

where $C_{i,s}$ is the concentration of occupied sites in the membrane, C_s is the concentration of free sites in the membrane, U_i is the mobility of cations i in the membrane, $U_{i,s}$ is the mobility of occupied sites and $K_{i,s} = 0$ when the sites are fully dissociated.

2.2.9. SELECTIVITY COEFFICIENTS AND INTERFERENCES

An important factor in the specificity in the membranes is their discrimination to ions of the same charge [35]. In solutions containing more than one electrolyte, the membrane responds to the total cationic and/ or anionic concentration. If one ion has high mobility (H^+ ion) or is large, then some distinction can be generally made; they are preferentially selected or their diffusion into the membrane is blocked.

The response [28] for a permselective ion exchange membrane for two ions is similar to equation 2.35 and is given by:

$$\Delta \Phi_{meas} = \Phi^0 + \frac{2.203RT}{zF} \log(a_i + K_{i,j}^{pot} a_j) \quad (2.40)$$

The response of each ion is given by the selectivity coefficient K_{ij}^{pot} , assuming identical activity,

$$\Delta\phi_{meas}(i) - \Delta\phi_{meas}(j) = \frac{2.303RT}{zF} \log K_{i,j}^{pot} \quad (2.41)$$

Interfering ions are usually of the same charge as the principal ion. However, for neutral membranes, ions of the opposite charge cause significant interferences. For the K^+ selective membrane, the response is a Nernstian slope in aqueous KOH, KF and KCl. As the anion becomes more oil-soluble the salt solubility increases and anions are extracted into the membrane. This process is accompanied by a decrease in the potential response and in membrane resistance [36, 37].

Structural factors may also affect the membrane selectivity. For example, steric factors relate the ionic size to the membrane network. Small ions (relative to the membrane pores), may be taken up by the membrane. Large ions may be totally excluded from entering the membrane: the "ionic sieve" effect. This steric effect may be controlled by the film preparation, for example, a minimum quantity of ions above the radius of 5.5 Å diffuse into membranes that are more than 10 % cross-linked [25].

Inter-ionic effects may also be important, such as coulombic effects between polymer chains and counter-ions in the electrical double layer. This factor will lead to a variation in the activity of the counter-ions giving a different internal distribution for ions of different charge. Cation-anion interaction may also be important. The closest approach for ions of opposite charge depends on the size of their hydration shells and on the extent to which they interpenetrate.

Oil soluble ion-carriers give selectivity to the membrane by extraction of ions into the membrane phase. Oil soluble anions in the membrane material will exclude any encroaching anions resulting in the permeation of cations exclusively into the membrane. For example, interference has been observed in valinomycin PVC films [38], at low ion-carrier loadings, response degradation was attributed to other cations serving as counterions for the negative sites. Lipophilic salts are agents for adding anionic sites when the ion pair segregate thus producing sites available for binding and reducing membrane resistances [39].

2.2.10. TIME DEPENDENT EFFECTS

Time dependent selectivity coefficients and potentials are often observed when a fresh membrane is exposed to an electrolyte for the first time. Some time after exposure, ions that compete with the principle ion are replaced from the bulk electrolyte [26]. In low concentration electrolyte, the steady state is typically obtained after a few minutes.

The response times of electrodes are determined by several factors; mass transport effects (such as convection, diffusion and forced convection), solution concentration, membrane properties and the temperature of the system.

The recovery time of a membrane is the time taken to regain its potential after immersion in a test solution. The recovery time increases with increasing concentration, indicating more ions in the membrane which needs to be replaced before a new equilibrium potential difference is reached. Thus, measurements should be made from dilute to concentrated solutions and small cell volumes should be avoided. After immersion in an asymmetric salt solution (depending on the duration of soaking and whether there are any fixed sites), the electrolyte concentration inside the membrane is non-uniform.

Often, a thin layer clings to the surface when the electrode is withdrawn from a solution and dipped into another. Sometimes the stagnant layer is enhanced by the presence of a thin film adsorbed externally or by an encroaching water layer at the electrode surface.

Experiments and theories suggest that three response times are observed in practical applications of ion-selective electrodes: (1) The shortest time constant is the result of the charging of the external space charge regions. This is the shortest time within which potential development can normally be observed. Time constants range from 2 to 10 ms for Na⁺ sensing glasses and from 100 to 200 ms for pH glasses, depending on electrode area [28]; (2) A longer time constant may be observed which results from the coupling of ion transfer with the double layer capacitance at the membrane surface. Time constants between 1 and 10 seconds are common; (3) The longest time constant shown by liquid ion exchanger membranes is due to concentration polarisation of charge carriers by current flow or steady state flux at zero current. This time constant is roughly the transit time of an ion through the membrane. The rates of ion exchange through the membrane can be on the timescale of seconds (a small ion entering a finely divided membrane) or weeks (where a large ion enters a Highly cross linked membrane).

2.3. THE ELECTRIFIED INTERFACE

This section concerns aspects of the membrane/electrolyte interface such as the electrified interface and the streaming potential.

When a surface is in contact with an electrolyte solution, ions may adsorb onto the surface [29, 30] and the structure of water will change. An ionic atmosphere equal and opposite in charge to the adsorbed ions will develop in the solution next to the membrane. This phenomena is termed the double layer.

The first model of the electrochemical double layer, [29, 30] by Helmholtz, describes a surface having a fixed charge in the counter charge layer. The Guoy-Chapman model describes the counter charge subject to thermal motion and is an extension of the model by Helmholtz. The Stern model combines both Helmholtz and the Guoy-Chapman model. The counter charge is partially immobilised on the surface whilst the rest of the surface charge is neutralised by the counter ions in the solution under thermal motion.

The mathematical description of the electrified interface which gives the electric potential as a function of distance from the surface, uses the Poisson equation,

$$\nabla^2 \Phi = -\rho / \epsilon \epsilon_0 \quad (2.42)$$

where ϵ is the dielectric constant of the medium, ϵ_0 is the permittivity of free space, ρ the space charge density = $\sum_i z_i F C_i$.

Using the Poisson equation, the ionic concentration can be linked to the electric potential at any point. To find the distributions of ions at different points with particular electrostatic energies, the Boltzman equation is used:

$$\frac{C_i}{C_i^0} = \exp [-z_i F \Phi / RT] \quad (2.43)$$

which means that smaller concentration of positive ions are found next to a positive surface charge.

The variation of ionic composition with distance across the diffuse double layer is characterised by a thickness x_A (the Debye length). The term for the ionic thickness x_A is:

$$x_A = [\epsilon\epsilon_0 RT / F^2 I]^{1/2} \quad (2.44)$$

where I is the ionic strength, $I = 0.5 \sum_i z_i^2 C_i^0$.

Here, x_A can be regarded as a measure of ion atmosphere thickness at the charged surface and depends on the concentration and type of electrolyte. These factors can be manipulated to produce a small or large ion atmosphere thickness (e.g. up to 1.3 μm for a flow rate of 282 cm sec^{-1} with 0.001 mol dm^{-3} KCl over polystyrene sulphonic acid particles [40]).

The potential difference between bulk solution and the solution at the Debye distance from interface, Φ_A , is related to the net surface charge density, σ , in the following way, for a planar surface:

$$\sigma = \epsilon\epsilon_0 \Phi_A / x_A \quad (2.45)$$

where the system as a whole is electrically neutral and the net surface charge σ is balanced by the space charge in the Gouy layer.

The charging of the interface between a membrane and an electrolyte solution may be effected by the functional groups of the polymer membrane protruding into the electrolyte solution. This affects the behaviour of ions diffusing into

the membrane and the development of the membrane potential difference. Thus an understanding of the electric interface is needed.

2.3.1. THE STREAMING POTENTIAL

The streaming potential is one of a class of effects termed "electrokinetic effects" which arise as a consequence of the relative motion of an electrolyte solution and an electrified interface. This is an important aspect in understanding the processes which the membrane undergoes as it is immersed into solution: in the present work, for example, the potentiometric behaviour of co-cast PVC-PEO membranes changes with soaking (see chapter 4). This effect arises because the diffuse double layer is stationary at the interface and is sheared when either the surface or the solution moves at a plane or slipping surface at some distance, x , from the surface. The potential at the slipping surface is denoted by ζ . Consideration of the streaming potential is important in order to account for the effects in which there is bulk flow of the electrolyte through the membrane. To model the effect, a cylindrical pore is considered. The Poisson equation for this situation, if we assume Φ depends only on the distance from the surface of adsorption, is:

$$\rho(r) = \frac{-\epsilon\epsilon_0}{r} \frac{d(rd\Phi/dr)}{dr} \quad (2.46)$$

In the situation where the radius of the capillary is much greater than the Debye length x_d , the shear plane can be approximated as a flat planar surface located at position r and at potential:

$$\Phi(r) = \xi \exp[(r-a)/x_A] \quad (2.47)$$

where r is measured from the centre of the capillary, a denotes the radius of the capillary and a/x_A is large enough for the potential at the centre of the capillary to be nearly zero. Typical streaming potential values are 0.2 mV/atm for a phenolsulphonate membrane [40].

Solution flow through a membrane in a potentiometric cell could arise as a consequence of three effects: (1) osmotic pressure differences across the membrane, (2) hydration of a newly prepared membrane, (3) flow coupled with the potential difference across the membrane.

Water transference through a membrane caused by an electric potential difference is known as electroosmosis and is the complimentary phenomena to the streaming potential. Water can enter the membrane in the solvation sheath of ions or as free solvent. The latter effect is a consequence of ionic migration imparting momentum to the solvent molecules.

Oda et al [41] studied the transportation of water from one compartment in the electrochemical cell to another. Treatment of solvent transport was divided into that moving with the velocity of the ions and that moving with a velocity limited by the friction resistance from the membrane structure. The latter velocity being much less than that of the ions [41]. Swelling of the membrane accompanies the migration of solvent into its interior [42]. Volumes of transported water across cation exchanger membranes in NaCl solutions were reported to be greater than could be accounted for by the hydration number of NaCl. Oda et al also introduced the concept of fixed and free water present in the membrane resin. The fixed water was proposed to be mainly the hydration

water attached to the polar groups of the resin, and the free water that moving with the same velocity as the migrating ions.

Water absorption into the membranes studied in the present work was a particularly important phenomenon. When a new, dry membrane was immersed into an electrolyte solution, it was highly resistive. Some membranes were resistive to the extent that no useful potential differences were measurable. However, the potential difference of the membrane stabilised with time and the equilibrium was more quickly established with the older membrane.

The transport of ions across the membrane may be measured using potentiometry but the flow of water into the membrane may affect the concentration of diffusing electrolytes, possibly causing the electrolyte to become dilute and thereby reducing the recorded potential difference.

REFERENCES FOR CHAPTER 1

- [1] C. W., Davies, "Ion Association", ch. 14, Butterworths press, London, 1962.
- [2] O. Y., Samoilov, *Discuss. Faraday Soc.*, **24**, 141, (1957).
- [3] F., Franks, "Water, a Comprehensive Treatise", vol. 2, ch. 1, Plenum Press, New York, 1973.
- [4] R. U., Lamas, A. A., Pavia, J. C., Martin, K. A., Watanabe, *Can. J. Chem.*, **47**, 4427, (1969).
- [5] J., Koryta, J., Dvorak, L., Kavan, "Principles of electrochemistry", ch. 1, John Wiley and Sons, England, 1993.
- [6] J. T., Edsall, H. T., Clarke (ed), "Ion Transport Across Membranes", p. 221, Academic Press, New York, 1954.
- [7] P. H., Reiger, "Electrochemistry", ch. 2, Prentice Hall Int. Inc., U.S.A, 1987.
- [8] K., Hellsing, *J. Chromatgr.* **36** 270, (1968).
- [9] J. Y., Kolske, F. E., Bailey, "Poly(ethylene oxide)", ch. 4, Academic Press, New York, 1976.
- [10] J., Hermans, *J. Chem. Phys.*, **77**, 2193, (1982).
- [11] D. H., Atha, K. C., Inghan, *J. Biochem.*, **258**, 5710, (1983).
- [12] S. L., Hager, T. B., MacRury, *J. Appl. Polymer. Sci.*, **25**, 1559, (1980).
- [13] B., Bogdanov, M., Mihailov, *J. Polymer. Sci. Phys. Ed.*, **23**, 2149, (1985).
- [14] C. P. S., Tilcock, D., Fisher, *Biochim. Biophys. Acta.*, **688**, 645, (1982).
- [15] N. B., Graham, M., Zulfiquar, N. E., Nwachuku, A., Rashad, *Polymer*, **30**, 528, (1989).
- [16] R., Kjellander, *J. Chem. Soc. Faraday Trans. 2*, 2025, (1982).
- [17] K. J., Lui, K., Parsons, *Macromolecules*, **1**, 529, (1969).
- [18] N. R., Gombotz, W., Guanghui, T. A., Horbett, A. A., Hoffman, *J. Biomed. Mat. Res.*, **25**, 1547, (1991).
- [19] J. M., Harris, "Poly(ethylene glycol) Chemistry, Biotechnical and

Biomedical Applications", ch. 17, Plenum Press, New York, 1992.

[20] N. B., Graham, N. E., Nwachuku, D. J., Walsh, *Polymer*, **31**, 909, (1990)

[21] H., Freiser, (ed) "Ion Selective Electrodes in Analytical Chemistry", Volume 2, ch. 4, Plenum Press, New York, 1980.

[22] J. A., Kitchener, J. O., Bockris, (ed) "Modern Aspects of Electrochemistry", No. 2, p. 134, Butterworths Scientific Publication, London, 1959.

[23] Robinson, Harned, *Chem. Rev.* **28**, 419, (1941).

[24] K. W., Pepper, *J. Appl. Chem.*, **1**, 124, (1951).

[25] H. P., Greggor, K. M., Held, J., Bellin, *Anal. Chem.*, **23**, 620, (1951).

[26] M. H., Waxman, B. R., Sundheim, H. P., Greggor, *J. Phys. Chem.*, **57**, 969, (1953).

[27] J. A., Kitchener, J. O., Bockris, (ed) "Modern Aspects of Electrochemistry", No. 2, p. 98-105, Butterworths Scientific Publication, London, 1959.

[28] R. P., Buck, *Sensors and Actuators*, **1**, 197, (1981).

[29] P. H., Reiger, "Electrochemistry", ch. 3, Prentice- Hall International Editions, U.S.A., 1987.

[30] D. A., McInnes, "Electrochemistry", ch. 1, Reinhold Publ., New York, (1939)

[31] F., Conti, G., Eisenman, *Biophys. J.*, **5**, 247, (1965).

[32] F., Conti, G., Eisenman, *Biophys. J.*, **6**, (1966).

[33] B., Fu, E., Bakker, J. H., Yun, M. E., Meyerhoff, *Anal. Chem.*, **66**, 2250, (1994).

[34] J., Sandblom, G., Eisenman, J. L., Walker, *J. Phys. Chem.*, 3862, (1971).

[35] D. J. G., Ives, G. J., Janz, (eds) "Reference electrodes, Theory and Practice", ch. 9, Academic press, London, 1961.

[36] R. P., Buck, M. L., Inglehart, E., Pungor, *Anal. Chem.*, **60**, 290-295, (1988).

[37] E., Lindler, E., Graf, Z., Neigrisz, K., Toth, E., Pungor, *Anal. Chem.*, **60**, 295, (1988).

- [39] R. P., Buck, E., Lindler, E., Graf, Z., Neigreisz, K., Toth, E., Pungor, *Anal. Chem.*, **60**, 295-301, (1988).
- [40] N. Lakshminarayanaiah, "Transport Phenomena in Membranes", ch. 4-6, Academic Press, New York, 1969.
- [41] Y. Oda, T., Yawataya, T., *Bull. Soc. Chem. Japan*, **28**, 263, (1955).
- [42] A., Despic, G. J., Hills, *Discuss. Faraday Soc.*, **21**, 150, (1956).

CHAPTER 3
EXPERIMENTAL TECHNIQUES
AND EQUIPMENT

CHAPTER 3. EXPERIMENTAL TECHNIQUES AND EQUIPMENT

This chapter outlines the experimental methods undertaken in this thesis. First, the preparation of pure PEO membranes with a summary of the experiments performed are described. Then, the preparation of co-cast PEO-PVC composite membranes is given with a description of the analytical techniques such as potentiometry, thermal analysis, FTIR, polarised light optical microscopy and solid state deuterium NMR.

3.1. MATERIALS

All chemicals were analytical grade (purity > 99.9%) and used without further purification. Poly(vinyl chloride) $(\text{CH}_2\text{CH}_2\text{Cl})_n$ (very high molecular weight PVC, m.w. 161,000), poly(vinylmethyl ketone) and cyclohexanone were purchased from Aldrich. Poly(ethylene oxide) $(\text{CH}_2\text{CH}_2\text{O})_n$ (m.w. 10^6 PEO) was a gift from Union Carbide. The inorganic salts were purchased from Aldrich, Fluka or BDH Chemicals. Sodium dodecylsulphate (NaDDS) was from Fluka. The salt solutions were prepared using quadruply distilled water, the second distillation being from an alkaline solution of potassium permanganate. The water purity was checked by conductivity measurements and was consistently $2 \pm 0.2 \mu\text{S cm}^{-1}$.

3.2. MEMBRANE PREPARATION

3.2.1. AQUEOUS PEO GELS

Aqueous gels were prepared by adding poly(ethylene oxide) powder to hot water (from 0.7 to 2% weight in solution). The resulting viscous mixture was stirred for approximately 2 hours to produce a solution. Membranes were made

by sucking the gelatinous solution through a stack of poly(ethylene terephthalate) porous cloth discs (diameter 3 cm) on a piece of filter paper in a Buchner funnel. The purpose of the filter paper was to slow down the rate of flow and so ensure thorough soaking of the disc.

3.2.2. PROCESSED POLY(ETHYLENE OXIDE) GELS

Unsupported poly(ethylene oxide) gels were prepared by adding drops of water (each addition was 1 ml, total volume was 2.8 ml) to the polymer powder (5.4 g) in a mortar and grinding to form a white solid which was repeatedly rolled and folded through metal rollers until a smooth and homogeneous gel was formed. The gel tended to curl up and crease after the rolling process, so it was kept between two sheets of glass under a heavy weight until needed.

3.2.3. COMPOSITE POLY(ETHYLENE OXIDE)-POLY(VINYL CHLORIDE) MEMBRANES

Composite PEO/PVC membranes were made by dissolving polymers (typical composition of 0.02 g PEO, 0.48 g PVC) in cyclohexanone. The mixture was stirred and heated at 45°C-60°C until fully dissolved. This viscous solution was then poured into the reservoir of a home-built doctor-blade casting machine (figure 3.1). The cast thickness (75 to 150 μm) was adjusted using a micrometer controlled blade. The solution flowed under the blade on to an optically flat glass plate which rested on a trolley. The trolley was pulled from under the micrometer controlled blade at a speed of 0.74 cm/sec. The liquid film flowed further after casting, resulting in films of thickness significantly less than the blade clearance. The cast solution was then dried by either exposure to warm air (30°C) for 12 hours, or by exposure to a thermostatted resistive heating element (1-2 hours at 60°C).

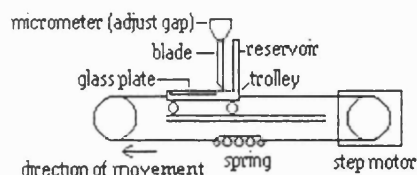


Figure 3.1: The Doctor-Blading co-casting machine is shown with the moving trolley on which the PEO-PVC membrane solutions were cast.

3.3. AQUEOUS POLY(ETHYLENE OXIDE) GELS

3.3.1. DENSITY AND VISCOSITY MEASUREMENTS

The density of aqueous PEO gel solution (2 to 0.16 mol dm⁻³) was measured using density bottles (purchased from BDH) calibrated with water at 25°C. The solutions were slowly poured into the density bottle (at 25°C) and any trapped air allowed to escape (15 minutes). The lids were replaced and the bottles were then weighed to obtain the density.

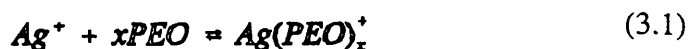
Viscosity measurements were made at room temperature with a Ostwald viscometer. The aqueous PEO gel solutions were pipetted into the viscometer and allowed to settle to eliminate any air bubbles before the experiment. This method measures the rate of flow of a liquid through a capillary under gravity and is valid only for streamline flow [1]. Water was measured as a reference liquid, eliminating the need to measure the dimensions of the viscometer.

3.3.2. CONDUCTIVITY MEASUREMENTS

The conductivity of aqueous PEO solutions was measured with a Phillips type 4016 conductivity meter. The matching probe was calibrated using 0.01 mol dm⁻³ KCl solution at 25°C. The instrument had an error of ± 0.5 μS.

3.3.3. STOICHIOMETRY AND STABILITY CONSTANT OF Ag/PEO COMPLEX

The possibility of a complexation reaction between silver and PEO in aqueous solution was studied by potentiometry of the Ag/AgCl electrode. Since the electrode potential measures the activity of the free Ag⁺ ions, the complexation reaction can be measured. The following reaction will occur in the complexation of one silver ion:



The equilibrium constant for this reaction is:

$$K = \frac{[Ag(PEO)_x^+]}{[Ag]^+ \cdot [PEO]^x} \quad (3.2)$$

The experimental procedure was as follows:

10 ml of 0.05 mol dm⁻³ AgNO₃ was added to 10 ml of 0.048 mol (ethylene oxide) dm⁻³ of PEO solution and stirred to mix the solutions. A reference

solution of saturated AgNO_3 was electrically connected to the PEO solution by a KNO_3 salt bridge. The reference electrode (Ag/AgCl) was placed in the saturated AgNO_3 solution and a Ag wire sealed in glass acted as the test electrode. The variation of potential of the Ag^+ electrode as the solution was diluted was measured.

3.4. PROCESSED POLY(ETHYLENE OXIDE) GELS

3.4.1. AC IMPEDANCE

Simple two-terminal impedance experiments were carried out to develop an understanding of the resistive properties of the film and bulk solution. The film was clamped in a standard 6 mm screw-cap joint. The resulting container was filled and immersed in a beaker of 0.1 mol dm^{-3} NaCl salt solution. Two platinum electrodes (surface area 1 cm^2) were placed on either side of the membrane. The AC impedance was measured using a Schlumberger 1253 Gain-phase analyser (GPA) and a computer to control and collect the data. The GPA has 3 components, the generator (to provide the sine wave perturbation to the system), the 2 analyser channels (to measure the response from the experimental points) and the display (for the operating menu and the results). The experiment measures the change in amplitude and phase resulting from a sine wave perturbation on the system. The frequency range was from 20×10^3 to 1×10^4 Hz in logarithmic steps (25/decade).

3.5. POTENTIOMETRY

All potentiometry experiments were carried out in a constant temperature environment of 25°C . This was effected by using a home-built system comprising a cupboard, a light bulb, an electric fan and a thermostat.

In potentiometry experiments on composite PEO/PVC films, the

electrochemical cell (figure 3.2) used was machined from Delryn (natural acetal). It consisted of two compartments clamped together with the test film held in place between each half by two O rings, which defined the electrode area and prevented leakages across the membrane.

In potentiometry experiments, on the cloth supported aqueous PEO gel membranes and the processed PEO gels, the cell used for measurement consisted of a glass tube with a screw cap joint at one end. The membrane was clamped against the glass tube underneath the screw cap. The potential difference was measured between Ag/AgCl electrodes mounted in the two compartments. The pH solutions used in tests on co-cast PEO-PVC membranes were made as described in table 3.1.

Prior to each experiment, the potential of the reference electrodes was checked versus a standard reference electrode (error of ± 1 mV). The potential difference across the film was measured with a Keithly 197A Autoranging microvolt DMM.

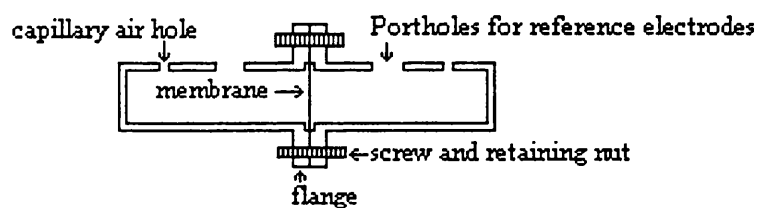


Figure 3.2: The concentration cell used in the potentiometry experiments on co-cast PEO-PVC membranes. The membrane is placed between the two compartments, secured with O rings and screwed together to prevent leakage of electrolyte solution from one compartment to another. There are holes machined for the reference electrodes and air holes for when excess electrolyte solution flows out after the electrodes are immersed into electrolyte solution filled compartments.

pH	Buffer Solution at 25 °C
1	25 ml of 0.2 M KCl + 67 ml of 0.2 M HCl
3	50 ml of 0.1 M Potassium hydrogen phthalate + 22.3 ml of 0.1 M HCl
5	50 ml of 0.1 M Potassium hydrogen phthalate + 22.6 ml of 0.1 M NaOH
7	50 ml of Potassium dihydrogen phosphate + 29.1 ml of 0.1 M NaOH
10	50 ml of 0.025 M Disodium tetraborate + 18.3 ml of 0.1 M NaOH
13	25 ml of 0.2 M KCl + 66 ml of 0.2 M NaOH

Table 3.1: The pH solutions used in the potentiometry tests on co-cast PEO-PVC membranes.

3.6. COMPOSITE POLY(ETHYLENE OXIDE)/ POLY(VINYL CHLORIDE) MEMBRANES-NON ELECTROCHEMICAL METHODS

3.6.1 THERMAL ANALYSIS

These methods probe the response of the films to temperature perturbations and provide an understanding into the thermal behaviour and the mixing of the polymers.

3.6.2. DIFFERENTIAL SCANNING CALORIMETRY (DSC)

This experiment measures the enthalpy changes in the composite PEO/PVC membranes with temperature. The instrument used was a Shimadzu DSC 50 machine, and the heating rate was controlled using the accompanying Shimadzu microprocessor controller (figure 3.3). The technique of power compensated DSC was employed: this utilises isolated sample and reference crucibles with their own heating elements and a temperature sensing device to measure the temperature difference between them. The instrument controller ensures that both the crucibles are heated at a constant rate and that the temperature difference between them is zero. The difference in power supplied to each crucible is recorded. If there are any enthalpic changes (i.e. for an endothermic reaction), then more heat is put into either crucible to ensure both equal heating rates. Power, heat flow and enthalpy changes can all be measured in this way [2].

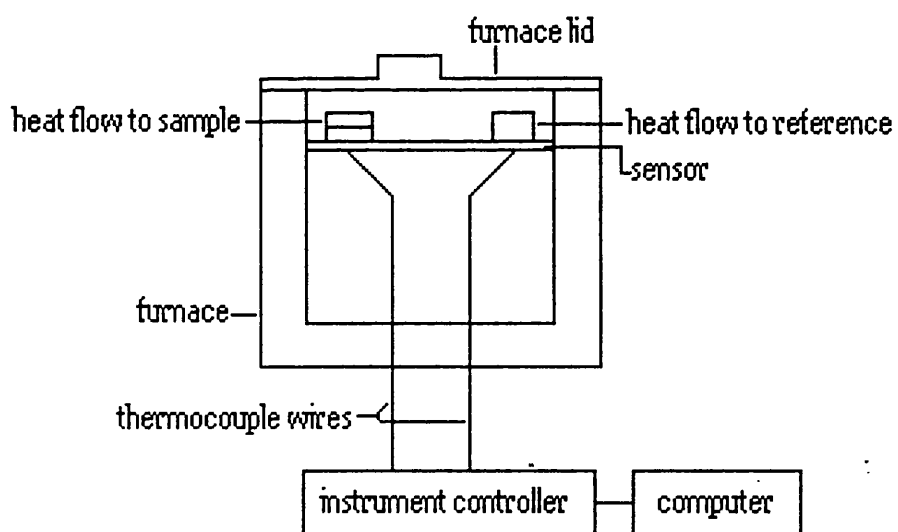


Figure 3.3: The Shimadzu DSC 50 recording instrument showing the heating chamber and control mechanism.

3.6.3. THERMO-MECHANICAL ANALYSIS (TMA)

The deformation characteristics (and hence the glass transition temperature) of the PEO-PVC composite films was measured against temperature. The effects of incompatibility between the polymers are accentuated in the deformation profile [3]. The instrument used for this experiment was a Stanton Redcroft TA 691 (figure 3.4), the heating rate (typically 5 °C/ minute), the temperature range (from -50°C to 150°C) was controlled using a Stanton Redcroft instrument controller and the deformation profile recorded using a chart recorder. The position of the quartz probe was monitored by a linear variable differential transformer (LVDT). The furnace temperature was measured using a Chrome Alumel thermocouple (reference junction at 0°C). The thermal mechanical probe was checked before each experiment to ensure that it was suspending freely. The load on the films during each experiment was always 20 g. A test run was performed using Poly(ethylene terephthalate) (PET) discs.

The thickness of the constant humidity conditioned composite PEO/PVC films (55% humidity, established by exposure to the vapour of 48 weight % 7 mol dm⁻³ H₂SO₄ and 52 weight % water at 25°C for 7 days), was measured with a digital micrometer. The films were then coated in silicone oil and cut into a square of about 5 mm × 5 mm to fit the stage of the machine.

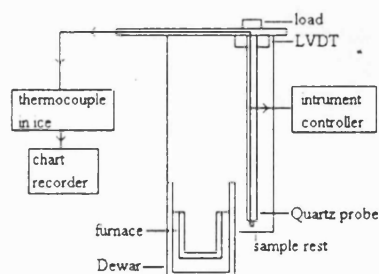


Figure 3.4: The thermo-mechanical setup showing the Stanton Redcroft instrument controller with the quartz tipped probe.

3.6.4. THERMOGRAVIMETRY (TG)

The mass change of these composite PEO-PVC membranes were measured as a function of temperature. The apparatus used was a Perkin Elmer TGA7 machine with TAS7 software (figure 3.5). The thermobalance encompasses a microbalance coupled to a furnace in which the sample is suspended freely on quartz wires. Nitrogen was used as the purge gas and all heating rates were controlled using a Perkin Elmer instrument controller coupled to the Perkin Elmer 7500 professional computer. Calibration of the instrument was done using Fe with the Curie point of 770°C [4].

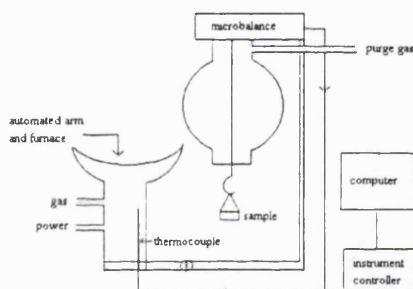


Figure 3.5: The setup for the thermogravimetry experiment showing the Perkin Elmer instrument controller coupled to the furnace and balance.

3.6.5. FOURIER TRANSFORM INFRARED SPECTROSCOPY (FTIR).

The infrared spectrum of the polymers and the composite films were obtained to explore any changes in the composite which might result from interaction of the polymers [5]. The amount of solvent in the film could also be deduced in this way. The spectroscopy was performed on films which had been supported with a piece of card with a window for the beam path and inserted into the sample holder of the Nicolet 205 FTIR machine.

3.6.6. OPTICAL MICROSCOPY.

Optical microscopy reveals any birefringence behaviour in the polymer film. This may be the result from: phase separation (any amorphous or crystalline states relating to composition or preparation) or stress and molecular orientation during preparation [6]. The optical properties of the composite films were recorded using a Jenalab optical microscope (resolution was $0.5\ \mu\text{m}$) with crossed polarizers coupled with a video camera head, monitor and a video printer to record the images.

Birefringent materials have a varying refractive index according to the direction of incident light and the orientation of optically anisotropic materials, to the plane of polarisation. The electric vector component of polarised light is split into two perpendicular plane polarised waves. The birefringent material has different refractive indices for the two polarised waves which pass through the material; one retarded relative to the other. The changed polarised waves pass through the sample which appears to be brightly coloured when using crossed polarisers with white light (the view being dark through crossed polarisers, in the absence of sample and residual strain in the optical glass). Birefringent materials have either uniaxial (one optic axis) or biaxial (two optic axes) such that, when viewed along the axes, the material appears isotropic. The refractive index of a material is at a maximum when the plane of polarisation contains the optic axes.

Generally, there are three types of birefringence: (1) orientation birefringence describes the degree of interaction between the electromagnetic wave and the bonding electrons in the molecule. Maximum interaction between the electric vector and the bond occurs when they are parallel, giving the highest refractive index. Hence birefringence depends on molecular orientation and bond polarisability. (2) Stress birefringence occurs on the application of stress leading to a change in bond polarisability dependent on the principal axis. (3)

Form birefringence results from a material with two or more phases of different refractive indices, hence a distortion of the electromagnetic field at the interface. Molecular extension occurs when a molecule exists in different conformations. The arrangement of an anisotropic molecule with links that show significant orientation in one plane but small end to end separation, has significant birefringence. There may be little orientation but significant end to end separation, giving small birefringence. If the links form a closed polygon, or are arranged with an equal orientation distribution with a large end to end separation, the result is a net birefringence of zero [7]. All these factors could describe the composite polymer film birefringence behaviour.

3.6.4. ^2H NUCLEAR MAGNETIC RESONANCE SPECTROSCOPY (NMR)

Using films equilibrated with D_2O , this method probes the mobility of deuterium nuclei, giving information on the states of water in the polymer film [8].

The D_2O conditioned films (equilibrated in pure D_2O vapour for 24 hours at room temperature) were packed into a standard NMR tube and sealed with teflon tape. The NMR machine was a MSL 300. A spectrum was taken at 213 and 293 K, and each spectrum was a combined average over 6 hours.

REFERENCES FOR CHAPTER 3

- [1] R. A. Robinson, R. H. Stokes (eds), "Electrolyte Solutions", ch. 11, Butterworths and Co. Ltd., London, 1959.
- [2] G. Van De Plaats, "The Practise of Thermal Analysis", ch. 7, Mettler, 1990.
- [3] D. Campbell, J. R. White, "Polymer Characterisation, Physical Techniques", ch. 12, Chapman and Hall, London, 1989.
- [4] R. C. Weast (eds), "The Handbook of Chemistry and Physics", Section E, p. 120, C. R. C. Press, 1978.
- [5] D. Campbell, J. R. White, "Polymer Characterisation, Physical Techniques", ch. 5, Chapman and Hall, London, 1989.
- [6] D. T. Grubb, L. C. Sawyer, "Polymer microscopy", ch. 2, Chapman and Hall, London, 1987.
- [7] C. E. H. Bawn, "The Chemistry of High Polymers", ch. 6, Butterworths, London, 1948.
- [8] H. Menge, T. Steurich, *Electrochim. Acta*, **13**, 1971, (1994).
- [9] D. Campbell, J. R. White, "Polymer Characterisation, Physical Techniques", ch. 6, Chapman and Hall, London, 1989.

CHAPTER 4
ELECTROCHEMICAL
RESULTS

CHAPTER 4. ELECTROCHEMICAL RESULTS

The results are presented in four parts. Firstly, some general aspects concerning the stability of the various films; secondly, some background studies concerning the interaction between PEO and ionic species in aqueous solution; thirdly, studies on pure PEO membranes and fourthly, studies on co-cast membranes.

4.1 DEVELOPMENT OF THE FILM PREPARATION METHOD

Initial studies were of pure PEO membranes. First, membranes were prepared by supporting an aqueous PEO solution on PET cloth discs. These films proved to be highly unstable with respect to time. Membrane puncture occurred after 20 minutes of immersion. Processed PEO gelatinous films (as described in chapter 3) were thicker and took some time first to hydrate and then to become completely permeable. This process took ~40 minutes. Figure 4.1 shows the resistance across such a membrane during the potentiometry experiment. Three stages are discernable: an initial phase of hydration of the membrane; a stage when both membrane resistance and potential difference were stable; followed by the membrane becoming completely permeable.

The first composite membranes co-cast from an organic solvent were hand cast onto a glass surface and allowed to dry at room temperature. These films were more stable in aqueous solution than both the aqueous films. They were able to separate two salt solutions for a period of 16 hours. The appearance of these films was heterogeneous and large domains of two optically different phases could be seen.

The films prepared using the casting machine (with cyclohexanone as solvent) were hydrophilic and stable in water over a period of at least 2 weeks and these films were used in later potentiometric experiments. The casting machine could reproducibly make homogeneous co-cast composite films. Films prepared

in this way were allowed to dry in a warm room at 30°C or radiant heated to a temperature in the range of 60 to 100°C. The films dried at the lower temperature took approximately 24 hours to dry sufficiently, so that they could be lifted from the casting plate. They were cloudy and white but homogeneous in appearance. The films dried in the range from 60 to 100°C took about 30 to 60 minutes to dry. These films were clear and homogeneous in appearance.

Membranes that had been dried using the heater at 30°C for a period of 12 to 60 hours gave a potentiometric response similar to the rapidly dried PEO-PVC films (60°C for 1 hour). Those membranes which had been dried for 12 hours gave immediate responses on exposure to solution whilst those dried for 60 hours had a very high resistance. When these membranes were first assembled into an electrochemical cell they behaved like an open circuit.

Rotary evaporated membranes were prepared to show the effect of the drying method in the preparation process on the potentiometric behaviour. In the co-cast membranes, the stationary polymer solution was dried for 1 hour in the temperature range of 60-100°C. During this time the polymer in solution could have separated out into domains or polymer layers, where one polymer crystallises first. This could have affected the potentiometric behaviour. Polymer solutions of rotary evaporated membranes were constantly in motion during the preparation, hopefully ensuring full integration of the polymers. The behaviour of rotary evaporated membranes is described in part four of this chapter.

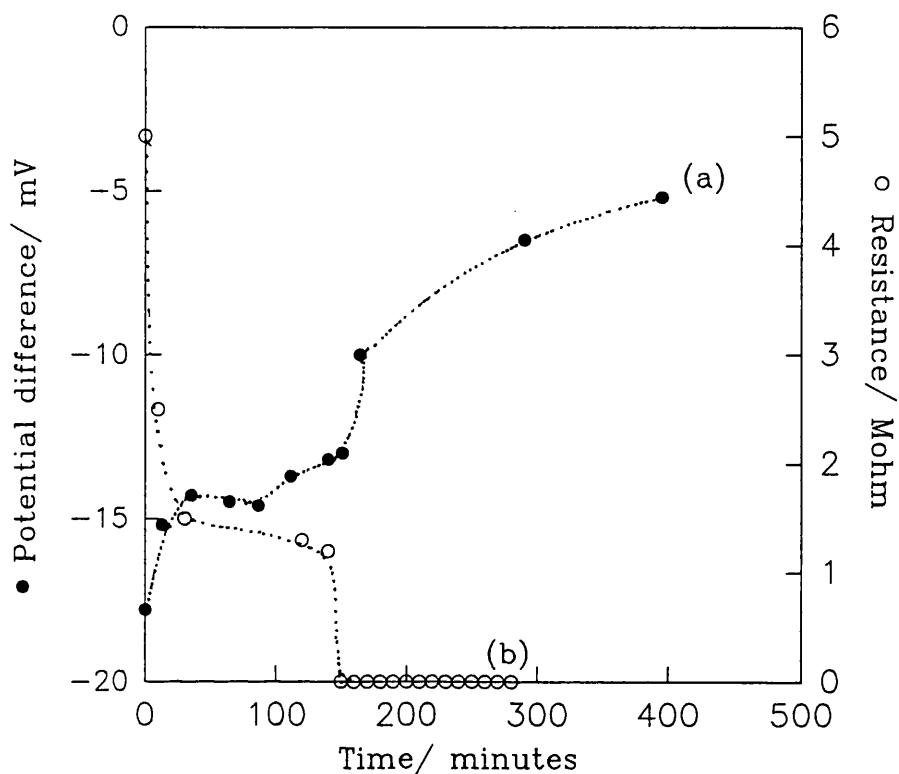


Figure 4.1: The potential difference vs. time for processed PEO films immersed between 0.1 and 0.01 mol dm^{-3} NaCl solutions at 25°C and the resistance across the membrane at the time of potentiometry measurement. The cell configuration was: (+) reference electrode/ 0.01 mol dm^{-3} NaCl/ membrane/ 0.1 mol dm^{-3} NaCl/ reference electrode (-).

The expected junction potential between the two solutions, calculated using the Henderson equation is -5 mV (aqueous transport numbers of the ions were used). If the membrane were ideally permselective, the potential difference would be 59 mV [1]. As the membrane hydrated the resistance dropped and the potential difference decreased. This continued until the membrane became completely permeable. That the membrane potential difference is more smaller than the junction potential difference implies that the mobility ratio $U_{\text{Cl}^-}/U_{\text{Na}^+}$ is greater in the membrane than in aqueous solution (see Chapter 6).

4.2 BACKGROUND STUDIES ON AQUEOUS PEO SOLUTIONS

4.2.1 CONDUCTIVITY OF SALT SOLUTIONS CONTAINING PEO

The conductivity of various salts in water and in aqueous PEO solutions are shown in figure 4.2, and limiting equivalent conductivity ratios (water/ aqueous PEO) are given in table 4.1. The ratio $(\Lambda_{aq}^0)_{\text{expt}}/(\Lambda_{aq}^0)_{\text{literature}}$ was consistent for the different salts, implying an error in the cell constant correction (applied automatically by the conductance meter used).

The molar conductivity of salts in PEO are be compared to those in water. The molar conductivity of NaCl and NaNO₃ increased in PEO. The greatest change was for NaNO₃, whose limiting conductivity in PEO solution was increased significantly, from 105 to 150 S cm² mol⁻¹.

The variations in the slope $d\Lambda/d(C)^{1/2}$ were: a slight decrease in the presence of PEO for NaCl, remained unchanged for Na(pTS) and increased notably for NaClO₄ and increased significantly for NaNO₃. The characteristic conductivity curve of the sodium-dodecylsulphate indicates micelle formation [2], with the critical micelle concentration somewhat lower in the presence of PEO.

4.2.2. VISCOSITY RESULTS

The viscosity η of the aqueous PEO solutions at 25°C is given in table 4.2. The viscosity of pure water η_0 was taken to be 1.002 centipoise (cp) at 25°C [4] and was used in the viscosity ratios (η/η_0). The specific viscosity is calculated from the following relation: $\eta_{sp} = (\eta - \eta_0) / \eta_0$ which expresses the change in viscosity of the polymer solution compared to the pure solvent. The viscosity is determined by the concentration, of the dissolved polymer, hence the viscosity number is expressed as: $\eta_{sp}C$ where C is the polymer

concentration [5]. The viscosity increases exponentially with increasing polymer concentration: $\ln(\eta/\eta_0)/C$ was constant.

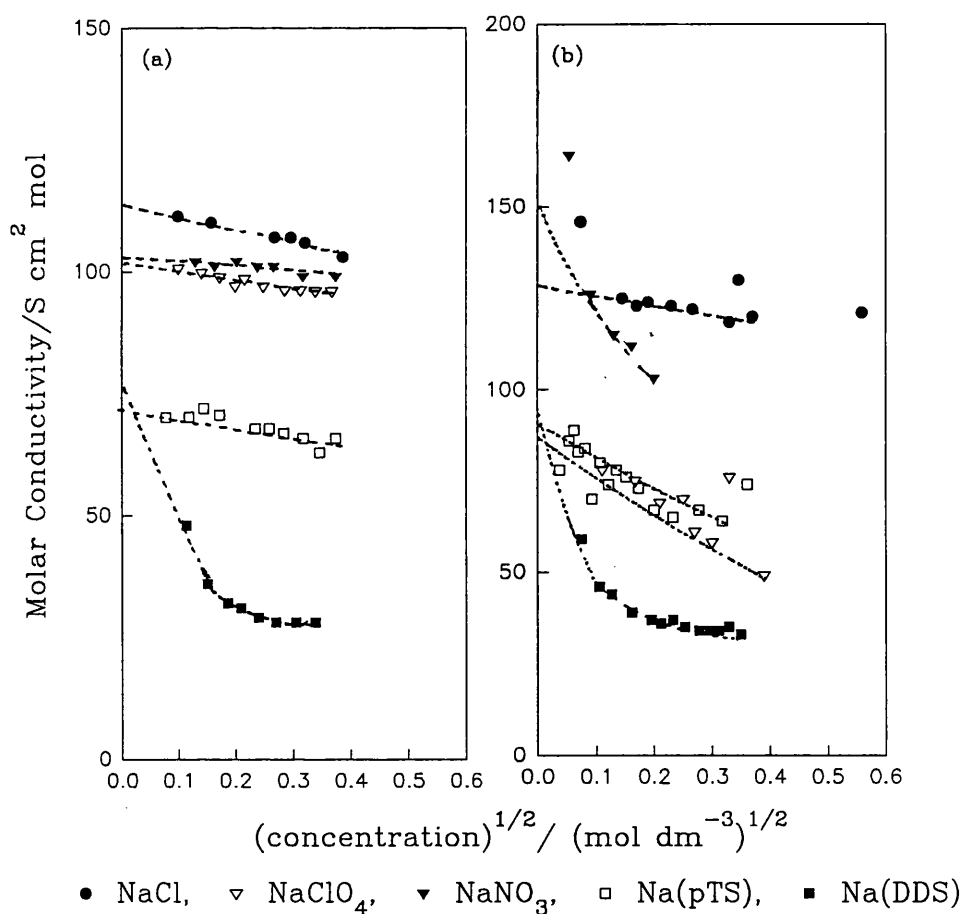


Figure 4.2: Molar conductivity vs. the square root of the solute concentration for (a) various salts dissolved in water with a regression plot to obtain the limiting molar conductivity, (b) various salts dissolved in 1 weight % aqueous PEO solution. The behaviour of the various salts changed from water to the PEO solution.

Salt	$\Lambda_{\text{PEO}}^0/\Lambda_{\text{H}_2\text{O}}^0$	Experimental	Literature Λ_{aq}^0
NaCl	1.16	115	126.5
NaClO ₄	1.37	102	117.4
NaNO ₃	1.46	105	121.5
Na(pTS)	1.06	72	-
Na(DDS)	1.10	-	-

Table 4.1: The limiting molar conductivity ratios for salts in PEO and water and the literature values of aqueous molar conductivities at 25 °C [3]. The molar conductivity ratios show that there is an increase in the molar conductivities in PEO compared to water: the largest increase being for the NaNO₃ salt, the smallest being for the sodium p-toluenesulphonate salt.

concentration g cm ⁻³	η/cp	$\eta_{\text{sp}}/\text{cp}$	$[\ln(\eta/\eta_0)]/C$ cm ³ g ⁻¹
13.6	2	1.0	1.15
27.3	4	3.0	1.15
38.6	6	5.0	1.05
50.0	10	9.0	1.04
56.8	14	13.0	1.05
68.2	24	23	1.05
79.5	34	34	1.01
91.0	45	44	1.0

Table 4.2: Concentrations and specific viscosities of aqueous PEO solutions of various concentrations. This shows that the specific viscosity increases significantly on increase in concentration. The $\ln(\eta_{\text{sp}}/C)$ term changed only slightly with a large increase in concentration and specific viscosity.

4.2.3. COMPLEXATION OF Ag^+ BY AQUEOUS PEO: POTENTIOMETRIC TITRATION

The cell configuration was (-) S.C.E/ Saturated NH_4NO_3 : KNO_3 salt bridge: 0.05 mol dm^{-3} AgNO_3 , 0.05 mol dm^{-3} PEO solution, $x \text{ dm}^3$ distilled water/ Ag wire electrode (+). The initial concentration of AgNO_3 was 0.05 mol dm^{-3} and 0.05 mol dm^{-3} PEO; the solution was diluted with water.

The results in figure 4.3 show the quantity $\ln[(n_i/cV)-1]$ vs. $\ln V$ where n_i is the total number of moles of silver ions present, V the total volume of the titration and c is the quantity

$$c = \frac{C}{C^0} = \exp\left(\frac{(E-E^0)F}{RT}\right) \quad (4.1)$$

where E is the experimentally determined potential of the silver electrode.

The experiment was repeated until the readings were consistent.

The potentiometric measurement changed slightly on addition of the PEO to the AgNO_3 solution (a change of 10 mV) and a further change of 30 mV on the total addition of water. Figure 4.3 shows a variation in the silver ion activity with increase in total volume indicating the amount of silver ion-PEO complexation. The average formation constant of silver ion-PEO complex was found to be 0.019 ± 0.002 and the average stoichiometry of the silver ion-PEO complex was 0.66 ± 0.012 . When n_i/cV was plotted against $1/V$, the limiting value of the formation constant at infinite dilution (when $1/V \rightarrow 0$), was found to be 0.135 ± 0.044 . In view of PEO solutions used directly with Ag/AgCl reference electrodes, minimum complexation of the silver ions can thus be assumed. Hence the liquid junction potential between the reference electrodes in contact with PEO solution may be assumed to be constant [6]. This observation is also of importance in connection with the later discussion of the generation of membrane potential.

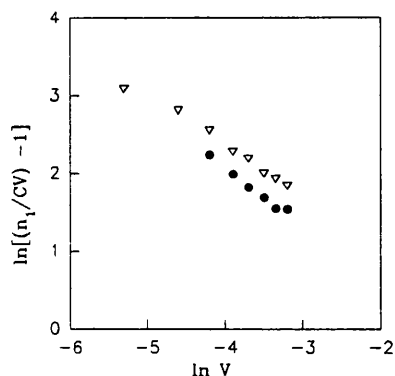


Figure 4.3: The variation of $\ln[(n_1/cV)-1]$ vs. $\ln V$ from which the complex formation constant and the silver ion-PEO ratio was calculated. Symbols are defined in the main text.

4.2.4. POTENTIOMETRY MEASUREMENT OF SALT COMPLEXATION BY PEO

A potentiometric cell with a liquid junction was constructed to assess the possibility of complexation of other cations by PEO. The potentiometric cell consisted of:

(+) reference electrode/ 0.1 mol dm^{-3} salt solution and $x \text{ cm}^3$ PEO solution : 0.1 mol dm^{-3} salt solution / reference electrode (-).

In the experiment 10 cm^3 of a 0.1 mol dm^{-3} salt solution was connected to 10 cm^3 of the same concentration salt solution, using a salt bridge in the same salt concentration. The expected potential difference is zero. On addition of PEO solution to one compartment and thorough mixing, the potential difference reading should be approximately the same if very little or no complexation occurs. However, the potential difference would be large if there was complexation of the salt and PEO molecules.

Figure 4.4 shows the variation of the potential with salt concentration and demonstrates that there is no significant complexation of Na^+ , K^+ or Mg^+ by PEO in dilute aqueous solution.

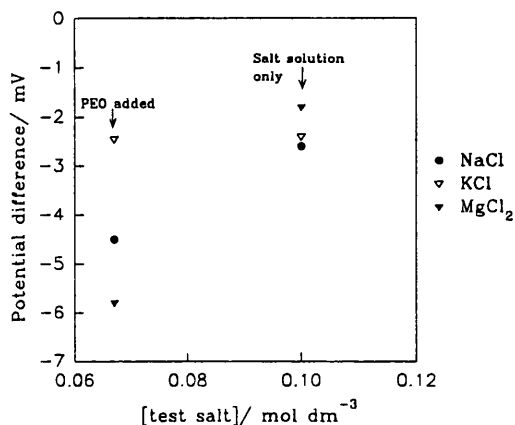


Figure 4.4: The effect of PEO on salt activity. The change in the potential difference upon the addition of 0.1 mol dm^{-3} aqueous salt solution to 1 wt % (weight percentage) PEO solution is shown. The potential difference change can be attributed simply to the effect of the small dilution of the salt in the test compartment.

4.3. POTENTIOMETRIC BEHAVIOUR OF PURE PEO MEMBRANES

Membranes described in this section are those formed by using PEO and water only. The potential difference vs. time for one such type of membrane has already been presented (figure 4.1). The tests on both the supported aqueous and processed PEO membranes were made using a vertical screw type cell (chapter 3.5). The salts used in these tests were HCl and various sodium salts.

4.3.1 SUPPORTED AQUEOUS PEO MEMBRANES

Membranes described in this section are those formed by supporting an aqueous PEO solution on PET mesh. The behaviour of these membranes to HCl activity are shown in figure 4.5 and for the other salts in figure 4.6. Apparent transport numbers in the membrane were calculated from equation 2.21 and are shown in table 4.3. The measurements on these membranes had

to be taken quickly in order that the whole concentration range be measured with one membrane before it became totally permeable (time taken ~20 minutes).

The film shows no perm-selectivity to H^+ in HCl solutions, the t_{H^+} calculated being the same as that for an aqueous solution (table 4.3). The response for the Na(pTS) and Na(DDS) salts showed cation selectivity over the anion. For the other salts, $NaClO_4$, KCl, KNO_3 and CsCl, the transport numbers of the cation and anion are both similar. In general, transport numbers of ions in these membranes were similar to those in aqueous solution.

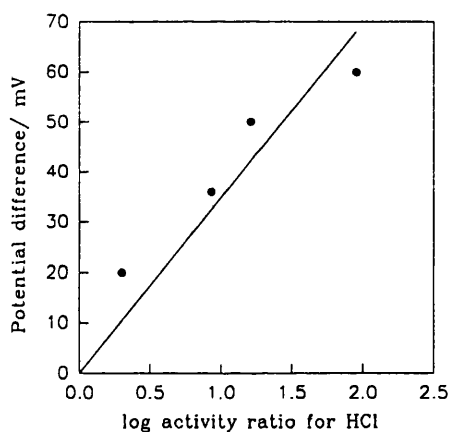


Figure 4.5: The behaviour of aqueous supported PEO films in HCl with the least square curve fit from which the apparent transport numbers are calculated. The cell configuration was:

(+) reference electrode/ X m HCl/ membrane/ 0.1 m HCl/ reference electrode (-).

The deviation from the expected straight line may be due to the potential difference not having reached its equilibrium value.

4.3.2. PROCESSED PEO MEMBRANES

The behaviour of these membranes in NaCl solution is reported in figure 4.7. Although the transport numbers derived from graphs such as figure 4.7 are the same as (within the experimental error) those in aqueous solution. The direct comparison found in figure 4.1 confirms that the t_{Na^+} was slightly diminished.

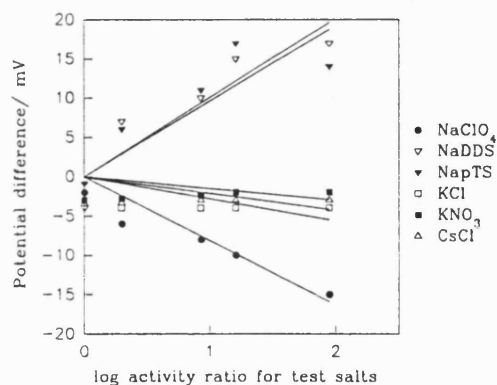


Figure 4.6: The behaviour of aqueous supported PEO films in various salt solutions.

The cell configuration was:

(+) reference electrode/ X m test solution/ membrane/ 0.1 m salt solution/ reference electrode (-).

Each salt solution was tested with a new membrane because these membranes became completely porous after the series of solution tests.

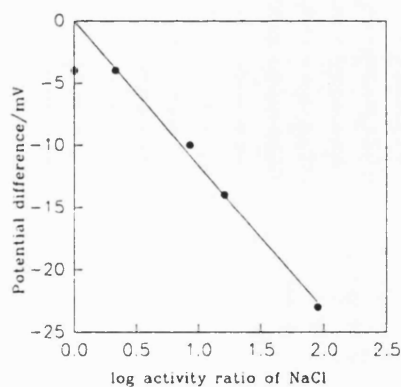


Figure 4.7: The potentiometric behaviour of processed PEO membranes with NaCl with the least squares curve fit from which the apparent transport numbers were calculated. The last measurement was an activity ratio of zero but there was a non-zero response. This could be due to the dissolved membrane in the test solution resulting in a non-zero activity ratio across the membrane. The activity ratios are calculated from activity coefficients from literature [7].

Salt	t_+	literature t_+
HCl	0.80	0.82
NaClO ₄	0.44	0.43
Na(pTS)	0.57	-
Na(DDS)	0.58	-
KCl	0.53	0.49
KNO ₃	0.52	0.51
CsCl	0.53	0.50
NaCl *	0.39	0.40

Table 4.3: The apparent transport numbers of various salts in the aqueous supported PEO membranes at 25 °C compared with the literature values of aqueous salt solutions. The apparent transport number of processed PEO membranes in NaCl are also given (marked with *), compared to the literature value [7].

4.4. POTENTIOMETRIC BEHAVIOUR OF CO-CAST PEO-POLYMER MEMBRANES

The ionic transport across co-cast membranes was investigated using potentiometry. Variations in the membrane composition and preparation procedure were explored to observe any effects in the membrane transport properties. This section is divided into five main sections; firstly, slowly dried PEO-PVC membranes, prepared at a temperature of 30°C for 12 hours; secondly, quickly dried PEO-PVC membranes, prepared at a temperature > 60°C; thirdly, PVC-Polymer membranes that were prepared at 60°C

incorporating Poly(methacrylate) (PMA), Poly(vinylmethyl ketone) (PVMK) or carboxylated PVC-PEO; fourthly, some PEO-PVC membranes using a different source of PVC and finally, some membranes which had been dried using a rotary evaporator.

4.4.1. POTENTIOMETRIC BEHAVIOUR OF SLOWLY DRIED PEO-PVC MEMBRANES

A typical time-potential difference behaviour of slowly dried membranes first immersed in solution is given in figure 4.8. Figure 4.8 shows that a steady potential difference was not achieved until typically after 30 minutes. This is attributed to the slow hydration of the polymer. The rate of hydration depends on composition i.e. 45% > 25% > 15%. After a series of tests, the clear membranes became cloudy-a consequence of soaking in water. This effect was not seen for the rapidly dried membranes, the hydration of PEO occurring in smaller domains which was not visible. The potential response for the 45% PEO membrane was opposite in sign to that for the 15 and 25% membrane, indicating that the Cl^- ion was transported faster than the Na^+ ion across the 45% PEO membrane. The 45% membrane showed little variation of the potential difference with time (< 2 mV). Figure 4.9 shows the variation of the potential difference with the solution activity ratio, for NaCl. There was a regular and reproducible trend in behaviour. Membranes with 5%, 15% and 25% PEO were cation selective with a response magnitude decreasing in the order 5% > 15% > 25% PEO. The 41% PEO membrane gave similar cation and anion transport numbers, whilst the 45% PEO membrane showed transport numbers similar to those in aqueous solution (see table 4.4).

The variation of potential with time following replacement of NaCl by HCl, on both sides of the membrane, is shown in figure 4.10. The corresponding potential difference variation with solution activity ratio in figure 4.11.

The response was around 42 mV per decade of solution activity, without a

pronounced regular trend with membrane composition. The apparent transport numbers in these membranes were similar to those in aqueous solution (see table 4.5)

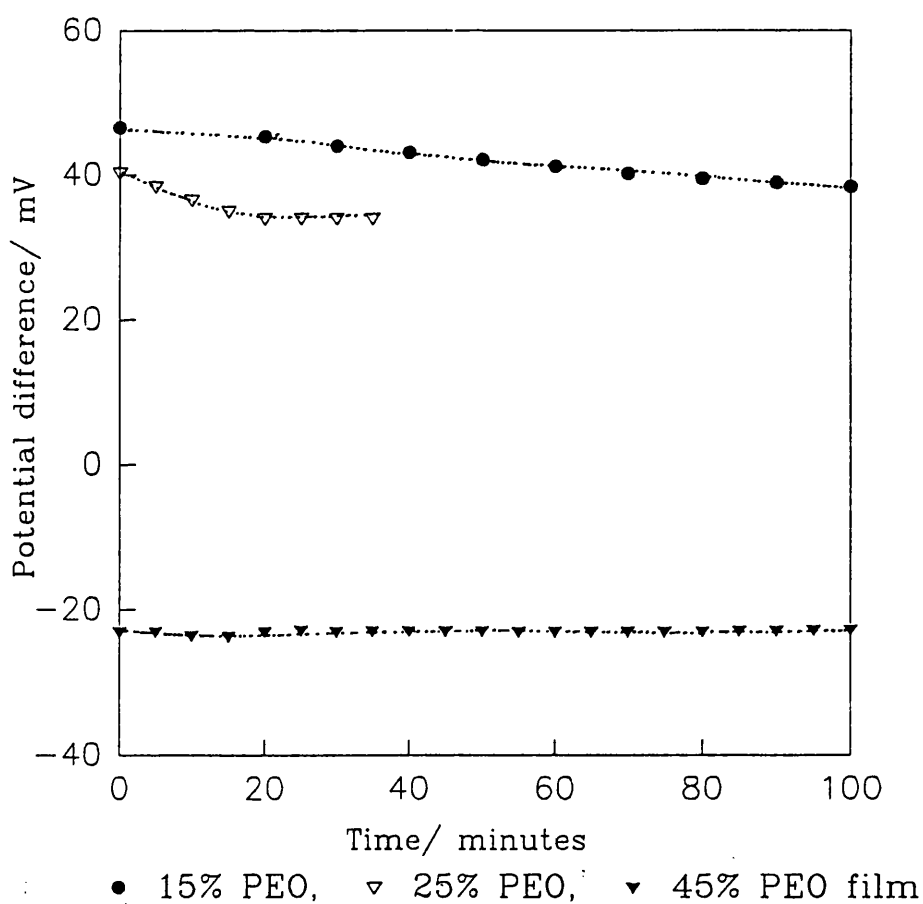


Figure 4.8: The potential difference vs. time response for co-cast composite PEO-PVC films dried at 30°C for 12 hours. The membranes were immersed as fresh, non-hydrated membranes. The cell configuration was:

(+) reference electrode: 0.001 mol dm⁻³ NaCl; membrane: 0.1 mol dm⁻³ NaCl; reference electrode (-).

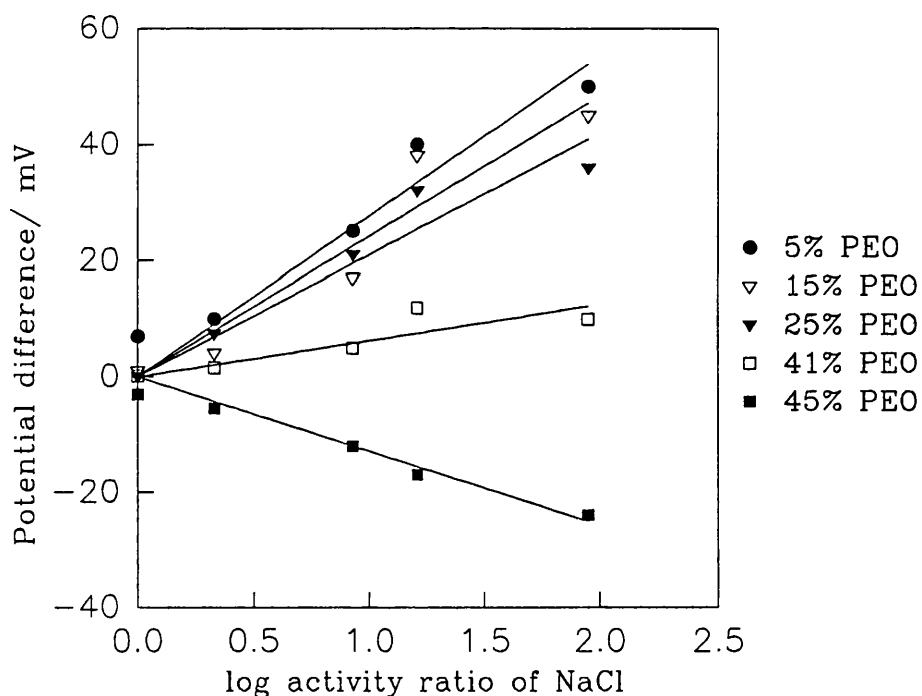


Figure 4.9: The potentiometric behaviour of slowly dried co-cast PEO-PVC membranes in NaCl. The solid lines show the least square fit used to calculate the apparent transport numbers. The cell configuration was: (+) reference electrode/ X m NaCl/ membrane/ 0.1 m NaCl/ reference electrode (-). Activity ratios are from literature [7].

The change in sign indicates that increasing the PEO content results in a steady decrease in the Na^+ ion transport number, which finally approaches the value for aqueous solution.

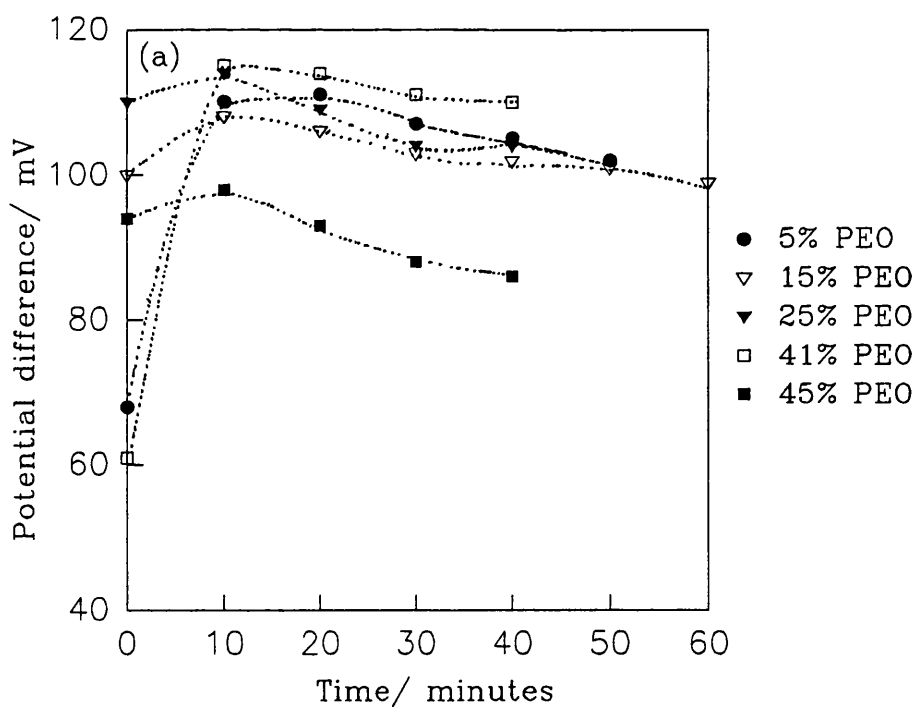


Figure 4.10: The potentiometric response of slow dried PEO-PVC films with time, following the replacement of NaCl with HCl, on both sides of the membrane. The cell configuration was:

(+) reference electrode/ $0.001 \text{ mol dm}^{-3} \text{ HCl}$ / membrane/ $1 \text{ mol dm}^{-3} \text{ HCl}$ / reference electrode (-).

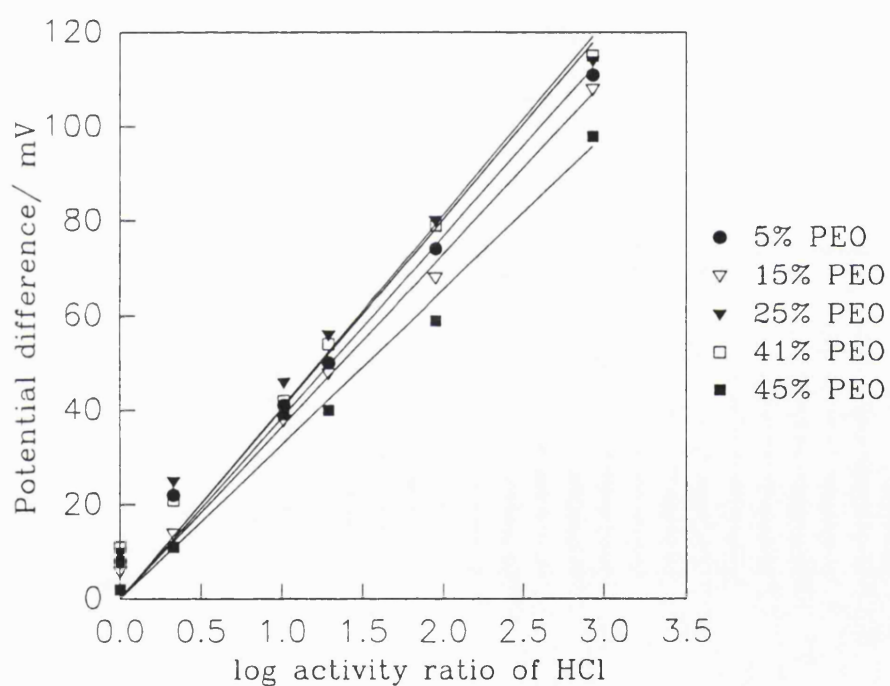


Figure 4.11: The potentiometric behaviour of slow dried PEO-PVC films in HCl. The solid lines show the least squares fit used to calculate the apparent transport numbers.

The cell configuration was:

(+) reference electrode/ X m HCl/ membrane/ 1 m HCl/ reference electrode (-). The activity ratios were computed from literature [7].

% PEO	t_{Na^+}
5	0.74
15	0.68
25	0.65
41	0.56
45	0.39
Aqueous solution	0.40

Table 4.4: The apparent transport numbers for the slowly dried, 30°C for 12 hours, co-cast PEO-PVC membranes in NaCl, calculated from figure 4.9 from the Nernst equation (refer to theory chapter).

% PEO	t_{H^+}
5	0.82 ± 0.02
15	0.80 ± 0.02
25	0.84 ± 0.02
41	0.84 ± 0.02
45	0.77 ± 0.04
Aqueous solution	0.82

Table 4.5: The apparent transport numbers for slowly dried, 30 °C for 12 hours, co-cast PEO-PVC membranes in HCl as calculated from figure 4.11. The 5% PEO membrane matches closely to the literature transport value of H⁺ ions in water of 0.82. The cation transport numbers are all the same within the experimental error.

4.2.2. POTENTIOMETRIC BEHAVIOUR OF QUICKLY DRIED PEO-PVC MEMBRANES

The potential time-variation of freshly immersed membranes is shown in figure 4.12. Maximum drift time response was shown for the highest concentration ratio, the first measurement in the sequence, the potential difference increasing from 35 mV to 120 mV in the first 20 minutes of exposure. The other solution tests did not vary in such a manner, although there was usually a slight variation in the first 10 to 20 minutes of the measurement before the equilibrium potential difference was reached. In figure 4.13, the time course of a sequence of experiments, in which exposure to HCl is followed by NaCl on the same membrane, shows the effect of residual ions inside the membrane on the subsequent potential measurements and also shows the time taken to reach an equilibrium potential difference.

Freshly immersed dry membranes were highly resistive. However, this changed with immersion time. Older membranes established equilibrium much faster. Films of thickness $> 100 \mu\text{m}$, dried at 60°C , particularly with low PEO content ($<20\%$), exhibited very high resistances. However, such rapidly dried films that were resistive could be used by soaking them in 1 mol dm^{-3} HCl for 2 weeks. It was postulated that this effect was due to hydration of the membrane brought about by the permeation of the H^+ ions into its interior.

The steady-state potentiometric response of these membranes to different acids and solutions of various pH is given in figure 4.14.

Some differences in behaviour (transport numbers are shown in table 4.8) and apparent anomalies may be noted. The HNO_3 response was linear for the 5% PEO film but not for the 40% which showed an anomalous potential difference value in the first test solution ($\log_{10} a_1/a_2=2.9$). This may have been because the equilibrium potential had not been reached. In contrast, the 5% PEO membrane

behaved well for the HCl and H₂SO₄. The potential difference variation with pH depended on the membrane composition, and fluctuated for pH > 2. This indicates that transport of some buffer ions may be hindered in the 5% and 20% PEO membrane, resulting in a membrane response which is indifferent to changing pH. The 40% PEO membrane shows a steady response to the pH solutions indicating that there is a concentration gradient of buffer ion across the membrane.

The response in NaCl and various single salt solutions is given in figure 4.15. The sequence of experiment was: NaCl, NaNO₃, HNO₃, H₂SO₄, KCl, CaCl₂, MgCl₂ and CsCl. The potential difference response of the membranes stabilised with time, the potential response was also affected by sample history. Well used samples varied little with time and it was noticed that as the membranes got older they became opaque, a sign of membrane hydration. The behaviour of the 5% PEO membrane in the salt solution was very irregular, in contrast to that in acid solution and that of membranes with higher PEO content. Transport numbers are shown in tables 4.6 and 4.7 and were very similar to values in aqueous solution (tables 4.6, 4.7, 4.8). This is in contrast to the behaviour of the slowly dried membranes which showed a Na⁺ ion selectivity in membranes with a low PEO content.

The potentiometric response was measured in mixed solutions of HCl and NaCl (fig 4.16) and compared to the ideal response given by the Henderson equation [1] for a permeable membrane using mobilities from ions in water [7]. The experimental values and calculated values are in close correspondence deviating by 20 mV for the HCl solution and 25 mV for the NaCl solution. The differences do depend on PEO content but a regular trend was not observed. Thus confirming that the apparent ion mobilities in these membranes are similar to those in pure water.

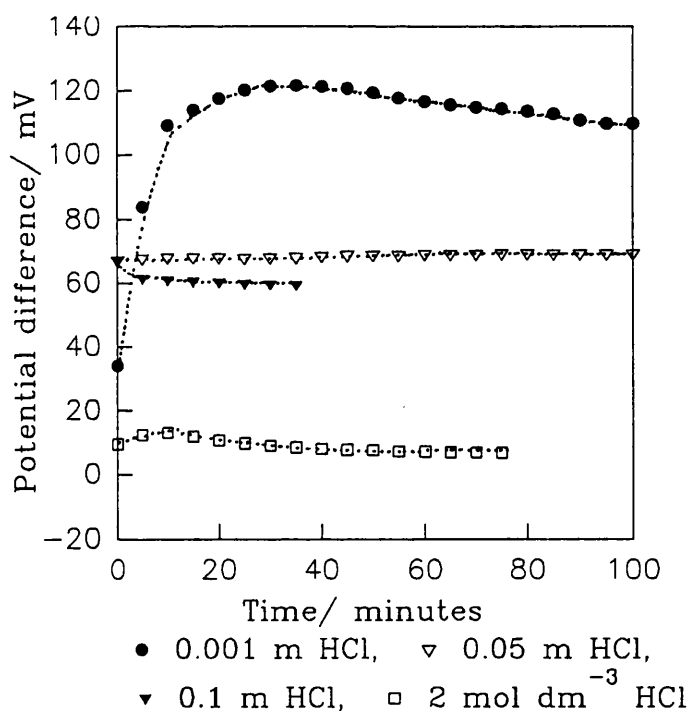


Figure 4.12: Potential difference vs. time response for a 10% PEO co-cast rapidly dried PEO-PVC film. The film was new and this figure illustrates the variation in the potential difference at the start of most measurements. Cell configuration was: (+)reference electrode/ test solution/membrane/ 2 mol dm⁻³ HCl/reference electrode (-).

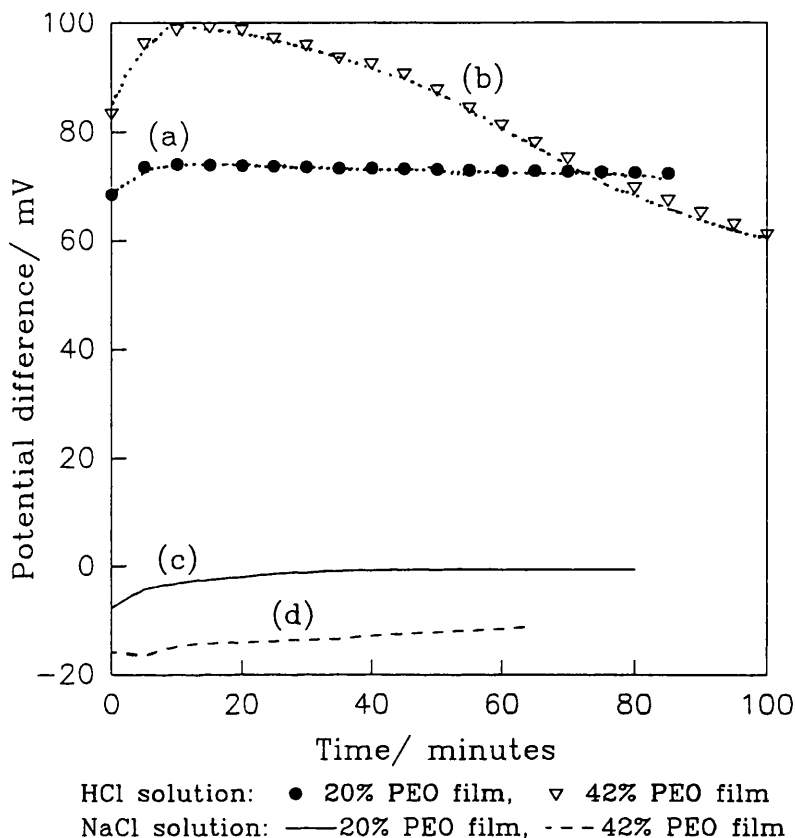


Figure 4.13: The potential difference-time response of rapidly dried new membranes of (a) 20% and (b) 42% PEO in HCl. The cell configuration was :
(+) reference electrodes/ $0.01 \text{ mol dm}^{-3} \text{ HCl}$ / membrane/ $2 \text{ mol dm}^{-3} \text{ HCl}$ / reference electrodes (-). Then they were immersed into NaCl, (c) 20% and (d) 42% PEO membrane. The cell configuration was:
(+) reference electrode/ $0.01 \text{ mol dm}^{-3} \text{ NaCl}$ / membrane/ $0.1 \text{ mol dm}^{-3} \text{ NaCl}$ / reference electrode (-).

Although the 42% membrane potential difference drifted by 40 mV in HCl solution over 100 minutes, the subsequent test with NaCl showed a stable film. The 20% PEO membrane had a potential difference drift of 10 mV in the first HCl solution and a smaller drift of 5 mV in the first 10 minutes of the subsequent measurement in NaCl.

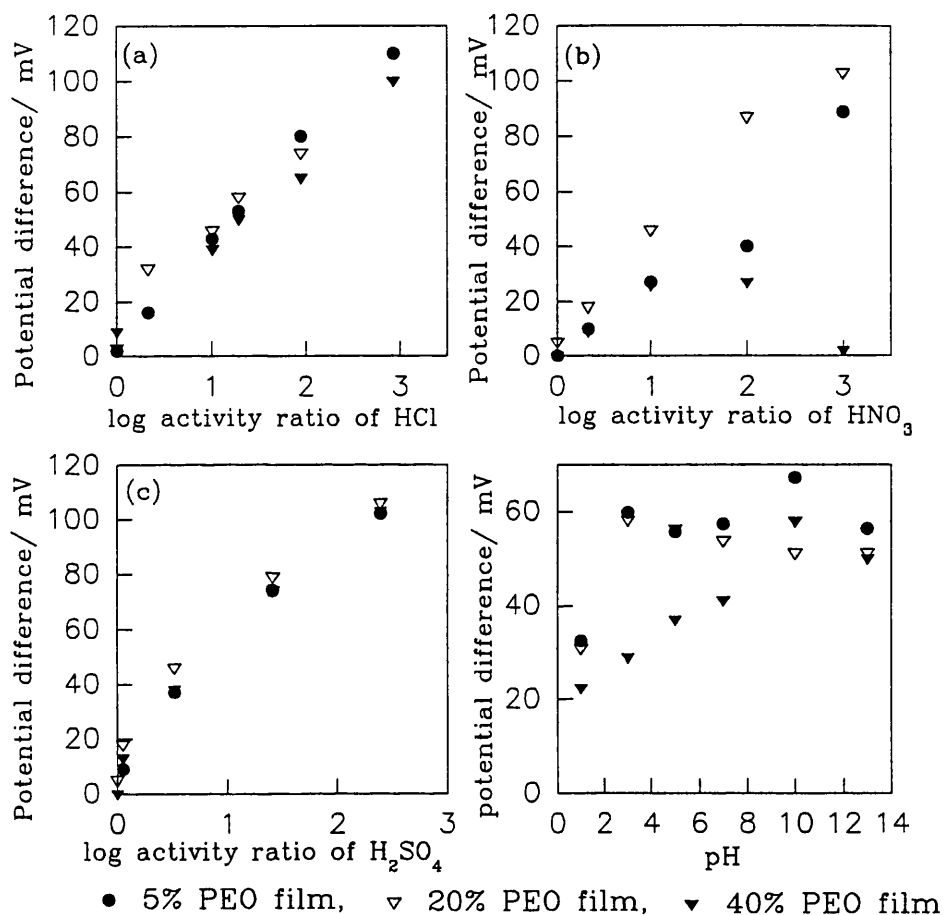


Figure 4.14: The potentiometric behaviour of quickly dried co-cast PEO-PVC membranes of various compositions in acid and pH solutions. The cell configuration was:
 (+) reference electrode/ test solution/ membrane/ constant salt solution/ reference electrode (-).

In section (a) the test solution was HCl, 1 mol dm⁻³ HCl was the constant solution; (b) in HNO₃, the constant solution 1 mol dm⁻³ HNO₃, (c) in H₂SO₄, the constant solution 1 mol dm⁻³ H₂SO₄ and (d) where the test solution varied in pH (as described in the experimental chapter 3), the constant solution was 1 mol dm⁻³ HCl.

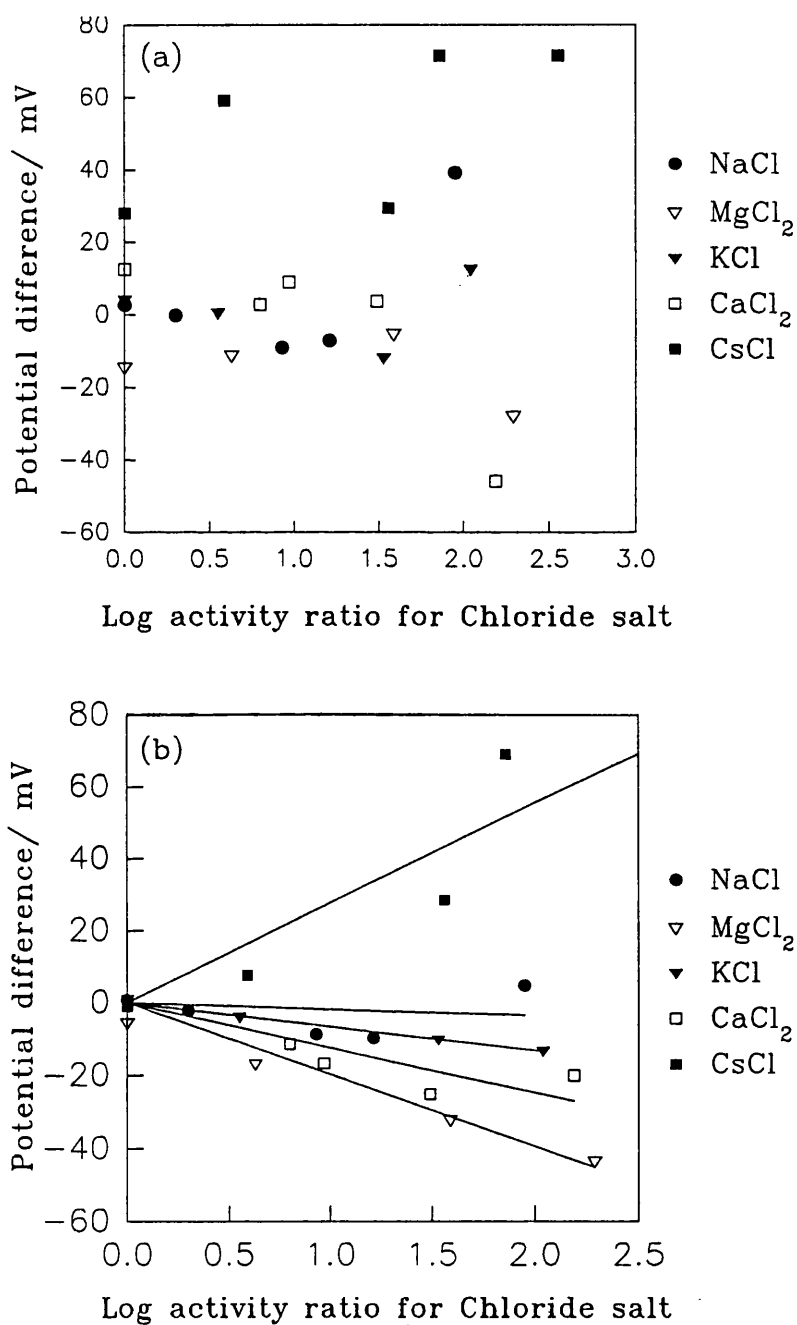


Figure 4.15: The behaviour of quickly dried PEO-PVC membranes in various salts, for a (a) 5% PEO membrane and (b) a 20% PEO membrane with a least squares curve fit from which the apparent transport numbers were calculated.

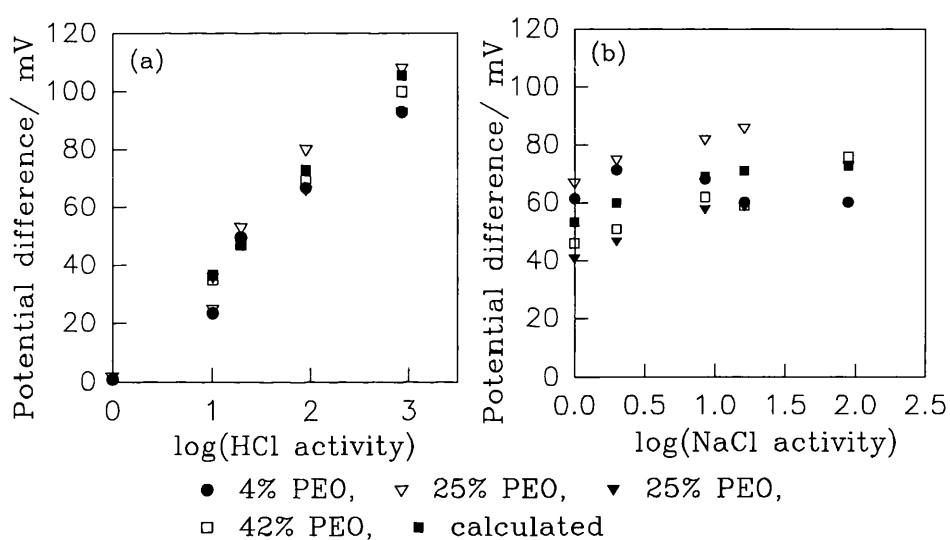


Figure 4.16: The potentiometric behaviour of quickly dried co-cast PEO-PVC membranes in mixed HCl, NaCl solutions compared to that calculated using the Henderson equation [7] using aqueous solution ion mobilities. The cell configuration was:

(+) reference electrode/ mixed salts/ membrane/ 1 mol dm^{-3} HCl, 0.1 mol dm^{-3} NaCl/ reference electrode (-). The mixed salt solution was, for HCl variation 0.001 to 1 mol dm^{-3} with NaCl fixed at $0.001 \text{ mol dm}^{-3}$, for NaCl variation, 0.001 to 0.1 mol dm^{-3} with HCl fixed at 0.01 mol dm^{-3} .

% PEO	Drying conditions	t_{H^+}
4	60°C, 1.5 hours	0.84
0	60°C, 1 hour	0.86
25	60°C, 1.5 hours	0.84
35	60°C, 1.5 hours	0.80
35	65°C, 1.5 hours	0.80
42	60°C, 1 hour	0.80

Table 4.6: The apparent cation transport numbers for quickly dried co-cast PEO-PVC membranes in HCl at 25°C solution (fig 4.14).

The H^+ transport number in these membranes is quite similar to the literature value for H^+ ions in water: 0.81 and did not change with drying conditions and PEO content.

% PEO	Drying conditions	t_{Na^+}
4	60°C, 1 hour	0.42
25	60°C, 1 hour	0.43
35	60°C, 1 hour	0.43
35	65°C, 1.5 hours	0.43

Table 4.7: The apparent cation transport numbers of Na^+ in quickly dried co-cast PEO-PVC membranes in NaCl solution at 25° C calculated from figure 4.15. These transport numbers did not change with drying conditions and PEO content.

% PEO	HCl	HNO ₃	H ₂ SO ₄	KCl	KNO ₃	NaCl	NaClO ₄	NaNO ₃	NaDDS	CsCl	MgCl ₂	CaCl ₂
5%	0.86	0.72	0.93	0.35	0.50	0.41	0.56	0.70	0.58	0.70	0.32	0.35
20%	0.86	0.84	0.93	0.45	0.50	0.42	0.63	0.58	0.70	0.56	0.58	0.39
40%	0.83	-	0.90	0.44	0.50	0.42	0.46	0.44	0.67	0.43	0.32	0.20
Water	0.82	0.83	0.90	0.49	0.51	0.40	0.43	0.41	-	0.50	0.26	0.28

Table 8: The apparent transport numbers of cation in the quickly dried co-cast PEO-PVC membranes. The salts which are similar to ions in water are HCl, KNO₃ and NaCl in the PEO compositions shown. For the NaNO₃ and CsCl salts, their transport numbers are greater at the 5% PEO compositions and the value at 40% is similar to that in water. Other salts such as HNO₃, KCl, MgCl₂ and CaCl₂ have transport numbers fluctuating in magnitude from the values in water. H₂SO₄ and NaClO₄ have cation transport numbers higher than that in water. For H₂SO₄, 5% PEO has the highest cation transport number; 20% and 40% PEO show the same value. The NaClO₄ cation transport number fluctuates from 0.56 to 0.46 but is greater than the value in water. The transport numbers for the 5% PEO membrane were forced fit through zero, the potential near low activity ratio was considered since those at high activity ratio showed the most drift.

4.4.3. POTENTIOMETRIC BEHAVIOUR OF PVC-POLYMER MEMBRANES

4.4.3.1. POTENTIOMETRY OF PVC-POLY(METHYLACRYLATE) AND PVC-POLY(VINYLMETHYLKETONE) MEMBRANES

The time-variation of PVC-PMA dry membranes immersed in HCl is shown in figure 4.17. The potential difference drifted upwards from the initial reading and then reached an equilibrium value after typically 60 minutes. The next measurement (0.01 mol dm^{-3}) had a potential that started at the last membrane measurement of -50 mV and drifted up to its equilibrium value. This measurement took 10 minutes to stabilise to a value of -40 mV . The rest of the measurements followed this pattern of starting from the last measurement in the previous solution, and drifting upwards to a new equilibrium value.

Identical behaviour was observed for the PVMK-PVC films. The first measurement took the longest to stabilize (60 minutes). However, at higher HCl concentrations an abrupt transition was observed. The potential shifted to a new level (20 mV).

The behaviour of PVC-PMA and PVC-PVMK membranes in HCl, NaCl and solutions of various pH is given in figure 4.18. The behaviour of PVC-PMA, PVC-PVMK films to solutions of mixed salts is shown in figure 4.19.

The PVMK membranes follow the expected behaviour well but the PMA has a response opposite in sign to that expected, both in the mixed salt and in HCl solutions. That is, for PMA-PVC membranes, it was apparent that the transport number of H^+ was remarkably decreased from its value in aqueous solution. This is in complete contrast to the behaviour to NaCl, which was hardly altered.

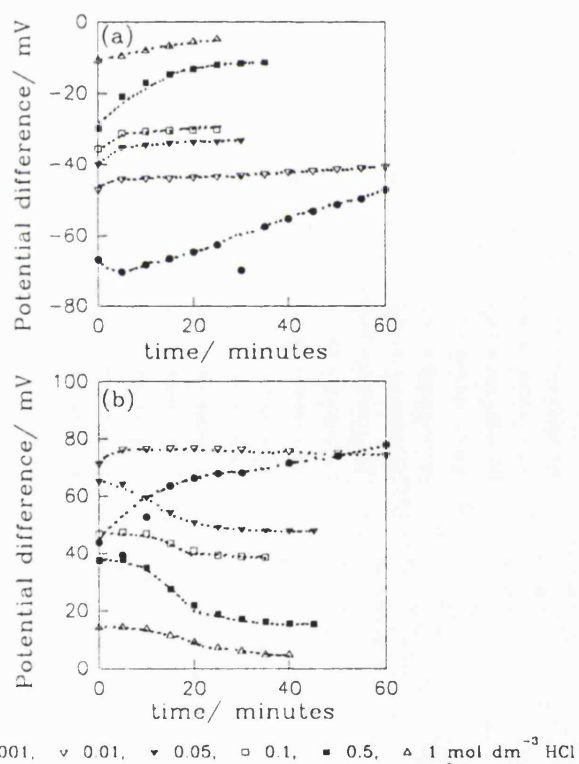


Figure 4.17: Potential difference vs. time response for a new co-cast rapidly dried, (a) PVC-PMA membrane and (b) PVC-PVMK membrane. The cell configuration was: (+) reference electrode/ test HCl solution/ membrane/ 1 mol dm⁻³ HCl/ reference electrode (-).

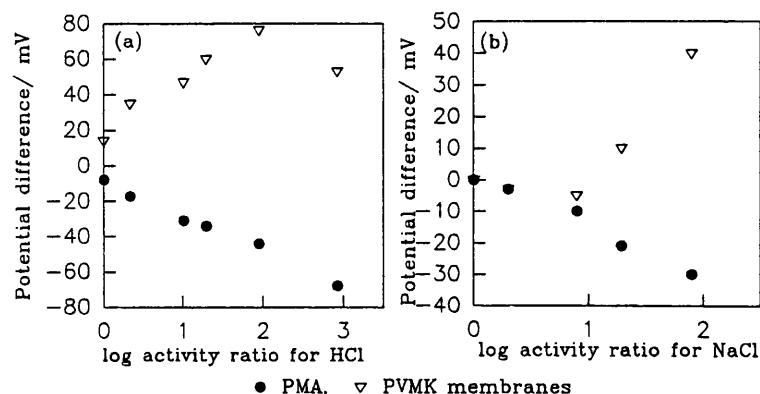


Figure 4.18: The behaviour of PVC-PMA and PVC-PVMK membranes to HCl and NaCl solutions. The cell configuration was: (+) reference electrode/ test solution/ membrane/ constant salt solution/ reference electrode (-); (a) in HCl, the constant solution is 1 mol dm^{-3} HCl; (b) in NaCl, the constant solution is 0.1 mol dm^{-3} NaCl.

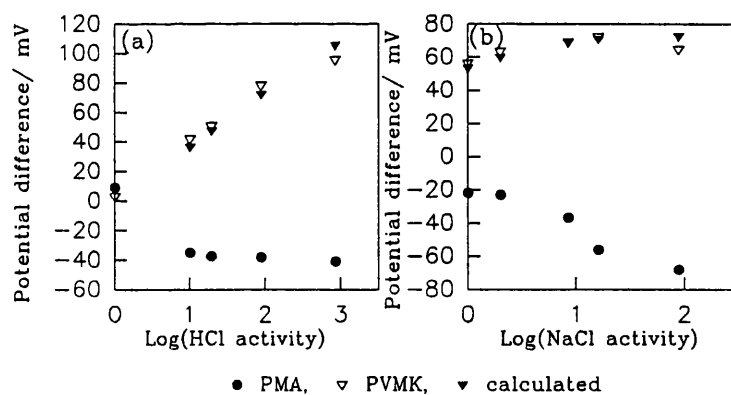


Figure 4.19: The potentiometric behaviour of PVC-PMA and PVC-PVMK films to mixed salt solutions compared to the Henderson equation calculated using mobilities of ions in water. The cell configuration was: (+) reference electrode/ mixed salts/ membrane/ 1 mol dm^{-3} HCl, 0.1 mol dm^{-3} NaCl/ reference electrode (-). The mixed salt solution were, for HCl variation 0.001 to 1 mol dm^{-3} with NaCl fixed at $0.001 \text{ mol dm}^{-3}$, and NaCl variation 0.001 to 0.1 mol dm^{-3} with HCl fixed at 0.01 mol dm^{-3} .

% PMA	Drying conditions	Salt tested	t_+
31.6	60°C, 1 hour	HCl	0.25
31.6	60°C, 1 hour 12 minutes	HCl	0.20
31.5	60°C, 1 hour	NaCl	0.37
31.5	60°C, 1 hour 10 minutes	NaCl	0.37

Table 4.9: The apparent cation transport numbers of HCl and NaCl in PMA-PVC membranes at 25°C from figure 4.18.

The transport number of H^+ in these films is much smaller than the literature values in water ($t_{H^+} = 0.81$) whilst that of Na^+ is hardly changed ($t_{Na^+,aq} = 0.40$).

% PVMK	Drying	Salt tested	t_+
12	60°C, 1 hour	HCl	0.87
12	50°C, 2 hours	HCl	0.84
12	60°C, 1 hour	NaCl	0.42
12	50°C, 2 hours	NaCl	0.42

Table 4.10: The apparent cation transport numbers of HCl and NaCl in quickly dried co-cast PVC-PVMK membranes at 25°C (fig 4.18).

These cation transport numbers is similar to those in aqueous solution. The apparent transport number of ions in the PMA-PVC and the PVMK-PVC membranes did not vary significantly with the drying time.

4.4.3.2. POTENTIOMETRY OF CO-CAST PEO-PVC (Fluka chemicals) MEMBRANES

Buck et al [8, 9, 10] have shown that PVC membranes contain fixed charges arising from trace impurities from the polymerization processes. They showed that PVC from different sources varied in concentration of charged sites present. Accordingly, the behaviour of membranes prepared using PVC from another source was explored. These membranes were prepared by co-casting the polymer solution and drying using the heater (60°C for 1 hour). Some membranes were dried at a lower temperature of 30°C for 12 to 60 hours.

The behaviour of PEO-PVC (Fluka) membranes in HCl, NaCl and solutions of various pH is shown in figures 4.20 and 4.21 which compares the responses for the films dried at low and high temperatures respectively. The response of both membranes in mixed salt solutions are shown in figures 4.22 and 4.23. Again, membranes with low PEO content and dried for a long time at 30 °C gave high membrane resistances, which slowly decreased upon hydration. In HCl solution, both 5% and 20% PEO membranes showed a fluctuating potential difference with increasing solution concentration, indicating a high resistance membrane. Only the 40% PEO membrane showed the expected regular, linear variation of potential difference with activity ratio. In HCl, the 20% membrane displayed a regular response since the film was hydrated. However, the 5% membrane remained unstable with large fluctuations in the potential response (-50 to 40 mV). Finally, the pH response for the 20% and the 40% PEO membranes varied regularly over the range from pH 1 to 10 whereas the 5% PEO membrane does not seem to be sensitive to the change in pH. In contrast, the membranes dried rapidly at higher temperatures showed a more regular behaviour.

Calculated apparent transport numbers are given in tables 4.11 and 4.12 and

are similar to those obtained with the Aldrich PVC. Any differences between the Aldrich and Fluka PVC membranes arose mainly because of the high electrical resistance of the slowly dried Fluka membranes. This arose as a consequence of a small but significant difference in the preparation procedure. The Aldrich PVC-PEO membranes were dried in a warm room at a temperature initially of 30 °C but slowly declining to ~20 °C over the 12 hours. The Fluka membranes were dried using a radiant element, maintaining an average temperature of 30 °C. It is reasonable to assume that, in this case, most of the water and cyclohexanone in the membrane was eliminated, thus giving rise to the resistive behaviour of the Fluka membranes.

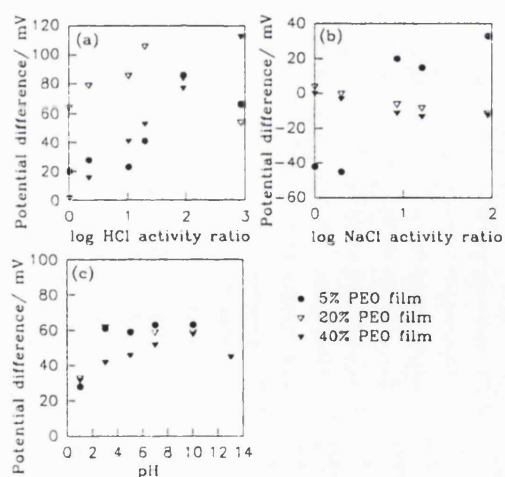


Figure 4.20: The response of PEO-PVC (fluka) membranes dried at 30°C to HCl, NaCl and solutions of various pH at 25°C.

The cell configuration was:

(+) reference electrode/ test solution/ membrane/ constant salt solution/reference electrode (-), (a) in HCl, the constant solution is 1 mol dm⁻³ HCl; (b) in NaCl, the constant solution is 0.1 mol dm⁻³ NaCl and (c) where the solution varies in pH and the constant solution is 1 mol dm⁻³ HCl.

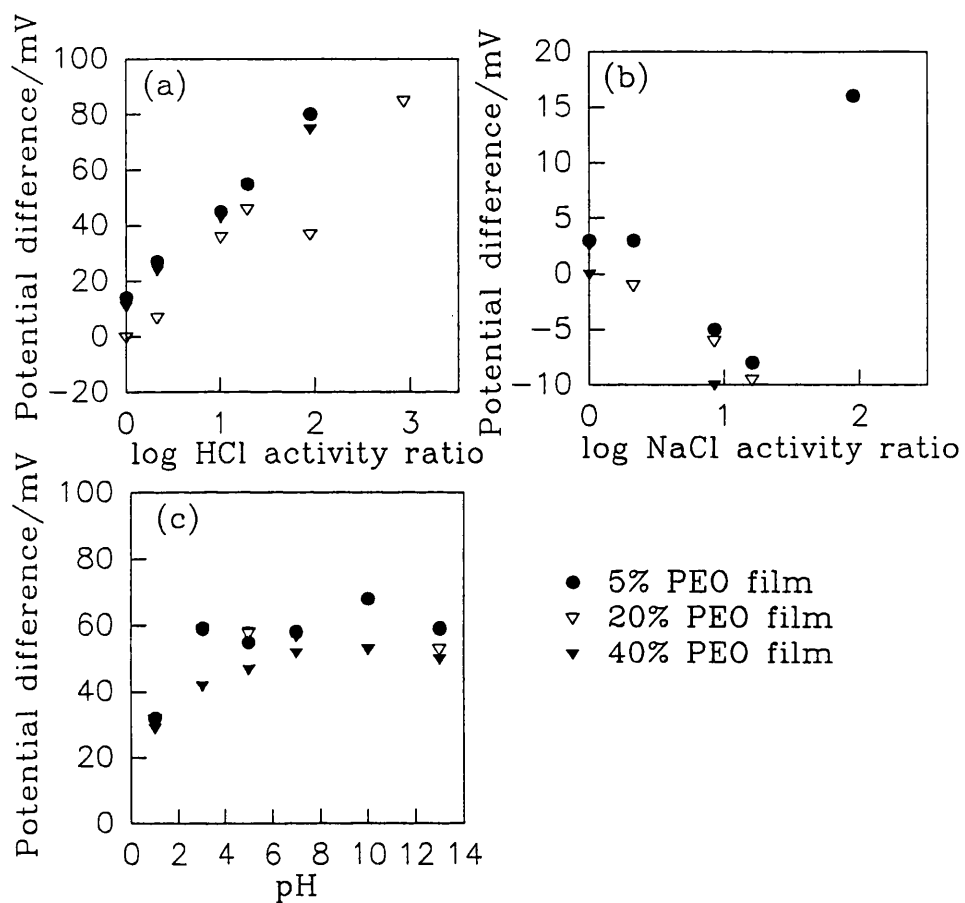


Figure 4.21: The response of PEO-PVC (fluka) membranes dried at 60°C for 1 hour to HCl, NaCl and solutions of various pH at 25°C.

The cell configuration was:

(+) reference electrode/ test solution/ membrane/ constant salt solution/reference electrode (-), (a) in HCl, the constant solution is 1 mol dm⁻³ HCl; (b) in NaCl, the constant solution is 0.1 mol dm⁻³ NaCl and (c) where the solution varies in pH and the constant solution is 1 mol dm⁻³ HCl.

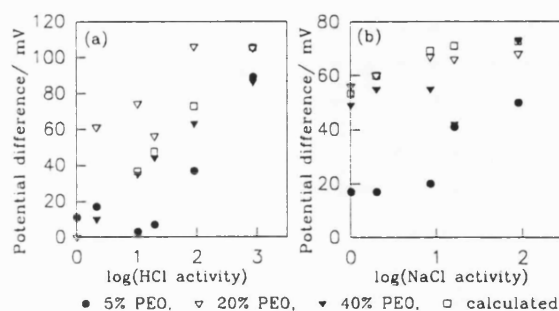


Figure 4.22: The potentiometric behaviour of PEO-PVC (fluka chemicals) membranes dried at 30°C, to mixed salt solutions at 25°C, compared to the Henderson equation calculated using mobilities of ions in water [10]. The cell configuration was: (+) reference electrode/ X mixed salts/ membrane/ 1 mol dm⁻³ HCl, 0.1 mol dm⁻³ NaCl/ reference electrode(-).

(a) 0.01 mol dm⁻³ NaCl, varying HCl, (b) 0.1 mol dm⁻³ HCl, varying NaCl.

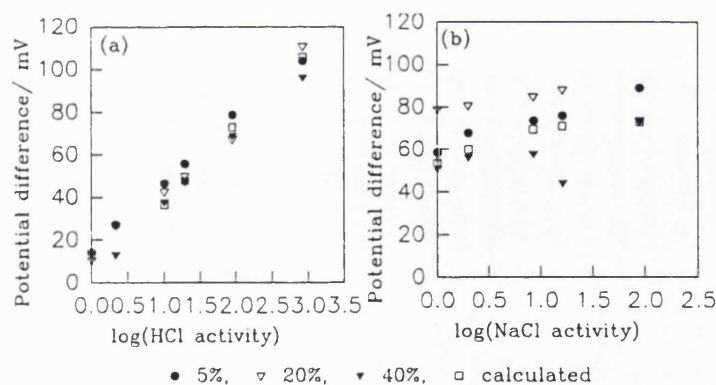


Figure 4.23: The potentiometric behaviour of PEO-PVC (fluka chemicals) membranes dried at 60°C for 1 hour, to mixed salt solutions at 25°C, compared to the Henderson equation calculated using mobilities of ions in water. The membranes were dried at 60°C for 1 hour. The cell configuration was:

(+) reference electrode/ X mixed salts/ membrane/ 1 mol dm⁻³ HCl, 0.1 mol dm⁻³ NaCl/ reference electrode (-).

(a) 0.01 mol dm⁻³ NaCl, varying HCl, (b) 0.1 mol dm⁻³ HCl, varying NaCl.

Salt	% PEO	t_+
HCl	5%	0.85 ± 0.02
	20%	0.84 ± 0.02
	40%	0.84 ± 0.02
NaCl	5%	0.63
	20%	0.46
	40%	0.40

Table 4.11: The apparent cation transport numbers of various salts in co-cast PEO-PVC (fluka) membranes at 25 °C, cast at 30 °C for 12 hours. The apparent H^+ transport numbers are invariant within experimental error. The apparent transport number of Na^+ decreases with increasing proportion of PEO to that found in aqueous solution.

Salt	% PEO	t_+
HCL	5%	0.85
	20%	0.82
	40%	0.72
NaCl	5%	0.45 ± 0.02
	20%	0.44 ± 0.02
	40%	0.42 ± 0.02

Table 4.12: The apparent cation transport numbers of various salts in co-cast PEO-PVC (fluka) membranes at 25 °C, cast at 60 °C for 1 hour. The apparent transport number for H^+ decreases with increasing PEO concentration and the apparent transport number for Na^+ seems to be invariant to the membrane PEO concentration within the experimental error.

4.4.3.3. POTENTIOMETRY OF CO-CAST PEO-CARBOXYLATED PVC MEMBRANES

In this series of experiments, co-cast membranes were prepared with carboxylated PVC. All other aspects of the membrane preparation were unchanged in that the membranes were quickly dried at 60 °C for 1 hour. Figure 4.24 shows the response of these films to HCl and figure 4.25 shows the response to various salt solutions.

The response of these films is close to the ideal Nernst equation behaviour (table 4.13). This behaviour is due binding sites, from the dissociated carboxylate functional group, which selectively transports cations across the membrane. Calculated membrane transport numbers decreased with increasing proportion of PEO.

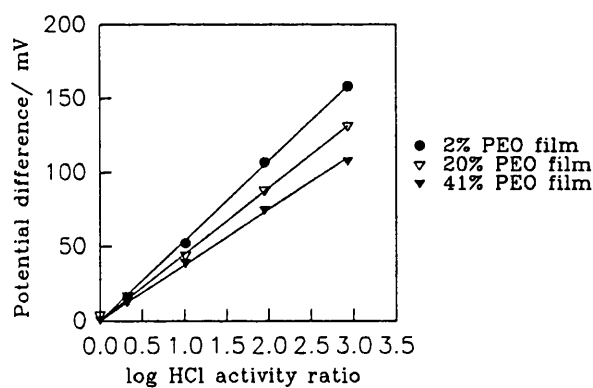


Figure 4.24: The response of co-cast PEO-carboxylated PVC membranes in HCl solutions at 25°C. The response is linear and for the 2% PEO membrane matches closely to the expected potential difference of 59 mV per decade for an ideal permselective membrane. The least squares curve fit is shown from which the apparent transport numbers are calculated.

The cell configuration was:

(+) reference electrode/ test solution/ membrane/ constant salt solution/ reference electrode (-); the test HCl solution varied from 0.001 to 1 mol dm⁻³ and the constant solution was 1 mol dm⁻³ HCl.

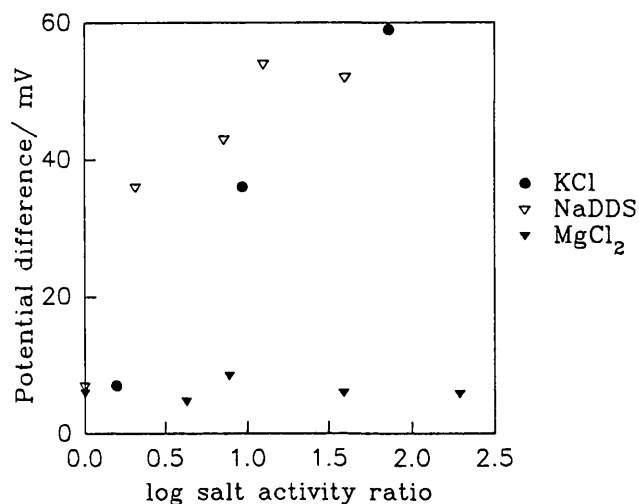


Figure 4.25: The behaviour of 2.2% co-cast PEO-carboxylated PVC membranes to various single salt solutions at 25°C. This behaviour is regular and the response time was within 1 minute. The cell configuration was:

(+) reference electrode/ test solution/ membrane/ constant salt solution/ reference electrode (-), where the constant solution concentration was 1 mol dm⁻³.

The potential difference was non zero when the salt activity ratio was zero. This could be due to the slightly resistive nature of the membrane since this first measurement was performed on a dry membrane and the higher PEO percentage membranes, which were more conducting, did not show this behaviour.

4.4.3.3. ROTARY EVAPORATED PEO-CARBOXYLATED PVC MEMBRANES

The preparation method of the co-cast membranes involved drying a stationary polymer solution. During this process, there is a hypothetical possibility that the polymers may separate into domains which might affect the potentiometric behaviour. The membranes whose behaviour is reported in this section were dried using a rotary evaporator, to see if this drying method affects the membrane behaviour. The membranes were generally rather thick (~0.4 mm)

and electrically resistive, which resulted in fluctuating potential differences in salts other than HCl.

Figure 4.26 shows the response of these rotary evaporated membranes to solutions of HCl and figure 4.27 the response to various salts, the order of experiments being HCl, KCl, NaDDS then $MgCl_2$. In HCl, the potential difference increased with increasing PEO concentration in the membrane. The response of the 10% PEO membrane was irregular at the high and low concentration ratios.

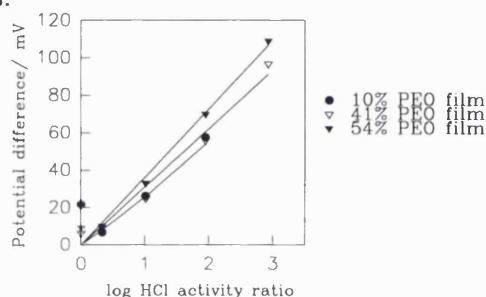


Figure 4.26: The behaviour of rotary evaporated PEO-carboxylated PVC membranes to HCl solutions at 25°C. The solid lines were forced fit through zero.

The cell configuration was:

(+) reference electrode/ test solution/ membrane/ constant salt solution/ reference electrode (-), where the constant HCl solution concentration was 1 mol dm⁻³.

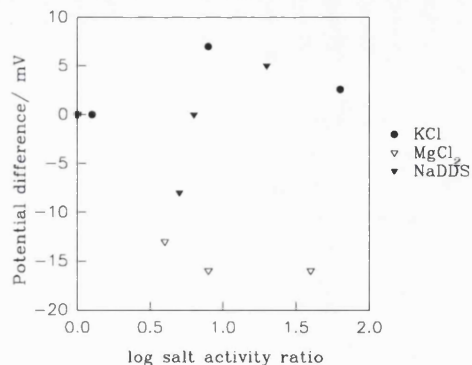


Figure 4.27: The behaviour of the 41% rotary evaporated PEO-carboxylated membranes to various salt solutions at 25°C.

The cell configuration was:

(+) reference electrode/ test solution/ membrane/ constant salt solution/ reference electrode (-), where the constant salt solution concentration was 0.1 mol dm⁻³.

Salt	%PEO	t_+ (co-cast membrane)	t_+ (rotary evaporated membrane)
HCl	10%	0.93	0.81
	41%	0.88	0.77
	54%	0.80	0.74
KCl	10%	0.92	-
NaDDS	10%	0.77	-
MgCl ₂	10%	0.50	-

Table 4.13: The apparent cation transport numbers of various salts in co-cast PEO-PVC-COOH membranes and rotary evaporated PEO-PVC-COOH membranes at 25°C.

REFERENCES TO CHAPTER 4

- [1] P. H., Reiger, "Electrochemistry", Prentice-Hall Inc., ch. 6, New Jersey, 1987.
- [2] D. B. V., Parker, "Polymer Chemistry", ch. 2, Applied Science Publ., London, 1974.
- [3] A. L., Horvath, "Handbook of Aqueous electrolyte Solutions", ch. 2, Ellis Horwood Ltd., England, 1985.
- [4] R. C., Weast, (ed), "The Handbook of Chemistry and Physics" C.R.C. Press, 1978.
- [5] P. W., Allen, (ed), "Physical Characterisation of polymers", ch. 6, Butterworth Scientific Publ., London, 1957.
- [6] D. J. G., Ives, G. J., Janz, (eds), "*Reference Electrodes, Theory and Practice*", ch. 1, Academic Press, London, 1961.
- [7] R. A., Robinson, R. H., Stokes, "Electrolyte Solutions", p. 463, Butterworths Scientific Publ., London, 1959.
- [8] F., Conti, G., Eisenman, *Biophysical Journal*, **6**, 227, (1966).
- [9] H. T., Clarke, (ed), "Ion Transport across Membranes", p. 145, Academic Press, New York, 1953.
- [10] R. P., Buck, E., Lindler, E., Graf, Z., Niegreis, K., Toth, E., Pungor, *Anal. Chem.*, **60**, 295, (1988).

CHAPTER 5
NON-ELECTROCHEMICAL
RESULTS

CHAPTER 5. NON-ELECTROCHEMICAL RESULTS

5.1. DIFFERENTIAL SCANNING CALORIMETRY (DSC)

Two types of membranes were studied using the DSC method. These were the slowly and quickly dried co-cast PEO-PVC films made using the casting machine. Both types of films were immersed in water for 48 hours at room temperature. Prior to measurement, they were blot dried, weighed and then placed in the DSC machine.

The results for the slowly dried membranes are shown in figure 5.1. The 10% PEO membrane sample weighed 1.16 mg and showed two peaks with onset temperatures of $-22.77\text{ }^{\circ}\text{C}$ and $-1.62\text{ }^{\circ}\text{C}$. The 20% PEO membrane weighed 10.79 mg and also showed 2 peaks. The onset temperature of the first small peak occurred at $-11.8\text{ }^{\circ}\text{C}$ and the other at $-0.08\text{ }^{\circ}\text{C}$. The 40% PEO membrane weighed 11.65 mg and showed just one peak, with an onset temperature of $-0.56\text{ }^{\circ}\text{C}$. The peak occurring near 273 K increases as the PEO content increases 10% > 20% > 40% PEO and corresponds to the phase change of free, unbound water in the membrane [1, 2]. The number of peaks in the membrane decreased with an increase in PEO content: the 10% and 20% PEO membranes showed two peaks whilst one peak was shown for the 40% PEO membrane, which implies that membranes with lower PEO content (10 and 20%) exhibits two types of water whilst the 40% PEO only shows the free water. The inset (in figure 5.1) shows clearly the transitions at the lower temperatures, (a) 10% PEO, (b) 20% PEO, (c) 40% PEO membrane. The DSC scan for the quickly dried PEO-PVC membrane is shown in figure 5.2. The quickly dried film proved to be more hydrophobic than the slowly dried membranes, and the first DSC scan showed no peaks. Subsequent measurements with a wet membrane showed one major peak near the freezing point of pure water [3]. The sample weighed 18.27 mg and the membrane showed two transitions. A peak which occurred at $\sim -40\text{ }^{\circ}\text{C}$ was found with the aid of a computer and had an onset temperature of $-36\text{ }^{\circ}\text{C}$. The larger peak occurred at $-1.00\text{ }^{\circ}\text{C}$. This result indicates that the quickly dried PEO-PVC membranes contain two types of

water, bound and free (although the bound water was difficult to detect). The inset (figure 5.2) shows the small transition which is obscured by the magnitude of the peak at $-1.00\text{ }^{\circ}\text{C}$.

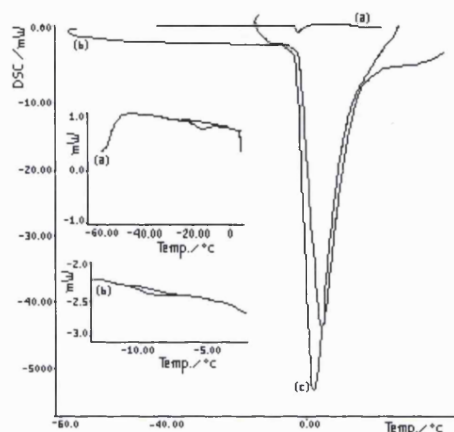


Figure 5.1: The DSC traces of co-cast PEO-PVC films, (a) 10% PEO film, b) 20% PEO film, c) 40% PEO film, all dried at 30°C , overnight. The membranes were soaked in distilled water at room temperature for 48 hours and blot dried prior to testing.

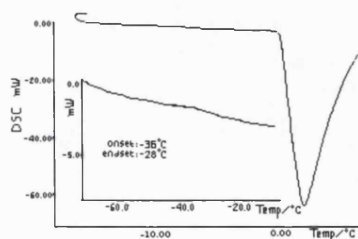


Figure 5.2: The DSC trace of co-cast 25% PEO-PVC film dried at 60°C for 1 hour.

5.2. THERMO-MECHANICAL ANALYSIS (TMA)

The thermo-mechanical analysis of co-cast polymer films gives the glass transition temperature of the membrane. It is important to find out whether there are one or two glass transition temperatures (and hence the number of phases in the membrane) [4]. The glass transition temperatures of the composite membrane indicate the extent of mixing between polymers and the solvent, and whether the combination of the polymers produces a membrane which incorporates the physical properties of both polymers, giving the membrane tensile strength (due to PVC) with a lower glass transition temperature (due to PEO) to ensure flexibility. Table 5.1 shows results from several scans of PEO-PVC membranes, of various compositions and preparation methods, under a 20 g load at the temperature range -50 to 150°C. The controls in this experiment were pure water and poly(ethylene terephthalate) which has a defined glass transition temperature of 64°C [5]. The glass transition temperatures of the pure polymers were: 85 °C for PVC [3] and -55 °C for PEO (m.w. 10⁶) [4].

These membranes showed varying glass transition behaviour dependant on the percentage of PEO (or PVC) in the membrane. Co-cast membranes with 5% PEO showed only one glass transition, whilst 10% to 20% PEO showed two glass transitions. The co-cast 40% PEO and the rotary evaporated 20% PEO membrane showed three glass transition temperatures.

These results were very sensitive to the experimental conditions, although every effort has been made to ensure continuity and consistency. The sensitivity of the thermo-mechanical scans is subject to the millivolt scale of the recording instrument. Previous to measurement, the millivolt settings are chosen to maximise signals from the probe (smallest mV setting for maximum sensitivity), as well as ensuring that full deflection from the probe is also

measured. This means that small transitions may not be measured for a thick film ($\sim 50 \mu\text{m}$) which requires a large millivolt setting to ensure that full deflection of the probe is recorded.

A reproducible result is dependant on constant environmental factors such as temperature and humidity. When these factors change (and all other experimental variables remain constant) different results are obtained. For example, the 20% PEO film consistently produced two glass transitions. On another day, the same sample gave three glass transitions. This could be due to a warm, humid environment causing a softening of the membrane resulting in the lower glass transition not being observed. For this reason, all the membranes were measured in one day.

The number of temperature transitions shown by the quickly dried co-cast membranes increased with PEO concentration. The 5% and 10% PEO membranes showed only one transition at similar temperatures. The 20% PEO membrane showed two transitions, one similar to the 5% PEO and 10% PEO membranes, and another at a higher temperature of $71 \text{ }^\circ\text{C}$. The 40% PEO membrane showed three transitions; one peak at $32 \text{ }^\circ\text{C}$, which was smaller than the previous lower PEO content membranes, one peak at $52 \text{ }^\circ\text{C}$, which was the same size as the previous membranes, and one small peak at $80 \text{ }^\circ\text{C}$.

The rotary evaporated membrane showed three transitions with temperatures dissimilar to previous co-cast membranes. There was one transition at $-23 \text{ }^\circ\text{C}$ which indicates that this membrane is significantly softer than the co-cast membranes. The other two transitions occurred at $41 \text{ }^\circ\text{C}$ and $107 \text{ }^\circ\text{C}$. The transition at $41 \text{ }^\circ\text{C}$ was slightly lower in temperature than the co-cast transition in the region of $45\text{-}50 \text{ }^\circ\text{C}$. The transition at $107 \text{ }^\circ\text{C}$ was much higher in temperature than previous transitions at around $70\text{-}80 \text{ }^\circ\text{C}$.

5.3. THERMOGRAVIMETRY (TG)

Thermogravimetric scans of co-cast, slowly dried membranes (conditioned by soaking for 1 week in distilled water at room temperature), showed transitions due to loss of water (100°C) and cyclohexanone (155°C) and due to decomposition of the polymers (PVC and PEO ~ 450 °C) [6]. There was a significant amount of cyclohexanone remaining in the film which may contribute to the membrane plasticity. It was indeed observed that membranes which were heat dried longer were less flexible. Table 5.2 shows the % weight fraction of water and cyclohexanone in each membrane.

The temperatures at which the weight loss occurred for the 45% co-cast membrane was slightly higher than for the rest of the PEO-PVC composite membranes.

The weight loss near the temperature of 100 °C indicate the loss of water from the membranes. Weight loss near the temperature of 155°C (boiling temperature for pure cyclohexanone) indicate a loss of the membrane solvent. All membranes show a weight loss near the ≈ 100 °C region corresponding to the loss of water molecules bound to the membrane.

The transition at 100 °C increases in temperature as the percentage of PEO increases: for the 45% rotary evaporated PEO membrane, this transition occurs at 139 °C. The next transition, corresponding to the loss of cyclohexanone, occurs near the temperature of 155 °C. This transition seemed to decrease with the increase in PEO content and the highest PEO content of 45% co-cast and rotary evaporated membranes did not show this transition. The following transition, corresponding to the charring of the polymers) is in the region of 300 °C. The pattern of this transition in the membranes is irregular. The trend was an increase from 0% PEO (279 °C) to 300 °C for the 15% and 315 °C for the 45% and decreasing for the 20% rotary evaporated membrane at 296 °C. The next transition did not occur for all of the membranes (the 5%, 45% co-cast PEO membranes and the 45% rotary evaporated PEO membrane). The

membranes that did show a transition had wide ranging temperatures from 279 ° C for the 0% PEO membrane to 379 ° C and 382 ° C for the 10% and 15% PEO membranes respectively.

% PEO	Temperature of	Comments
5%	46	only one peak measured
10%	50	Peak at 70°C smaller
20%	45 71	Both peaks the same size
40%	32 52 80	smaller peak at 32°C compared to the 52°C peak. The peak at 80 °C was gradual.
20% *	-23 41 107	The peak at -23 °C was small compared to the large peak at 41 °C. The peak at 107 °C was the same size as the one at -23 °C

Table 5.1: The Thermo-mechanical transitions of co-cast PEO-PVC films,

* represents a rotary evaporated PEO-PVC film.

% PEO	Temperature at Which Weight loss occurred/°C				
0	101	241	279	297	436
5	116	178	301	-	456
10	115	172	294	379	436
15	119	170	304	382	436
45	123	-	315	-	461
45*	139	-	296	-	460

Table 5.2: Transition temperatures of slowly dried PEO-PVC films, * represents a film soaked in water before the measurement and 0 % PEO is a pure PVC co-cast film.

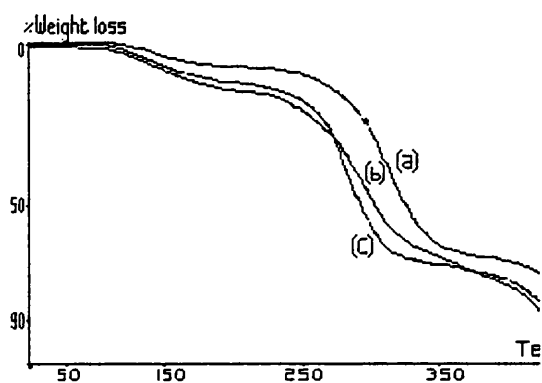


Figure 5.3: The temperature vs. percentage weight loss derived from the thermogravimetric scans of slowly dried co-cast PEO percentage membranes, (a) 45% PEO film, (b) 15% PEO film, (c) 5% PEO film.

5.4. FTIR SPECTROSCOPY

FTIR Spectroscopy confirmed (figure 5.4) there were significant amounts of cyclohexanone and water present in the slowly dried films whereas the quickly dried films showed less solvent and less water.

There were no observed peak shifts in the co-cast polymer films compared to the spectrum of the individual pure polymers, implying no strong interaction between the different polymer molecules [7].

Figure 5.4 shows FTIR spectrum of membranes which were dried at 30 °C for 12 hours. These membranes show a significant amount of water with a broad peak in the OH stretch region of 3200 to 3800 cm^{-1} . These membranes also show a strong peak in the region of 2900 cm^{-1} . This corresponds to the CH_2 group symmetric stretch from the polymer carbon chain skeleton. The membranes show a strong peak in the region of 1700 cm^{-1} which is from the carbonyl group of the membrane solvent cyclohexanone [8]. In the fingerprint region of 400 to 1500 cm^{-1} the spectra did not change between the three polymer membrane compositions which were slowly dried.

Figure 5.5 shows the FTIR spectrum of PEO-PVC membranes which were quickly dried at 60 °C for 1 hour for the 5% PEO membrane, and 65 °C for 2 hours for the 20% PEO membrane and 70 °C for 1 hour for the 40% PEO membrane.

These membranes showed no peaks in the OH stretch region of 3200 to 3800 cm^{-1} indicating an absence of water molecules sorbed into the membrane. There was still a strong peak in the region of 2900 cm^{-1} , although these peaks have shifted approximately 50 cm^{-1} to 2950 cm^{-1} compared to the slowly dried PEO-PVC membranes. The 5% PEO membrane shows a strong peak at 1700 cm^{-1} whereas the 20% and the 40% PEO membrane do not show this peak. Thus the 5% PEO membrane has residual cyclohexanone and the 20% and

40% do not. There are slight differences in the fingerprint region of 400 to 1500 cm^{-1} in that some of the peaks in the 40% PEO membrane are sharper than the 5% and 20% PEO membrane and the peak points are more clearly illustrated. The very sharp peak around the region of 1350 cm^{-1} is quite characteristic of PEO. The 45% quickly dried membrane shows this peak. In the other membranes, it is perhaps broadened. Figure 5.6 shows the FTIR spectrum of the PMA-PVC membrane. This membrane shows no OH peaks. The peak at 2850 cm^{-1} is due to the CH_2 groups of the polymer backbone. There is a peak at 1750 cm^{-1} which corresponds to the ketone functional group in cyclohexanone. The peaks in the fingerprint region of 400 to 1500 cm^{-1} are also present in the PEO-PVC membranes.

The FTIR spectra of quickly dried co-cast pure PVC membrane with the spectra for PEO and cyclohexanone from literature [8] are given as a comparison in figure 5.7.

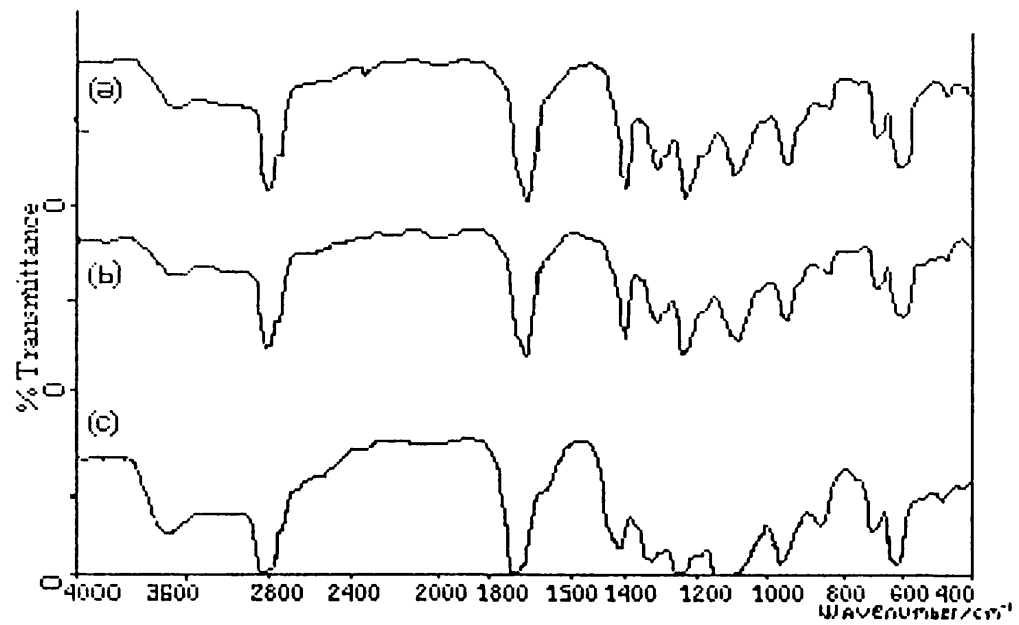


Figure 5.4: The FTIR spectrum of slowly dried co-cast PEO-PVC membranes, (a) shows the 5% PEO membrane, (b) 10% PEO membrane, (c) 25% PEO membrane.

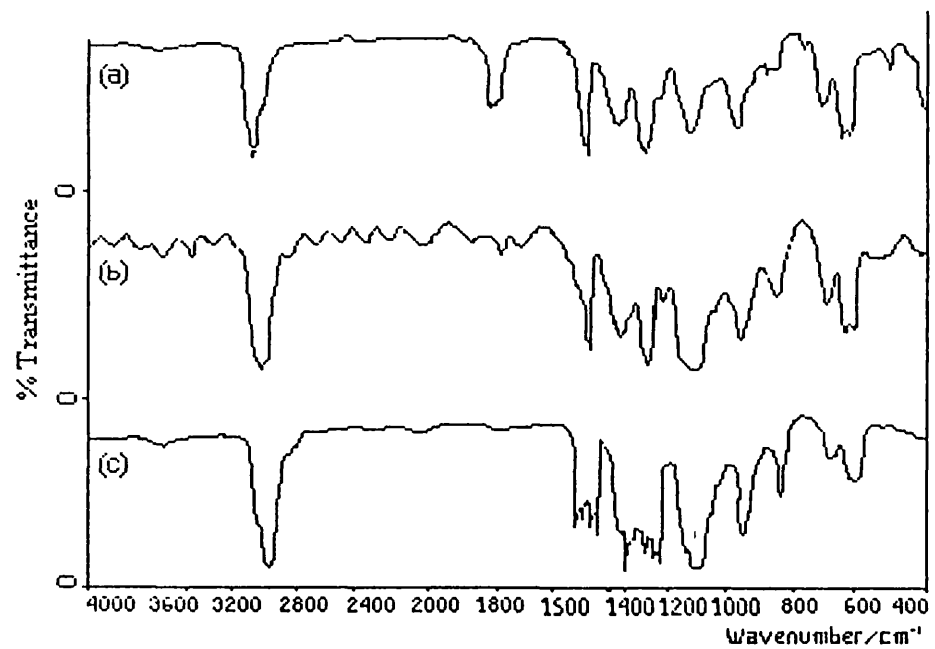


Figure 5.5: The FTIR spectrum of quickly dried co-cast PEO-PVC membranes, (a) shows the 5% PEO membrane, (b) 20% membrane, (c) 40% membrane.

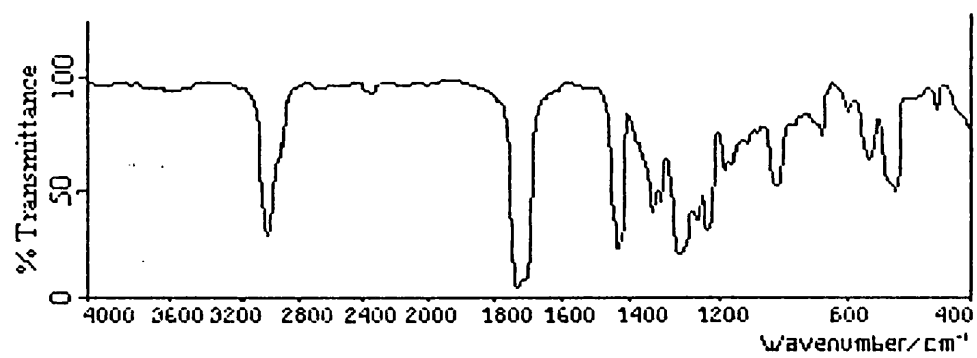


Figure 5.6: The FTIR spectrum of the quickly dried co-cast Poly(methylacrylate)-PVC membrane.

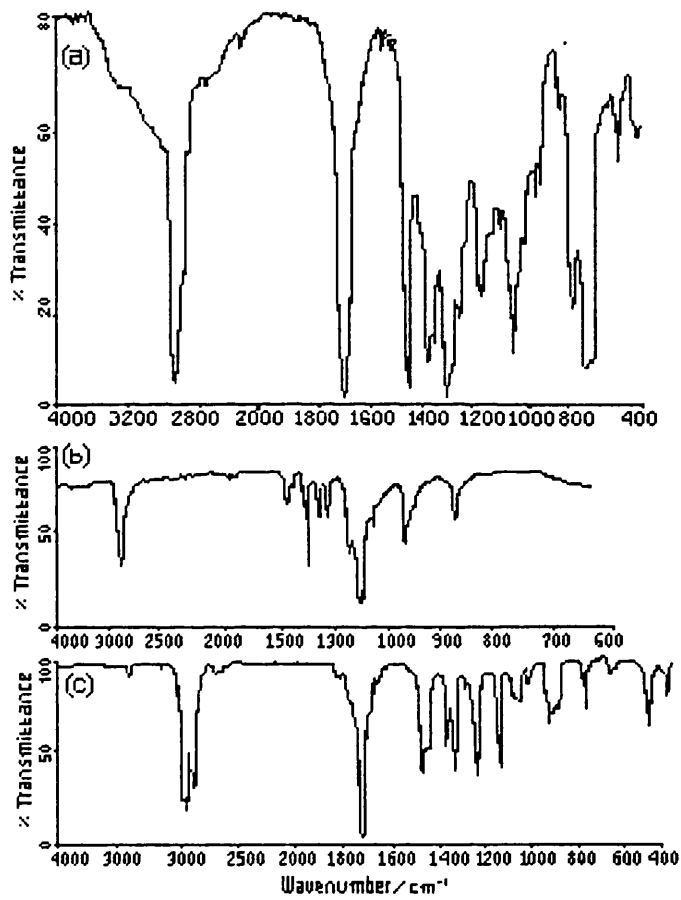


Figure 5.7: The FTIR spectrum of the individual polymers (a) quickly dried cast PVC, (b) PEO and (c) cyclohexanone [8].

5.5. OPTICAL MICROSCOPY

Optical microscopy shows any dissimilar phases in the composite film. The use of polarised light illumination picks out phases with different birefringence [9, 10]. Figure 5.8 shows large domains of different birefringent material for the slowly dried co-cast PEO-PVC films. Domain size is typically 2-4 μm across.

Quickly dried co-cast films show smaller domains of birefringence, typically of the width 1 μm in figure 5.9. Figure 5.10 and 5.11 show polarised optical microphotographs of quickly dried PMA-PVC and PVMK-PVC membranes respectively.

The 5% PEO slowly dried membrane show crystalline regions amongst an amorphous background. The 40% PEO slowly dried membrane shows a higher concentration of crystalline domains with many colours, which indicate a wide range of crystalline configurations.

The 4% PEO quickly dried membranes show fewer crystalline regions than the 5% slowly dried membrane. The sizes of the crystals are generally smaller with the occasional large crystal. The 40% PEO quickly dried membrane has more crystalline domains than the 4% quickly dried membrane. The crystal size was the same as the 4% PEO membrane with a few large crystals. The quickly dried 40% PEO membrane shows fewer colours than the 40% slowly dried membrane indicating that the quickly dried membrane has fewer crystalline configurations.

The PMA-PVC membranes show a lower density of crystallites after soaking. This indicates that the crystals may leave the membrane during immersion in electrolyte solution. The PVMK-PVC membranes also showed a marked difference upon soaking: the crystal density decreases and becomes non-uniform. These photomicrographs are of different regions, but they are representative of the whole membrane.

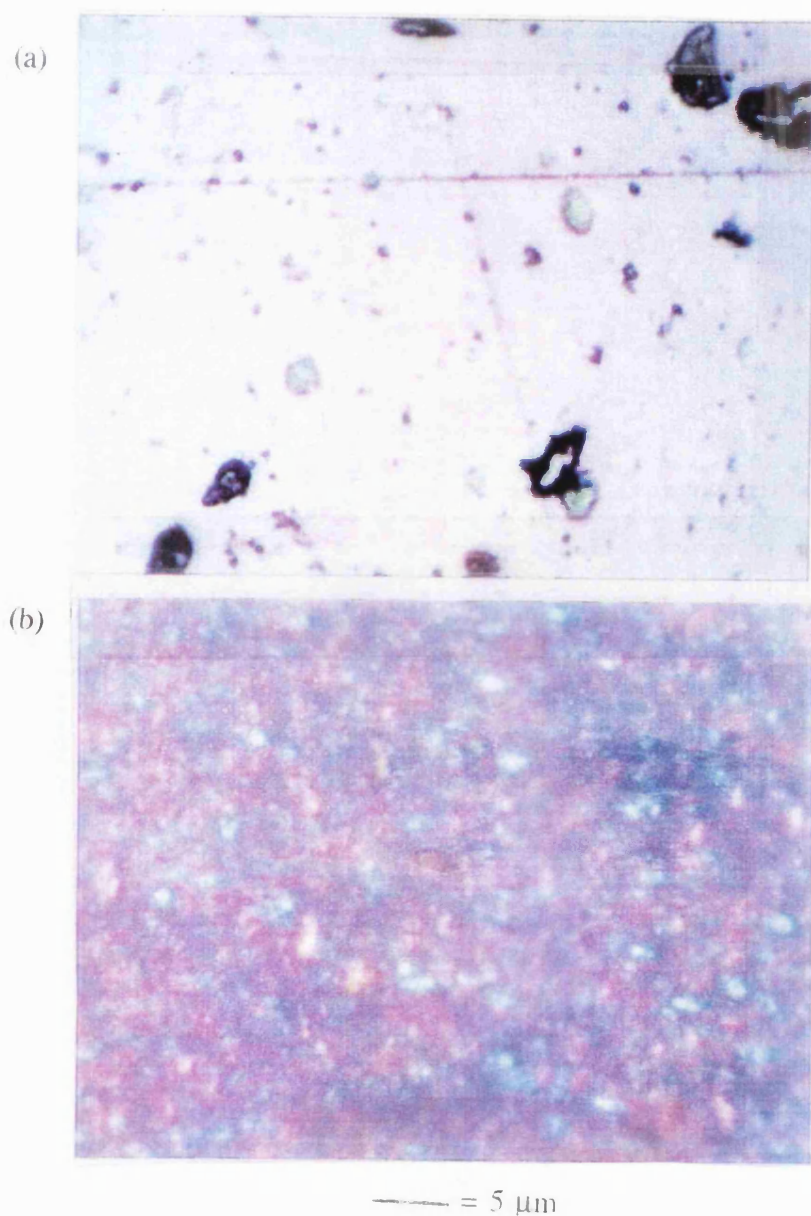


Figure 5.8: The polarised light optical photomicrographs of co-cast PEO-PVC membranes dried at 30°C for 12 hours of (a) 4% PEO, (b) 40% PEO.

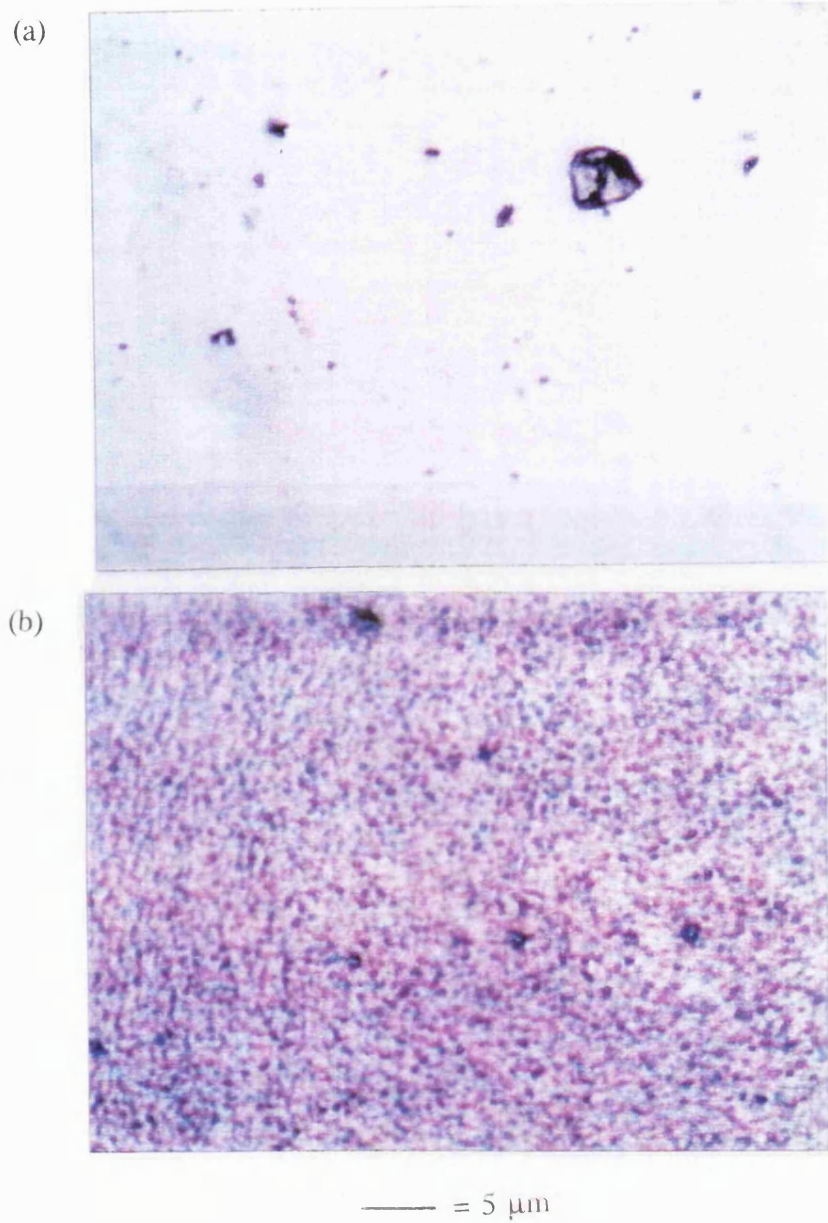


Figure 5.9: The polarised light optical photomicrographs of co-cast PEO-PVC membranes dried at 60 °C for 1 hour of (a) 4% PEO and (b) 40% PEO membrane.

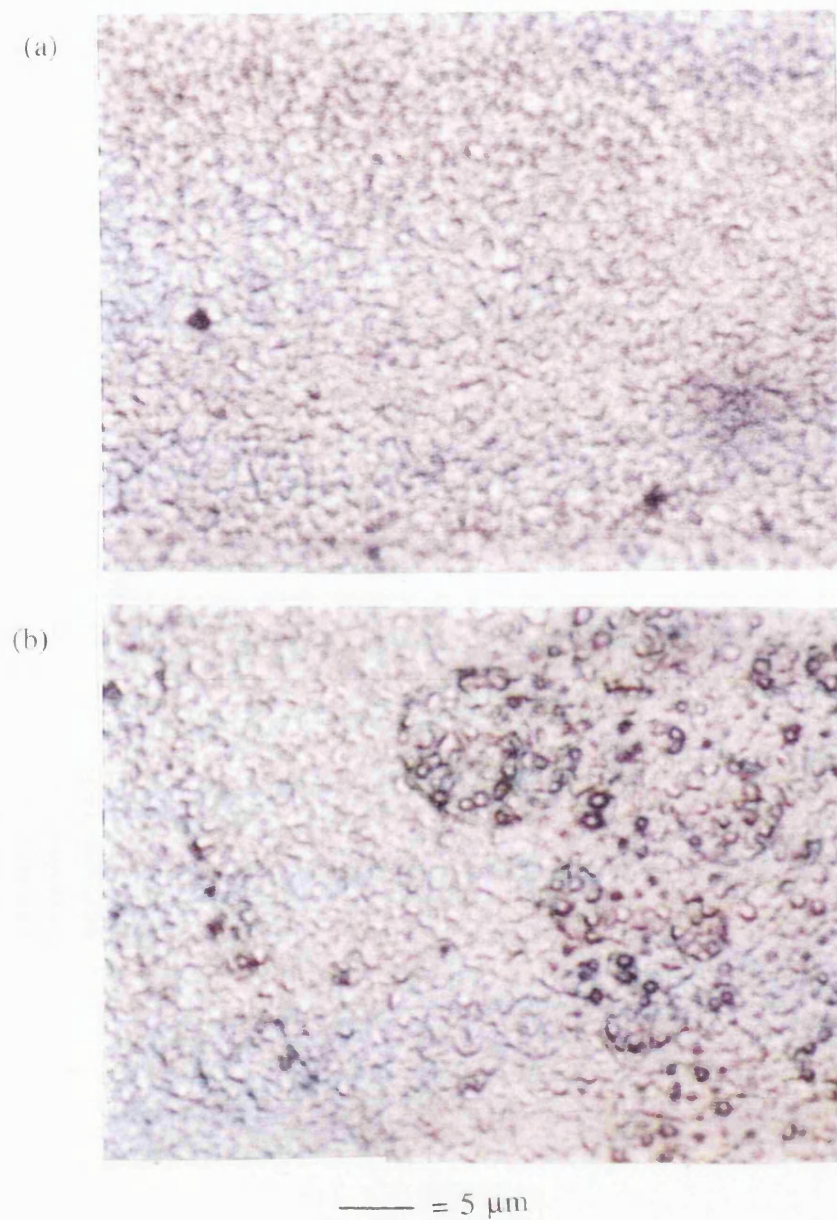


Figure 5.10: The polarized light photomicrographs of Poly(methylacrylate)-PVC films, (a) dry and (b) after soaking in water. The appearance of salt rings arises from soaking in salt solutions during electrochemical testing.

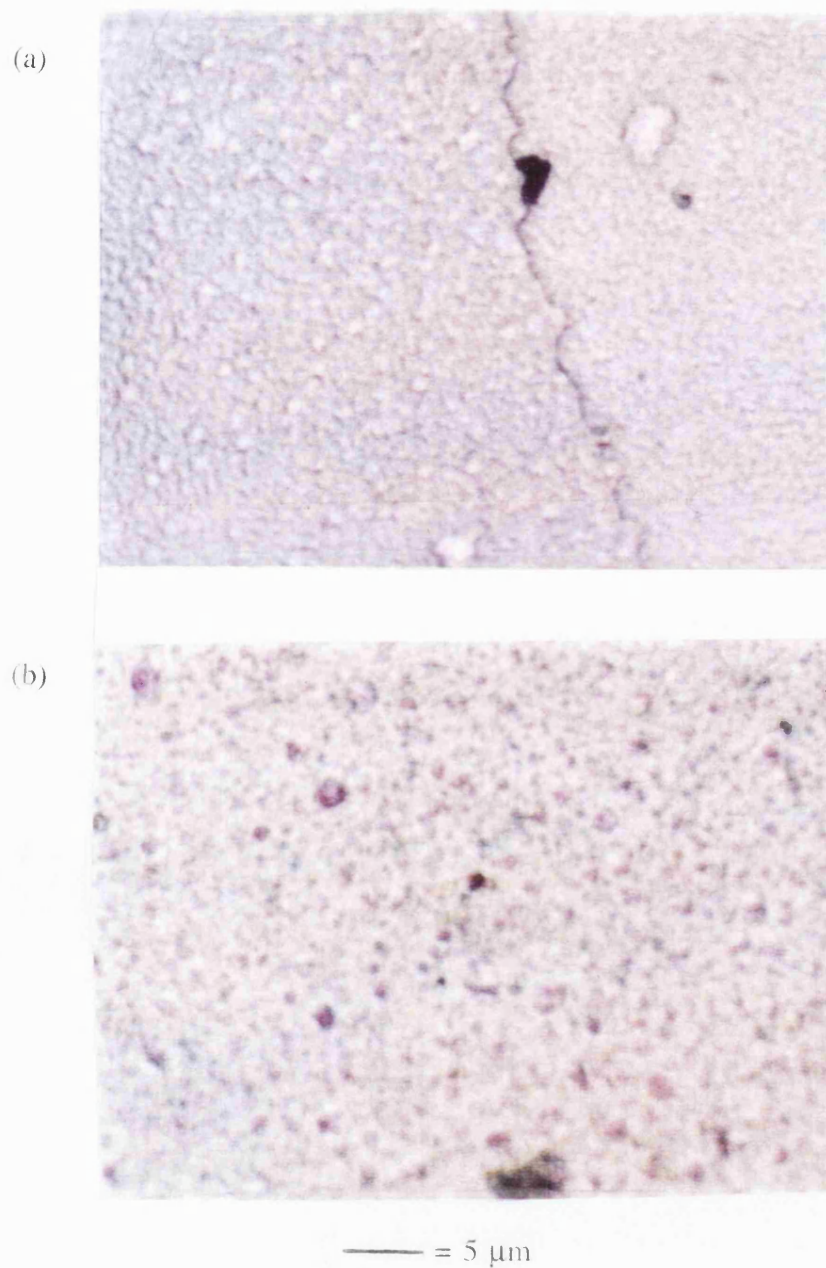


Figure 5.11: The polarised light photomicrograph of quickly dried Poly(vinylmethylketone)-PVC films in the dry state (a) and (b) after soaking in distilled water.

5.6. SOLID STATE NMR SPECTROSCOPY

The solid state NMR spectrum of D_2O equilibrated films shown in figure 5.12 was taken at 213 and 293 K. At 213 K, there was one large peak at 319 Hz and two less significant peaks at -72624 Hz. However, there was only one sharp peak of 221 Hz at the higher temperature of 293 K.

The sharp peak at 293 K indicates isotropic motion of D_2O molecules in figure 5.13. This behaviour is characteristic of free D_2O molecules as all molecular motions average out in the timescale of the scan [12]. The spectra at 213 K may be a superposition of two lineshapes due to two different molecular motions [13].

Pure D_2O at 250 K is given as a comparison in figure 5.13 b.

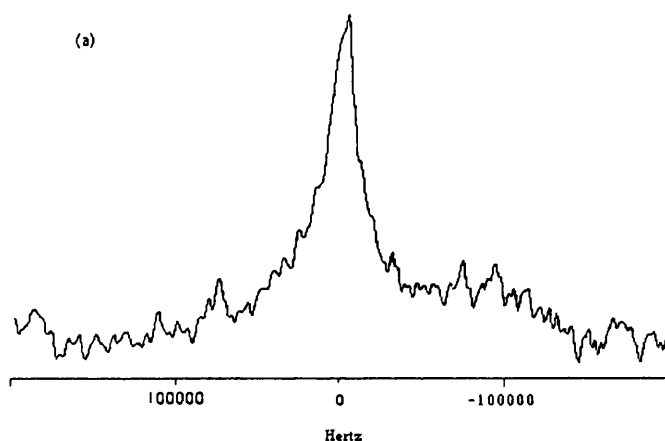


Figure 5.12: The solid state NMR spectrum of 20% PEO quickly dried at 60 °C for 1 hour, D_2O conditioned film at 213 K. The lineshape of the spectrum indicates that the D_2O molecules are not stationary at this temperature compared to the spectrum of solid D_2O (figure 5.13 b).

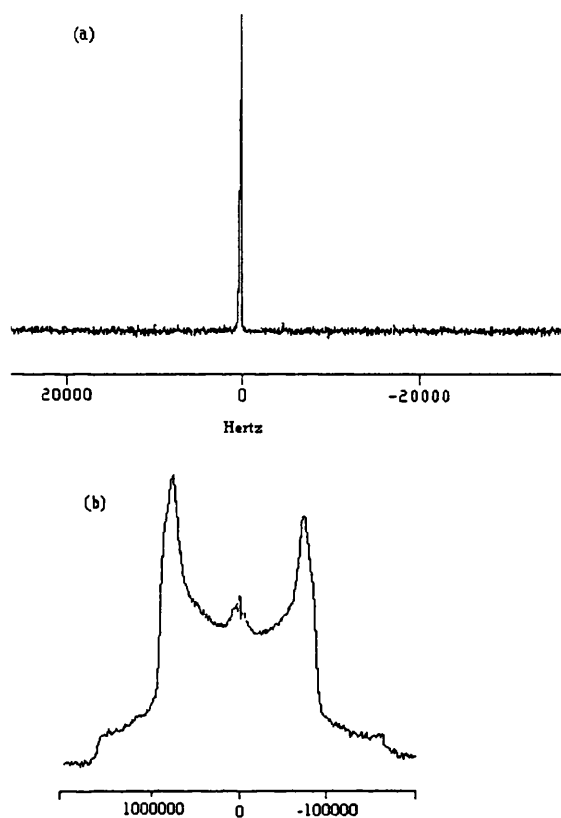


Figure 5.13: The solid state NMR spectrum of a) D_2O conditioned film at 298 K and b) pure D_2O at 250 K showing the characteristic lineshape [13]. The spectrum of the 20% PEO quickly dried membrane at 298 K suggests that the D_2O molecules are completely isotropic in their motion.

REFERENCES FOR CHAPTER 5

- [1] D., Campbell, J. R., White, "Polymer Characterisation, Physical Techniques", ch. 12, Chapman and Hall, London, 1989.
- [2] C., Booth, K., Kiros, C., Price, A., Ryan, Z. G., Yan, *Macromol.*, **28**, 1, (1995)
- [3] G., Van De Plaats, "The Practise of Thermal Analysis", ch. 7, Mettler, 1990.
- [4] F. E., Bailey, J. V., Koleske, "Poly(ethylene oxide)", ch. 6, Academic Press, London, 1976.
- [5] G., Van De Plaats, "The Practise of Thermal Analysis", ch. 1, Mettler, 1990.
- [6] F. E., Bailey, J. V., Koleske, "Poly(ethylene oxide)", ch. 3, Academic Press, London, 1976.
- [7] D., Campbell, J. R., White, "Polymer Characterisation, Physical Techniques", ch. 5, Chapman and Hall, London, 1989.
- [8] C., Pouchet, "The Aldrich Library of Infrared Spectra", Edn. 3, Aldrich U.S.A., 1981.
- [9] D., Campbell, J. R., White, "Polymer Characterisation, Physical Techniques", ch. 11, Chapman and Hall, London, 1989.
- [10] D. V. B., Parker, "Polymer Chemistry, ch. 4, Applied Science Publ. Ltd., London, 1974.
- [11] V., Voss, B., Boddenberg, "Surface Science", p. 241, Elsevier Science, Holland, 1993.
- [12] B., Boddenberg, R., Grobe, *Lehrstuhl Fur Phys. Chemie*, *42a*, 497, (1988)
- [13] T., Menge, T., Steurich, *Electrochim. Acta*, *13*, p. 1871, (1994).

CHAPTER 6
DISCUSSION

CHAPTER 6. DISCUSSION OF RESULTS

It is proposed that the dominant effect on permselectivity in the membranes studied here is a modification of the interaction between ions and water within the membrane channels formed by a hydrated polymer. The key result illustrating this is in figure 4.9.

The hypothesis is that the membranes are a nano-scale composite structure comprising interpenetrating networks of hydrophobic and hydrophilic regions. The size of these regions determine the transport properties of ions moving through the membrane.

6.1. CONDUCTIVITY OF IONS IN AQUEOUS SOLUTIONS CONTAINING PEO

These experiments indicated that PEO, even in dilute solution, could modify the hydration of ions also present. Thus, the limiting molar conductivities of salts in pure water and in the PEO solution were found to differ. For some salts i.e. NaCl, NapTS, the limiting molar conductivity was greater with PEO present but for NaClO₄, the conductivity decreased.

The changes in Λ^0 can be explained in terms of the effective hydrodynamic radius of the ions at high dilution being changed as a consequence of the presence of PEO in solution. In other words, the size of the ionic hydration sheath depends on the structure of water about the polymer molecule.

The effect of ions upon the local structure of water has traditionally been considered in two ways. Firstly, the ratio of Stokes law radius to crystal radius increases in the sequence $K^+ < Na^+ < Li^+$ implying a greater local structuring of water around the smaller ion.

Hydration of an ion can conceptually be regarded as breaking of the structure of liquid water followed by its reorganisation around the ion. Three zones

could then be envisaged: a tightly structured zone around the ion where water molecules are oriented by the electric field of the ion; a zone far from the ion having the original tetrahedral organisation of liquid water and, in between, a zone of mismatch (of increased disorder). The viscosity B coefficient has been taken to indicate the net effect of the ion on the system. Thus a positive B coefficient (chapter 2.1) for an ion in solution is interpreted as promotion of the water structure. Anions such as NO_3^- and ClO_4^- have a negative B coefficient (-0.04, -0.02 respectively) indicating the hydrogen bonds of water molecules, neighbouring the ion, are weakened. Thus the solvated anion is larger with lower ionic mobility and lower conductivity at high dilution [1]. In general, according to this interpretation, Na^+ is "net structure making" whilst K^+ and anions are "net structure breaking". This distinction can be used to describe how the hydrated ions interact with hydrated polymers. Wiggins [2] has used such arguments to discuss the relative exclusion by living cells of K^+ compared to Na^+ and explored the postulated effects in a number of model systems. Therefore, it is proposed that the increased Λ^0 value for NaCl in PEO solution is a result of the interaction of the hydration shell of Na^+ and polymer, affecting ionic radii and mobility.

The slope of $d\Lambda^0/d(C^{1/2})$ is affected by the degree of ion association in solution. In concentrated salt solutions (0.09 mol dm^{-3}), ion pair association will increase due to long range electrostatic ionic interaction [3]. Oppositely charged ions in a concentrated electrolyte solution may form associated ion pairs with one or more molecules of water separating the two ions. This results in the ions being unable to show independent Brownian motion, so when an electric field is applied, they will migrate as one unit. The ion pair will not contribute to the electric current and the conductivity is lowered with increasing concentration. This behaviour is observed for NaClO_4 and NapTS whose conductivity decreases in PEO solution from the value in water. The B coefficient for the ClO_4^- ion is negative (-0.02) which indicates a disruption of the hydrogen bonds between the water molecules, leading to diminished

resistance to the Na^+ and ClO_4^- ion pair formation. It is proposed that the interaction of the hydrated ion and polymer in PEO solution leads to ion pair formation. In contrast, for NaCl, the conductivity decreased normally with increase in concentration in PEO solution. Thus NaCl does not form ion pairs in PEO solutions.

An increase in the Na(DDS) concentration from zero resulted in a considerable decrease in the specific conductivity which then remained steady with further increase of concentration. This behaviour suggests micelle formation [4]. The characteristic change in conductivity is due to aggregation of the dodecylsulphate ions to form micelles of colloidal size. This results in the association of the charged micelles and the oppositely charged ions, which produces the decrease in conductivity. The critical micelle concentration for the Na(DDS) in water was $0.0256 \text{ mol dm}^{-3}$ and was lower in PEO solution ($0.0144 \text{ mol dm}^{-3}$). The critical micelle concentration would be lowered if the electrical repulsion between the charged species is lowered, such as when the ions of the micelles interact with PEO molecules.

6.2. DISCUSSION OF PEO MEMBRANES

6.2.1. SUPPORTED PEO MEMBRANES

The potential response of supported PEO membranes was determined by the ionic transport numbers and the activity ratio of the electrolyte solutions across the membrane, resulting in a response which is characteristic of a permeable membrane (fig. 6.1). Thus, there is no evidence for specific interaction between PEO and the Na^+ ion, even though the effective concentration of the PEO in the membrane phase was very large.

However, the results from the concentration cells show that there is a potential

difference generated when the membrane is immersed in electrolyte solution which is bigger than expected on the basis of the junction potential. The effects of PEO on ion mobility were small but distinct and are summarised in table 6.1.

Salt	effect of PEO membrane on U_+/U_-
HCl	0
NaClO ₄	0
Na(pTS)	+
Na(DDS)	+
KCl	0
KNO ₃	0
CsCl	0

Table 6.1. The effect of the PEO membrane on the relative ionic mobility of various salts, where + indicates a small increase; 0 = no effect; - indicates a small decrease.

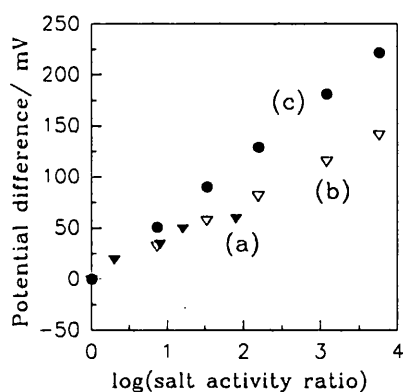


Figure 6.1: The potential difference response of the (a) supported aqueous PEO membrane in HCl compared to the (b) ideal response of a liquid junction for a permeable membrane (c) ideal semipermeable membrane response.

6.2.2. BEHAVIOUR OF PROCESSED PEO MEMBRANES

These gelatinous processed membranes showed no great permselectivity to NaCl. The potential response of these membranes indicating that they behaved like permeable membranes, hydrating with time and becoming porous. The fully hydrated membrane offered no resistance to electrolyte mixing, typically after 40 minutes, as indicated by the increase in the potential difference response from a negative value towards zero. At the same time, the membrane resistance decreased from 4 M Ω to zero. The potential difference response of the processed PEO membranes to NaCl may be described as that of a permeable membrane rather than a semipermeable membrane (fig. 6.2).

The result from a direct comparison of the potential response with time of the processed PEO membranes shown in figure 4.1. It indicates that the relative mobility of ions in the membrane is changed slightly from that in aqueous solution. The expected potential response for a liquid junction potential is -5 mV and the membrane potential response was about -15 mV. The mobility ratio U_{Cl^-}/U_{Na^+} had therefore increased, but the change in ionic mobility from the aqueous value was small. The relative ionic mobilities may be changed because the interaction of ions with water is changed in the presence of PEO.

The state of the water molecules neighbouring the PEO molecules are an important consideration in discussing ionic mobilities, since the hydration shells of the ions and PEO interact during transport across the membrane. As discussed in section 6.1, the viscosity B coefficients indicate the influence of the particular ion on the structure of neighbouring water molecules. A positive B coefficient may indicate promotion of the tetrahedral network of the water structure by way of hydrogen bonding of the water of solvation, such that the ion occupies a space within the water network causing no spatial disruption. A negative B coefficient may indicate a disruption in the water bonding network of the water molecules by the ions, effecting a lowering of the

viscosity.

In table 6.2 the ratio $R_U = (U_+/U_-)_{\text{membrane}} / (U_+/U_-)_{\text{aq}}$ is shown for the various salts. The viscosity B coefficients for aqueous solution are also tabulated. Unfortunately, for further development of the interpretation, no regular trend can be discerned.

Salt	R_U	B_+	B_-
HCl	0.8	+0.07	0.00
NaClO ₄	1.9	+0.08	-0.02
Na(pTS)	-	+0.08	-
Na(DDS)	-	+0.08	-
KCl	1.2	0.00	0.00
KNO ₃	1.0	0.00	-0.04
CsCl	1.1	-0.04	0.00
NaCl *	0.96	+0.08	0.00

Table 6.2. The membrane to aqueous ionic mobility ratio and the viscosity B coefficients of the cation and anions for the supported PEO solution membrane (unmarked) and the processed PEO gel membrane (*)

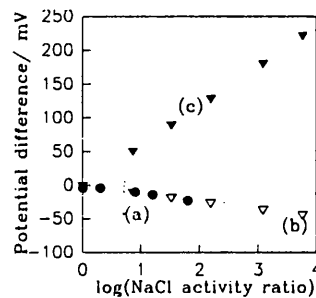


Figure 6.2: The potential difference response of (a) processed PEO membranes in NaCl solution compared to the (b) ideal permeable and (c) semipermeable behaviour calculated from literature.

6.3. BEHAVIOUR OF THE CO-CAST PEO-PVC MEMBRANES

In this section, the ideas presented in sections 6.1 and 6.2 are developed further. It is suggested that the permselectivity of the membranes, investigated in this project, is a result of interactions between ions and water within the membrane channels formed by the hydrated hydrophilic polymer. It is proposed that the factors which determine the dimensions of the hydrophilic polymer channels, within the hydrophobic polymer matrix, will also affect the selectivity of the membrane. The membrane preparation method is considered to affect the membrane microstructure, which influences the domain size of the hydrophilic polymer and hence the dimensions of the hydrated channels. These variables modify the state of water molecules within the hydrated channels which influence the ionic mobility as the ions are transported through the membrane.

6.3.1. EVIDENCE FOR DIFFERENT FORMS OF WATER IN THE MEMBRANE

There are two sources of evidence concerning the different forms of water in the membrane: Differential Scanning Calorimetry (DSC) analysis and ^2H NMR spectroscopy.

Previous studies on PEO gels and solutions have shown that there are three types of water states bound by the poly(ethylene oxide) molecule [5]: water I, in which the water molecules resemble free, unperturbed water, with freezing temperature near 273 K; water II, in which the water molecules are weakly bound by the polymer and freeze at lower temperatures; and water III, where the water molecules are strongly bound to the polar groups of the polymer, do not freeze and are not detected calorimetrically [6].

DSC of the slowly dried co-cast PEO-PVC membranes showed only 2 types

of bound water. The transition temperature of the largest peak corresponds to free unperturbed water, the onset temperature occurring about 0 °C. The surface water of these membranes may be measured as the free water but since these membranes were methodically blot dried, this contribution may be minimised. The second phase transition occurred at about -11 to -25 °C and is interpreted as membrane bound water. The 10% and the 20% PEO membrane showed this type of water but not the 40% PEO membrane. The types of water present, therefore, correspond to the type of ion transport exhibited by the membranes. The 10% and 20% PEO co-cast membranes showed some cation permselectivity to NaCl and HCl solutions and have both bound water and free water associated with the polymers. The DSC scans of the 40% PEO membrane only showed the unperturbed, free water and this membrane exhibited permeable membrane behaviour. Thus ions that travel through the 40% PEO membrane past the hydrated PEO molecules with free, unperturbed water molecules give aqueous transport numbers. Whereas, ions transported through the 10% and 20% PEO membranes are exposed to both the free and bound states of water and give transport numbers different to the aqueous value.

^2H NMR spectroscopy shows the state of water molecules in the membrane by observing the changes in the spectra with varying temperature. A typical solid state NMR lineshape consists of two components: a broad absorption arising from non-isotropic behaviour with a narrower central component from isotropic molecular orientations superimposed [7]. In the case of D_2O spectroscopy, differences in lineshape arise from the orientation of these molecules relating to their environment shown at different temperatures [8]. The correlation time for molecular chain motion should be less than 10^{-4} seconds for line narrowing to occur at NMR frequencies. Since there is a distribution of different states of water within the PEO-PVC membranes, the result should be a broadening of the response peaks. If the water molecules in the PEO-PVC membrane were to freeze, then the pure D_2O lineshape (chapter 5.6, Fig. 5.13 b) would be

observed [8].

At 213 K, the D₂O spectra of a quickly dried co-cast 20% PEO membrane only showed a single, broad peak meaning that the water molecules continue to exhibit isotropic behaviour, as in the spectra of the PEO-PVC membrane at 293 K. That is, at 213 K, there was some fraction of the water that was not frozen.

Those water molecules frozen at 213 K would correspond to water I and II types of water molecules described by differential scanning calorimetry. The freezing temperatures of water II is typically 240-260 K [6], just the range observed here by DSC. Thus, the solid state NMR spectra reveal those adsorbed D₂O molecules correspond to water III which are strongly bound to the polar groups of the polymer but not registered calorimetrically.

6.3.2. CORRELATION OF FORMS OF WATER AND POTENTIAL RESPONSE OF CO-CAST MEMBRANES

The response of the slowly dried co-cast PEO-PVC membranes in HCl solutions suggests that the transport numbers of these ions are within the experimental error of their aqueous transport values. The potential response of these slowly dried membranes to NaCl solutions suggest that there is a difference in the relative ionic mobility U_{Cl^-}/U_{Na^+} from that in water. At low PEO concentrations (5%), the Na⁺ ion is transferred across the membrane with a mobility greater than the Cl⁻ ion. This is contrary to what is found in water. Membranes with a high PEO concentration (45%) show a higher Cl⁻ ion mobility compared to the Na⁺ ion, similar to that found in water. Thus the potential response of the slowly dried PEO membranes show a trend in ionic mobility dependent on the concentration of PEO.

The DSC analysis of the slowly dried membranes showed that ones with a low

PEO concentration exhibit water molecules which are bound to polar groups melting at a reduced temperature (< 273 K) and free water which melts at about 273 K. This result corresponds to ion-water interactions which are different from those in aqueous solution giving rise to apparent transport numbers quite distinct from aqueous values. Slowly dried membranes with a PEO content of 45% showed only one type of water which conforms to the state of water which is free and unbound by polar groups, so that the ion-water interaction can be considered as in an aqueous solution. The apparent transport numbers of these ions in the 45% PEO membrane are similar to those found in water.

The potential response of the quickly dried membranes in HCl and NaCl showed apparent transport numbers similar to those found in aqueous solution. A quickly dried 25% PEO membrane analysed with DSC did show two peaks corresponding to free and bound water (but the small peak corresponding to bound water could only be found with the aid of computer enhancement to pick the peak from the baseline noise). Thus the properties of the quickly dried membranes should be dominated by the free water. This theory also correlates with the apparent transport numbers, which are within experimental error of aqueous values.

6.3.3. EVIDENCE FOR VARIATIONS IN MICROSTRUCTURE IN THE CO-CAST MEMBRANE

Evidence concerning microstructure comes from polarised light optical microscopy, FTIR spectroscopy and thermo-mechanical analysis (TMA). Polarised light optical microscopy shows the variation in the size and distribution of birefringent domains with membrane composition and preparation method. Low PEO percentage membranes had fewer crystalline (PEO) domains compared with higher PEO percentage membranes. These

crystalline domains were smaller with the quickly dried membranes. The quickly dried membranes had a few rather large PEO crystallites.

The high percentage PEO membranes had small (quickly dried PEO-PVC membrane) to medium sized (slowly dried PEO-PVC membrane) crystalline regions. Thus, supposing these crystals hydrate, they give channels in which the water molecules may be described as weakly bound. The transport of ions through these membranes would then be determined by their transport number as in pure water, as observed. This conclusion further relates to the results from differential scanning calorimetry, since only the 10% and 20% PEO membranes showed the free and bound water associated with semipermeable membrane behaviour whilst the 40% PEO membrane only showed the free water molecules associated with permeable membrane behaviour.

The expected vibrational spectra of molecules rely on the concept that the vibrational frequencies of chemical groups behave independently of the rest of the molecule of which they are a part. Interactions that occur between vibrating groups then lead to shifts in the absorption frequency which may be interpreted in terms of changes in the molecular environment [10]. The main differences in the spectrum of co-cast membranes differently prepared is that the peaks representing water and cyclohexanone (3800 to 3000 cm^{-1} and 1750 to 1700 cm^{-1} respectively) are absent in the quickly dried co-cast PEO-PVC membranes compared those slowly dried.

The differences between the co-cast PEO-PVC membranes are illustrated in the peak due to PEO at 1325 cm^{-1} , for the 10% slowly and quickly dried membranes. This peak shifts towards 1350 cm^{-1} with increase in PEO content indicating a difference in interaction between PEO and PVC with increase in PEO content.

The peak due to PVC at 1475 cm^{-1} is present in the slowly and quickly dried

PEO-PVC membranes and is clearly seen in the 40% PEO membrane. This peak shifts from 1475 cm^{-1} in the 40% PEO-PVC membrane to 1450 cm^{-1} in the PVC-PMA membranes indicating vibrational interactions between the PVC and PMA molecules. The other differences between the PVC-PMA membrane spectra and the PEO-PVC membranes are absent peaks due to replaced PEO (at 1100 cm^{-1} and 1360 cm^{-1}) and peaks present due to PMA (1025 cm^{-1} , 950 cm^{-1} and 750 cm^{-1}).

Thermogravimetric analysis (TG) is complementary to FTIR analysis in that it identifies and determines the proportion of the chemical species in the polymer sample from its temperature of evolution in a controlled heating programme. Water was initially evolved as the slowly dried co-cast PEO-PVC membranes were heated in nitrogen gas. The temperature of this transition increased with PEO content, presumably because the water molecules can interact with the PEO via strong hydrogen bonds. The previously soaked 45% PEO membrane showed the highest temperature of transition for water ($139\text{ }^{\circ}\text{C}$) indicating a large proportion of adsorbed water interacting with the PEO in the membranes. The next temperature transition corresponded to the evaporation of the polymer solvent cyclohexanone from the slowly dried co-cast PEO-PVC membranes. The temperature of this transition decreased with increase in PEO content. An increase in PEO content results in the binding of water molecules to the membrane. Presumably the interaction of water with the solvent cyclohexanone will lower the temperature of evaporation. The higher transition temperatures (in the region of 300 to $500\text{ }^{\circ}\text{C}$) correspond to the charring of the polymer.

Thermomechanical analysis (TMA) shows the extent of mixing of the two polymers on the scale of the probe area (1 cm^2) [11]. For example, a thermomechanical scan showing just one peak indicates a thorough mixing of the two polymers and two peaks indicates heterogeneity in the membrane.

The TMA scans showed the number of glass transitions increasing with the proportion of PEO in the membrane. There was, also, a larger number if the rotary evaporation method was used to prepare the membrane. An interpretation based simply on the number of softening temperatures is that the 5% PEO membrane consisted of one fully mixed phase whilst the 10% and 20% PEO membranes showed segregated polymer regions.

The 40% co-cast and the 20% rotary evaporated PEO membrane both showed transitions which indicate the presence of mixed and segregated polymers regions having softening temperatures that correspond to both the pure polymers and, in between, some softening temperatures indicating mixed phases.

Thus, thermomechanical analysis showed that the homogeneity of these membranes decreases with increasing proportion of PEO. The homogeneity of the membranes can be linked to its electrochemical behaviour. The homogeneous 5% slowly dried co-cast PEO-PVC membrane behaved like a semipermeable membrane and the heterogeneous 40% slowly dried co-cast PEO membrane behaved like a permeable membrane.

6.3.4. CORRELATION OF MICROSTRUCTURE AND MEMBRANE POTENTIAL

The results found in polarised light optical microscopy, FTIR spectroscopy and thermomechanical analysis can be related to the potential response of the co-cast membranes.

The observations on membrane microstructure indicate that the PEO is organised in hydrated channels penetrating the membrane. These channels

would range from single molecule dimensions up to the micrometer scale features observed by optical microscopy. It can be proposed that the loosely bound water is associated with large channels. Since the transport behaviour is supposed to depend upon the interaction of the hydrated ion with the solvation sheath of the PEO, it may be proposed that the relative mobility of different ions varies with the PEO channel diameter.

The second postulate needed is that the absolute mobility of the ions decreases with decreasing channel diameter. Now, the observations can be explained qualitatively. Large PEO channels (large crystallites observed by microscopy) would behave like the pure PEO membranes, with ion mobility and transport numbers changed from that in water but not by much. So, if the behaviour of the co-cast membrane was determined by the large crystallites, the results should be similar to those from the pure PEO membranes. This is the case for all the rapidly dried membranes and for membranes with large PEO content. For the quickly dried membranes, there was a large number of very small channels, but these would have a low conductivity; the small number of large crystallites would act as an ionic short-circuit. Thus, these membranes have high electrical resistance but the transport behaviour would be similar to aqueous solution. This interpretation is also consistent with DSC showing mainly "free" water (presumably associated with the large crystallites) and only a very small amount of "bound" water.

It is the slowly dried membranes which show the effects of the channel size on ion transport. It is proposed, that if the channels are not too small they will have sufficient conductance such that the total membrane conductance would not be dominated by the larger channels. It is these membranes that show clearly a range of water binding sites, and in which the trend in potentiometric behaviour correlates with the physical measurement of microstructure.

The most startling effect is on the relative mobility of Na^+ . Other cations (K^+ ,

Cs^+) show mobility relative to Cl^- which is not much different to that in aqueous solution. However, the mobility of Na^+ relative to anions (and hence relative to K^+ , Cs^+) was greatly enhanced as the PEO channels got smaller. The postulate of Na^+/K^+ discrimination based on differential solvation, or "water structure", effects is not new.

Wiggins has studied the distribution of ions between bulk water and water in the pores of a silica gel [12] and concluded that the surface orientated water showed enhanced solvent powers for the water-structure breaking ions and decreased solvent powers for the structure-making ions. Dalton et al also [13] studied the exclusion of ions using silica gels and found that the exclusion of salts from the silica pores was due to the cation rather than the anion. The ability of an ion to change the structure of water and the effects of ionic charges, were considered in the interpretation of their results. Two explanations for the mechanism of ion exclusion were offered: size exclusion and the inability of solute species to approach a solid surface compared with the solvent molecules. The size exclusion factor was related to the viscosity B coefficient of the ions, which was interpreted in terms of the ability of an ion to influence the extent of water structure around the ion and thus affect the size of the ionic hydration shell. The other factor for ionic exclusion was considered the inability of a hydrated solute species, larger than a solvent molecule, to be concentrated near a solid surface. Thus a centre for an aluminium hydrate, for example, cannot for purely geometrical reasons approach a solid surface as closely as a centre of a water molecule, causing an enrichment of the ion concentration in the bulk solution. Dalton et al also postulated a mechanism whereby an aluminium hydrate reacts with the silica gel by exchange of the hydration water molecules with the silica molecule, or by dissociation of a H^+ entity from the hydrate, which then reacted with the silica gel.

Comparison between the FTIR spectrum of the quickly dried and the slowly

dried PEO-PVC membranes revealed that there were small shifts in the peaks. These correspond to interactions between the polymers when incorporated into the co-cast membrane. FTIR spectroscopy also showed that the role of cyclohexanone is important although unclear. Co-cast membranes, which were dried for a period longer than 30 hours, showed behaviour similar to an open circuit. This long drying process could diminish the water and cyclohexanone content in these membranes which perhaps may be necessary to produce an ion-conducting membrane.

6.3.5. EFFECT OF VARIATION OF PVC IN THE MEMBRANE

The effect on permselectivity of the membranes by modification of PVC was investigated by changing its source or adding a functional group to the carbon chain.

When the source of the PVC was changed to Fluka (m.w. 80,000) problems were encountered with low membrane conductivity. In particular the slowly dried membranes were very resistive and gave a very erratic potential difference response (in contrast to the results obtained with Aldrich PVC, m.w. 161,000). The resistive behaviour may be a result of over-drying the membrane; drying for a long period at a constant 30 °C whereas the drying temperature for the Aldrich PVC membranes dropped from 30 °C to room temperature after 2-3 hours.

The quickly dried Fluka type PEO-PVC membranes, on the other hand, were very similar to the PEO-PVC (Aldrich) membranes, with the exception of the results in HCl. All the PEO-PVC (Fluka) membranes gave apparent transport number for NaCl similar to those in water.

Incorporation of a carboxylate functional group endows the co-cast membrane

with cation selectivity from binding sites of the carboxylate anion [14]. The potential response of the co-cast and rotary evaporated membranes in HCl showed that the membrane was cation selective. The potential response decreased with a decrease in the carboxylated PVC content, indicating the cation permselectivity was indeed due to the carboxylate group. In this case, the hydrated PEO channels would provide a short-circuiting path. The other salts tested were KCl, NaDDS and $MgCl_2$, of which the K^+ and the Na^+ ions gave a membrane response, indicating that the carboxylate group in the membranes bound K^+ and Na^+ ions as well as H^+ ions.

6.3.6. EFFECT OF CHANGING THE HYDROPHILIC POLYMER IN THE MEMBRANE

The effect of changing the membrane component PEO was studied by replacement with PVMK ($[CH(CH_3)CO]_n$) and PMA ($[CH_2CH(CO_2CH_3)]_n$). The potential responses of these membranes was found to differ. The behaviour of HCl and NaCl in PVC-PVMK membranes were similar to that in water. The PVC-PMA membranes exhibited exclusive anion selectivity in HCl and NaCl single salt solutions and the mixed salt solutions. This observation is very interesting since the functional groups of the polymers differ only in that the PVMK contains a ketone and the PMA polymer contains an ester.

6.4. MODEL FOR THE CO-CAST PEO-PVC MEMBRANE POTENTIAL RESPONSE BASED ON MEMBRANE STRUCTURE

A model is proposed which describes the potential difference response of the co-cast PEO-PVC membrane where the membrane structure is modelled as a set of parallel, non-interacting channels. The model is developed in a way similar to the liquid junction potential equation in chapter 2.2.

similar to the liquid junction potential equation in chapter 2.2.

The conducting channels are considered to fall into classes, j , each class has a conductance per channel equal to σ_j , and this conductance is dependent on the radius of the channel. The total conductance per class of channels is $N_j\sigma_j$ and the total conductance of the membrane is $\sum_j N_j\sigma_j$.

If an increment of charge δQ is transported across the membrane, the charge for each class of channels is δQ_j , so $\delta Q = \sum_j \delta Q_j$. The transport number of each ion i in channel j is t_{ij} (different for different j) and also $\sum_i t_{ij} = 1$. The transport of the number of moles of ions i in channel j is δn_{ij} , so the transport number t_{ij} , can be expressed as,

$$t_{ij} = \frac{Fz_i \delta n_{ij}}{\delta Q_j}$$

or rearranged to give the number of moles of ions transported,

$$\delta n_{ij} = \frac{t_{ij} \delta Q_j}{Fz_i}$$

So, $\delta Q_j / \delta Q$ is simply the ratio of conductance of channel j to the total conductance, assuming that the channels are non-intersecting.

So, the increment of charge transported is

$$\delta Q_j = \frac{N_j \sigma_j}{\sum_j N_j \sigma_j} \delta Q$$

Now, the transported number of moles of ions can be expressed as,

$$\begin{aligned}\delta n_i &= \sum_j \delta n_{ij} = \frac{1}{Fz_i} \sum_j t_{ij} \delta Q_j \\ &= \frac{1}{Fz_i} \sum_j \left(t_{ij} \cdot \frac{N_j \sigma_j}{\sum_j N_j \sigma_j} \delta Q \right)\end{aligned}$$

This can be rearranged to give,

$$\delta n_i = \frac{\delta Q}{Fz_i \left(\sum_j N_j \sigma_j \right)} \cdot \sum_j t_{ij} N_j \sigma_j \quad (6.1)$$

that is, the contribution of each set of channels to the total transport is weighted by the conductance of that set of channels. For each ion moving some small distance dx , the change in electrochemical potential is,

$$d\mu_i = RT d \ln(a_i) + Fz_i d\Phi$$

At steady state, the net current is zero, i.e.

$$\sum_i d\mu_i \delta n_i = 0$$

i.e.,

$$\sum_i [RT d(\ln a_i) \cdot \delta n_i + Fz_i d\Phi \cdot \delta n_i] = 0 \quad (6.2)$$

this equation can be rearranged , using equation (1), to give,

$$Fz_i \delta n_i = \delta Q \cdot \frac{\sum_j t_{ij} N_j \sigma_j}{\sum_j N_j \sigma_j}$$

so, from equation 2, the above term can be expressed as,

$$\left[\sum_i RT d(\ln a_i) \cdot \frac{\sum_j t_{ij} N_j \sigma_j}{Fz_i (\sum_j N_j \sigma_j)} + \frac{\sum_j t_{ij} N_j \sigma_j}{\sum_j N_j \sigma_j} \cdot d\Phi \right] \delta Q = 0$$

which can be expressed as,

$$\sum_i \left[RT d(\ln a_i) \cdot \frac{\sum_j t_{ij} N_j \sigma_j}{Fz_i \sum_j N_j \sigma_j} \right] + \left[\frac{\sum_i \sum_j t_{ij} N_j \sigma_j}{\sum_i N_j \sigma_j} \cdot d\Phi \right] = 0 \quad (6.3)$$

When rearranged the following equation is obtained,

$$\frac{\sum_i \sum_j t_{ij} N_j \sigma_j}{\sum_j N_j \sigma_j} = \frac{\sum_j (N_j \sigma_j \cdot \sum_i t_{ij})}{\sum_j N_j \sigma_j}$$

By definition of the transport number, $\sum_i t_{ij} = 1$, in each channel. Thus the above ratio is equal to 1. From equation 6.3,

$$d\Phi = \frac{-RT}{F} \sum_i \frac{d(\ln a_i)}{z_i} \cdot \frac{\sum_j t_{ij} N_j \sigma_j}{\sum_j N_j \sigma_j}$$

Which may be integrated across the membrane to obtain the membrane potential difference, $\Delta\Phi$ (this procedure is the same as the standard expression except for weighting of the transport numbers). The next step is to simplify and approximate,

(a) t_{ij} is independent of position across the membrane,

(b) only a binary electrolyte is considered.

Which results in the following expression,

$$\Delta\Phi = -\frac{RT}{F} \ln(a_1) \left[\frac{1}{\sum_j N_j \sigma_j} \right] \left[\sum_j N_j \sigma_j \left(\frac{t_{+,j}}{|z_+|} - \frac{t_{-,j}}{|z_-|} \right) \right]$$

For a 1:1 electrolyte,

$$\Delta\Phi = -\frac{RT}{F} \ln\left(\frac{a_1}{a_2}\right) \left[\frac{\sum_j N_j \sigma_j (t_{+,j} - t_{-,j})}{\sum_j N_j \sigma_j} \right]$$

For simplicity, let $S_j = N_j \sigma_j / \sum_j N_j \sigma_j =$ total relative conductance of channels j

$$\Delta\Phi = -\frac{RT}{F} \ln\left(\frac{a_1}{a_2}\right) \cdot \sum_j S_j (t_{+,j} - t_{-,j}) \quad (6.4)$$

It is hypothesed that for very small channels in the co-cast membranes there would only be H^+ transport, via a Grotthus mechanism, along the water molecules in the hydrated channels, but that the few large crystals formed dominate the conductance of the membrane.

Equation 6.4 can be used to describe the behaviour of the membrane, for various assumptions of the values of S_j :

Now assume two classes of channels, one having $t_+ = 1$ and the other having t_+ , t_- equal to the values in aqueous solution. Then as S , the proportion of

permselective channels, varies between 1 and 0, the behaviour of the membrane varies smoothly between that of a semipermeable and that of a permeable membrane. Figure 6.3 show the potential difference response of a membrane to HCl and NaCl respectively, as modelled in this way. The expected potential difference response decreases with a decrease in the value of S . This means that as the conductance of the permselective channels decreases, the proportion of ions transported through these channels correspondingly decrease.

This trend in potential difference response is very similar to the response of the slowly dried co-cast PEO-PVC membranes in NaCl and HCl as shown in figure 4.9. The potential difference response of the slowly dried membranes decreases with an increase in PEO content. Thus the slowly dried co-cast PEO-PVC membranes with low PEO content (5%) may be represented as having a relatively high conductance of permselective channels. Whereas, the membranes with a high PEO content (45%) show a relatively high conductance of non-permselective channels. The permselectivity of the low PEO content slowly dried membranes results from a even distribution of medium sized, hydrated PEO channels which allow ion transport. Whereas the lack of permselectivity in the quickly dried low PEO content membranes is a result of the membrane conductance being dominated by a few large PEO clusters.

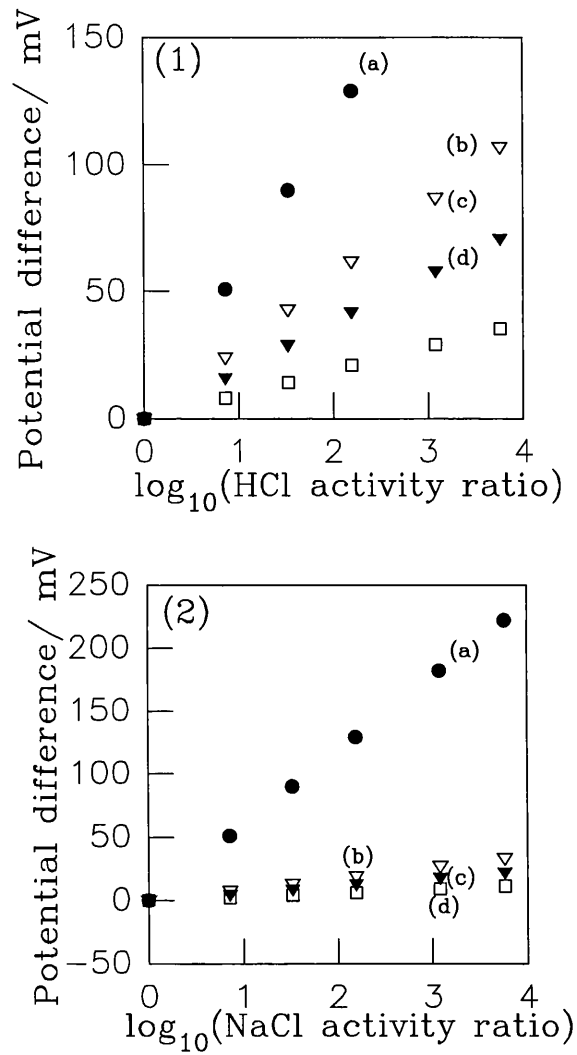


Figure 6.3: The expected potential difference response of a membrane in (1) HCl and (2) NaCl solution, modelled using equation 6.4 and on assumption of 2 classes of channels, shown with the various fractions of the total relative conductance of permselective channels to the membrane, (S_j), where the values for S_j are: (a)=1, (b)=0.75, (c)=0.5, (d)=0.25.

REFERENCES FOR CHAPTER 6

- [1] C. W., Davies, "Ion Association", ch. 14, Butterworths, London, 1962.
- [2] P. M., Wiggins, *J. Theor. Biology*, **32**, 131, (1971).
- [3] H. S., Harned, B. B., Owen, "Physical Chemistry of Electrolyte Solutions", ch. 7, Reinhold Publ., New York, 1950.
- [4] C. W., Davies, "Ion Association", ch. 11, Butterworths and Co., London, 1962.
- [5] J. M. Harris, "Poly(ethylene glycol), Biotechnical and Biomedical Applications", ch. 2, Plenum Press, New York, 1992.
- [6] V. A. Bershstein, V. M., Egorov, "Differential Scanning Calorimetry of Polymers", ch. 8, Ellis Horwood, New York, 1994.
- [7] H. Menge, T. Steurich, *Electrochim. Acta*, **13**, (1994), 1971.
- [8] B. Boddenberg, R. Grosse, *Lerhstuhl Fur Phys Chemie II*, **41a**, (1986), 1361.
- [9] D. Campbell, J. R. White, "Polymer Characterisation, Physical techniques", ch. 5, Chapman and Hall, New York, 1989.
- [10] D. Campbell, J. R. White, "Polymer Characterisation, Physical techniques", ch. 6, Chapman and Hall, New York, 1989.
- [11] D. Campbell, J. R. White, "Polymer Characterisation, Physical techniques", ch. 12, Chapman and Hall, New York, 1989.
- [12] P. M., Wiggins, *Biophys. J.*, **13**, 385, (1973).
- [13] R. W., Dalton, J. L., McClanahan, R. W., Maatman, *J. Colloid Sci.*, **17**, 207, (1962).
- [14] E., Pungor, E., Graf, Z., Niegreisz, K., Toth, E., Pungor, *Anal. Chem.*, **60**, 295, (1988).

CHAPTER 7
CONCLUSION

CHAPTER 7. CONCLUSION

The hypothesis, that a permselective membrane could be made from a nano-scale hydrated network of PEO supported by a strong flexible matrix of PVC with a polymer solvent cyclohexanone, has been sustained. The process of quickly drying the polymer solution hindered crystallisation resulting in an amorphous polymer.

Both the pure PEO membranes and processed gelatinous membranes were found to behave alike in aqueous solution. These membranes showed insignificant permselectivity and were structurally unstable in salt solutions, becoming porous after a period of about 20 to 40 minutes.

The co-cast PEO-PVC membranes were structurally stable in electrolyte solution for over a period of about 2 weeks and showed some permselectivity. The slowly dried co-cast membranes in NaCl solution exhibited permselectivity to Na⁺ ions, whereas the quickly dried co-cast membranes exhibited transport numbers similar to those found in aqueous solution.

The permselectivity of the slowly dried PEO-PVC membranes decreased with an increase in PEO content in the membrane, with the transport number of ions becoming similar to aqueous values in high PEO content membranes (45% PEO).

The decrease in permselectivity with an increase in PEO content for the slowly dried membranes could be characterised by the model described in chapter 6. Hydrated PEO channels are considered as non-intersecting pathways for ion transport, each characterised by its particular conductance σ . The expected potential difference response in the model decreased with a decrease in the fraction of permselective channels.

Physical characterisation techniques, by DSC and ²H NMR, demonstrated that the slowly and quickly dried co-cast PEO-PVC membranes of high PEO content (45%) contained unbound water molecules. The hydrated PEO

channels were representative of a wholly aqueous environment and these membranes gave transport numbers which were similar to that in water. The narrower PEO channels were considered to confer permselectivity to the membrane by size exclusion of hydrated ions, based on the interaction energy of the polymer's water of hydration with that of the ions. This effect was not observed when there was an abundance of the larger hydrated channels such as in the 45% PEO-PVC membrane. Thus only the slowly dried low PEO content (5%) membranes showed permselectivity to Na^+ ions.

It was found that changing the PVC and the PEO component changed the potential difference response of the membranes. Incorporation of a carboxylate group gave cation permselectivity to the membrane, as expected. Incorporation of a poly(methylacrylate) with a poly(vinyl chloride) matrix produced anion selective membranes, an effect which did not have an obvious explanation.

Recommendations for improving the permselective nature of the membrane involving changes to the preparation procedure would be to prevent the larger clusters of PEO from forming during the drying process, or, to remove them afterwards so that the transport properties of the smaller, permselective channels will dominate. This could be done by quickly drying the polymer solution as described in chapter 3, then removing the large PEO clusters by soaking the membrane in an aqueous solution of poly(acrylic acid) (chapter 1.1.4) which will complex the PEO, followed by casting another polymer layer over the membrane to fill holes which may form as a consequence of PEO extraction. There may be problems such as a high resistance associated with a thick multilayered membrane, but this might be overcome if each cast membrane had a blade clearance of less than about 20 μm when producing a membrane of three layers, and soaking the membrane on the casting plate in the aqueous poly(acrylic acid) to minimise damage which would occur when a thin fragile membrane is lifted off the casting plate.

In summary, the preparation of flexible, tough, water-stable composite PEO PVC membranes has been achieved. The potential difference behaviour of the slowly dried co-cast PEO-PVC composite membranes showed some permselectivity to Na^+ ions. Incorporation of a carboxylate ion into the PVC component of the co-cast and rotary evaporated membrane causes the membranes to be exclusively selective to monovalent cations, such as H^+ and Na^+ ions. Preparation methods have been suggested to improve the permselectivity of the co-cast PEO-PVC membranes.